GENETIC STUDY OF HEMATOPOIESIS IN ZEBRAFISH

QIAN FENG
(Bachelor of Medicine, Beijing Medical University, P.R.China)

A THESIS SUBMITTED
FOR THE DEGREE OF DOCTOR OF PHILOSOPHY
INSTITUTE OF MOLECULAR AND CELL BIOLOGY
DEPARTMENT OF BIOLOGICAL SCIENCES
NATIONAL UNIVERSITY OF SINGAPORE
2005

Acknowledgement

I would like to express my deepest and most sincere gratitude to my supervisor, Dr Zilong Wen, for guiding me throughout the course of this study. He not only provided insightful suggestions on my projects, but also built a conducive scientific environment in our lab. I am also grateful for his critical perusal of this thesis. Special thanks also go to my Ph.D. committee members, Dr Jinrong Peng, Dr Yunjin Jiang and Dr Peng Li for their valuable advice and suggestions.

I also want to thank the past and present lab members especially Fenghua Zhen and Chinthing Ong, who had worked with me to finish the microarray project. Many thanks go to our genetic screen team, both in our lab: Hao Jin, Yanmei Liu and Dr Peng's group: Lin Guo and Honghui Huang, for the joyous collaboration and forever friendship.

6 years of Ph.D work would be insurmountable without the professional support from the technical staff in TLL (ex-IMA) and IMCB. My gratitude to Chinheng Goh, Amy Lai and all the aunties in TLL fish facility and Dr Maysu You and all the members in IMCB fish facility for their hard work on the maintenance of our main experimental material: zebrafish. Heartfelt appreciations also go to sequencing facilities and IT departments in both institutes.

Lastly, I am enormously indebted to my parents for everything I am today and special thanks to my mother-in-law for her concern. I owe my loving gratitude to my wife, Evelyn Ng (and my baby boy Yong Jia for the joy he brings to us), for her continuous support and understanding during my countless hours spent in the lab over the past years.

Table of Contents

Summary

Hematopoiesis is a program for blood formation and is characterized by ventral mesoderm induction, hematopoietic stem cell specification and subsequent lineage cell differentiation. This program is highly conserved during evolution. Many key regulators have been identified through the studies in mouse, amphibians and birds. Recently, zebrafish (*Danio rerio*) has emerged as a good genetic model organism to study the early events and organogenesis during vertebrate development. The hematopoiesis in zebrafish has been shown to be very similar to that in mammals and other higher vertebrates. Almost all analogous blood cells have been identified in zebrafish and early hematopoietic events, like blood circulation and heart beating, can be visualized under the microscope after 24 hours post fertilization. In addition, unlike mouse, zebrafish early blood deficient mutants can survive up to 7 days post fertilization with normal body formation, which facilitate the in-depth study of early hematopoiesis during vertebrate development. Hence, complementary to mouse, zebrafish is a good vertebrate model system for the study of hematopoiesis.

Many zebrafish hematopoietic mutants have been identified through large-scale genetic screens. However, specific tissue or organ deficient mutants can not be isolated through these morphology-based screens. In order to study the T-cell development and thymic organogenesis, we carried out the whole mount *in situ* based forward genetic screen using *rag1* as a marker. After one year of primary screening and two rounds of re-screens, we identified 86 *rag1* deficient mutant families from 540 mutagenized genomes. Considering the criterions of general development, blood circulation and thymus rudiment marker *foxn1* expression, 13 mutants were selected and maintained for future study.

In addition to using forward genetic approach, we also used microarray techniques to compare the gene expression profiles between wild-type and early hematopoietic mutant, *cloche*, which has defects in both hematopoietic and vascular development. I developed a method to construct cDNA library from a single embryo of any desired development stage. Through this method, we could compare the gene expression profile of *cloche* mutant and wild-type at very early stage. We performed Affymetrix Array on *cloche* mutants at 18-somite stage and identified 18 previously uncharacterized zebrafish genes that were down-regulated in the *cloche* mutant. Further whole mount *in situ* analyses showed that 9 of these genes had tissue specific expression patterns in hematopoietic or vascular cells.

Through our forward genetic screening and microarray analyses, many hematopoietic mutants and hematopoietic or vascular related genes have been identified. Collectively, the mutants will serve as invaluable models and the genes as potential molecular markers to understand vertebrate hematopoiesis and human diseases.

List of Tables

List of Figures

List of Abbreviations

aa	amino acid
AP	alkaline phosphatase
BAC	bacterial artificial chromosome
BCIP	5-bromo-3-chloro-3-indolyl phosphate
bHLH	basic helix-loop-helix
bp	base pair
clo	cloche
DIG	digoxygenin
DNA	deoxyribonucleic acid
dNTP	deoxyribonucleotide triphosphate
dpf	days post fertilization
EGFP	enhanced green fluorescence protein
ENU	N-ethyl-N-nitrosourea
FBS	fetal bovine serum
FCS	fetal calf serum
GFP	green fluorescence protein
hpf	hours post fertilization
hr	hour
ICM	intermediate cell mass
IPTG	isopropyl b-D-thiogalactopyranoside
kb	kilo base pair
M	mole per liter
min	minute
MO	morpholino
mon	moonshine
mRNA	messenger ribonucleic acid
mt	mutant
NBT	nitroblue tetrazolium
ng	nanogram
nl	nanolitre
NTP	ribonucleotide triphosphate
PBS	phosphate-buffered saline
PCR	polymerase chain reaction
PFA	paraformaldehyde
PTU	1-phenyl-2-thiourea
rag1	recombination activating gene 1
RT	room temperature
RT-PCR	reverse transcription polymerase chain reaction
SSC	sodium chloride-trisodium citrate solution
UV	ultraviolet
µl	microlitre
wt	wild-type

List of Publications

1 Vrp1p Functions in Both Actomyosin Ring-Dependent and Hof1p-Dependent Pathways of Cytokinesis
Suniti N. Naqvi, Qian Feng, Victoria J. Boulton, Regina Zahn and Alan L. Munn; ***Traffic*** 2001 2: 189-201

2 Chromatin-remodelling factor BRG1 selectively activates a subset of interferon-α-inducible genes
Mei Huang, Feng Qian, Yuanyu Hu, Chengeng Ang, Zhong Li and Zilong Wen; ***Nature Cell Biology*** 2002 4: 774-781

3 Microarray Analysis of Zebrafish *cloche* Mutant Using Amplified cDNA and Identification of Potential Downstream Target Genes
Feng Qian, Fenghua Zhen, Chinthing Ong, Suk-Won Jin, Hui Meng Soo, Didier Y.R. Stainier, Shuo Lin, Jinrong Peng and Zilong Wen; ***Developmental Dynamics*** 2005 233:1163-1172

4 The 5' zebrafish *scl* promoter targets transcription to the brain, spinal cord, and hematopoietic and endothelial progenitors
Hao Jin, Jin Xu, Feng Qian, Linsen Du, Chee Yong Tan, Zhixin Lin, Jinrong Peng, Zilong Wen; ***Developmental Dynamics*** published online: 28 Oct 2005

Participation at Conference

1 Joint EMBO-IMA Workshop: Fish as model organisms in the genomic era, Singapore, 2001

2 3rd European Conference on Zebrafish and Medaka Genetics and Development, Paris, France, 2003

3 International Stem Cell Conference, Singapore, 2003

4 15th International Society of Developmental Biologists Congress, Sydney, Australia, 2005

5 Keystone Symposia: Stem Cells, Senescence and Cancer , Singapore, 2005

Chapter I: Introduction

1.1 Hematopoiesis Program in Vertebrate

1.1.1 General Concepts of Hematopoiesis

The blood is composed of a large array of cell types that circulate through the blood vessels to reach different tissues, where they provide oxygen (erythrocytes), produce platelets that are essential for clotting processes (megakaryocytes), supply the first barrier of defense against invasive pathogens (macrophages and neutrophils), and produce the specific protection system against foreign agents and abnormal cells (lymphoid lineage-T cells, B cells and natural killer cells). All these mature blood cells come from a common progenitor cell called hematopoietic stem cell (HSC), which can differentiate into multiple blood cell types and maintain the self-renewal activity (Kondo et al., 2003). The processes that HSC commit and differentiate to all blood lineage cells are defined as hematopoiesis.

1.1.2 The Ontogeny of Hematopoiesis

The development of hematopoiesis has been studied in many species, and several aspects of the program are conserved throughout vertebrate evolution. The initiation of hematopoiesis is ventral mesoderm induction conducted by bone morphogenic protein (BMP-4) and some other unknown growth factors (Kishimoto et al., 1997; Winnier et al., 1995). Following this induction, blood cells development occurs in two waves: the first wave of hematopoiesis arise in the blood island of yolk sac and leads to the production of primitive red blood cells, megakaryocytes, and macrophage progenitors (Maximow AA., 1909; Xu et al., 2001; Palis et al., 1999); the second hematopoietic wave (definitive wave of hematopoiesis) takes place in the fetal liver and produces long-term

hematopoietic stem cells (LT-HSCs) capable of reconstituting the blood system for life, shortly before birth and thereafter, the bone marrow becomes the major site of hematopoiesis (Shivdasani et al., 1995). In mouse, the first hematopoietic site was identified in the extra-embryonic yolk sac (Haar and Ackerman, 1971), termed as blood island; whereas similar extra-embryonic blood island counterparts were also found in bird and frog (Zon, 1995). For a long time, the extra-embryonic yolk sac was considered as the only initiation site of hematopoiesis (Moore and Metcalf, 1970). However, recent experiments from amphibians (Turpen et al., 1981; Kau and Turpen, 1983) and birds (Martin et al., 1978) demonstrated that the yolk sac is not the only site for the hematopoiesis commencement. During avian development, intra-embryonic hematopoietic cells appeared in the dorsal mesentery, in para-aortic foci, in the anterior region of the mesonephros in association with the postcardinal veins, or in the dorsal aorta (Dieterlen-Lievre and Martin, 1981; Cormier and Dieterlen-Lievre, 1988). Stem cells from this intra-embryonic region differentiate into the definitive erythrocyte population and also give rise to progenitors that colonize the thymus and bursa of Fabricious (Lassila et al., 1978; Lassila et al., 1982). The analogous compartment in the Xenopus embryo is the mesoderm of the dorsal lateral plate (DLP), which contributes to definitive erythroid and lymphoid populations (Turpen and Knudson, 1982). The corresponding intra-embryonic region termed either aorta-gonads-mesonephros (AGM) or para-aortic splanchnopleura (P-sp) in mouse were found to contain cells with the capability of long-term reconstitution of the hematopoietic system when injected into irradiated mice (Godin et al., 1993; Medvinsky et al., 1993), also supporting the presence of second hematopoietic initiation site in the intra-embryonic region. Thus, the ontogeny of hematopoiesis is initiated independently from two different anatomical locations during embryogenesis.

1.1.3 Hemangioblast Cell

The presence of two sites for early hematopoietic generation has led to much speculation concerning lineage relationships. The concurrent emergence of hematopoietic cells and vascular endothelium cells with the similar spatial gene expression patterns suggest the existence of a common progenitor, or hemangioblast (Dieterlen-Lievre, 1975). Mice with null VEGF receptor Flk-1 or TGFβ1 display the deficiency in generation or organization of both blood and vascular cells (Shalaby et al., 1995; Dickson et al., 1995), indicating interdependence between vasculogenesis and hematopoiesis. In the *in vitro* ES cell (embryonic stem cell) differentiation experiments, blast colony-forming cell (BL-CFC) was identified as presumptive hemangioblast cell that has the bipotential for hematopoietic and endothelial cell development (Kennedy et al., 1997; Choi et al., 1998). In addition, the zebrafish *cloche* mutant exhibits defects on both hematopoietic and endothelial lineage cells (Stainier et al., 1995), consistent with the requirement of a common progenitor cell. Recent study from embryo-derived blast colony found that the potential hemangioblast are first detected at the mid-streak stage of gastrulation, with a narrow developmental window spanning approximately 12-18h of mouse gestation, dramatically declining at the head fold stage (Huber et al., 2004). Although these experiments provide circumstantial evidence to highlight the inseparable relationship between hematopoietic cells and vascular endothelium cells and support the hypothesis of hemangioblast, isolation of these cells has not been successful.

1.1.4 Hematopoietic Stem Cell

The hematopoietic stem cells are the central kernels of the blood cell development. Featured with self-renewal and lineage commitment, the HSCs are the forefront of both basic stem cell research and clinical applications (Akashi et al., 2000). The bone marrow transplantation and peripheral blood stem cell transplantation have been widely used in

therapy of immune system deficient patients and for the recovery of the stem cells that have been destroyed by high doses of chemotherapy and/or radiation therapy. Although the clinical application reveals the powerful multipotenty of HSCs, the ontogeny of these cells is still a controversial issue. The cell transplantation experiments demonstrate that both yolk sac blood island and AGM have HSCs (Moore and Metcalf, 1970; Medvinsky et al., 1993). The yolk sac supports the generation of primitive HSCs and is the first homing site for definitive erythroid cell development (Palis and Yoder, 2001). However, the yolk sac HSCs can only reconstitute hematopoiesis after the injection to neonatal mice but not to irradiated adult host (Yoder et al., 1997). Whereas, the AGM contains the definitive HSCs, which possess the ability to reconstitute the hematopoiesis of lethally irradiated adult mice (Medvinsky and Dzierzak, 1996). The relationship between these two populations of HSCs is largely unknown (Keller et al., 1999; Yoder, 2001; Cumano and Godin, 2001). Some studies suggest independent origins of primitive and definitive HSCs(Dieterlen-Lievre, 1975; Medvinsky and Dzierzak, 1996), whereas others provide evidence for a common precursor population, which arises in the yolk sac to provide primitive hematopoiesis for the early embryo but also seeds the AGM and fetal liver as these sites become competent to support HSCs and hematopoietic cell development (Moore and Owen, 1967; Johnson and Moore, 1975). Recently, the discovery of placenta as an important site for HSCs development makes the parentage of HSCs more complex (Alvarez-Silva et al., 2003; Gekas et al., 2005; Ottersbach and Dzierzak, 2005). Nevertheless, the studies of HSCs commencement help us to define the suitable microenvironment for HSCs development and may provide information for *in vitro* culture of HSCs in HSCs based-therapy.

1.1.5 Hematopoietic Lineage Differentiation

The hematopoietic lineage differentiation is depicted in a hierarchical fashion, with HSCs producing first to progenitors and then to precursors with varying commitments to multiple or single pathways. After a transient harboring in the yolk sac and AGM, HSCs migrate to the secondary sites of hematopoiesis: the liver, spleen, thymus and bone marrow, where the totipotent HSCs give rise to transit populations with restricted differentiation capacity (Dzierzak et al., 1998; Delassus and Cumano, 1996). These transit progenitor cells, which can be identified by expression of specific lineage markers and bioassays of developmental potential in tissue culture or transplantation, eventually differentiate into different hematopoietic lineages, for instance, the common lymphoid progenitors (CLP) give rise to B-cells and T-cells (Kondo et al., 1997), whereas the common myeloid progenitors (CMP) give rise to monocytes, platelets, granulocytes and erythrocytes (Akashi et al., 2000). The developmental potential of these cells is generally limited to only one or two of the hematopoietic lineages and these cells progressively display the antigenic, biochemical, and morphological characteristic of the mature cells of the appropriate lineages and lose their capacity for self-renewal (Kondo et al., 2003).

1.1.6 Molecular Regulation of Hematopoiesis

The hematopoiesis program, from ventral mesoderm induction to final lineage cell differentiation, is controlled by multiple factors and pathways. Gene-targeting approaches have been widely applied to define the functions of these factors in the primitive and definitive hematopoiesis. In respective T-lymphoid acute leukemia oncoprotein Tal-1/SCL (for stem cell leukemia) (Porcher et al., 1996; Robb et al., 1995; Robb et al., 1996; Shivdasani et al., 1995) and LMO2 knockout mice (Yamada et al., 1998; Warren et al., 1994), the lack of precursor determination or maintenance both in yolk-sac and fetal liver is observed and indicate that these two genes play important

roles in early development of primitive and definitive hematopoietic progenitors. Whereas, in knock-out mice for another two transcription factors AML1/RUNX1 (Castilla et al., 1996; Wang et al., 1996) and c-MYB (Mucenski et al., 1991), the yolk sac hematopoiesis is normal, but the fetal liver hematopoiesis is blocked as HSC generation and proliferation are defective, suggesting the specific functions of RUNX1 and c-MYB in definitive hematopoiesis. Although no specific primitive hematopoietic deficient mutant has been identified so far, studies from these knock-out mice indicate that the requirements for primitive and definitive hematopoiesis are distinct. Similarly, the erythroid cell deficient in GATA1 knock-out mice (Pevny et al., 1991) and the absence of lymphoid cells in Ikaros knock-out mice (Georgopoulos et al., 1994; Nichogiannopoulou et al., 1999) demonstrated that GATA1 and Ikaros are key regulators in erythropoiesis and lymphopoiesis respectively.

Although a small number of “master” genes that control the development of different hematopoietic cells have been identified, recent studies from microarray analyses reveal that lineage differences extend to quantitative changes in the relative level of expression of most genes rather than absolute changes in the expression of a limited number of lineage-specific genes (Ivanova et al., 2002; Terskikh et al., 2003; Lambert et al., 2003; Bruno et al., 2004; Evans et al., 2004). Hence, the combination of biological experiments and math arithmetic can efficiently construct a molecular network of hematopoiesis, from which the transcriptional regulation mechanisms in different lineage specification can be elucidated fairly.

1.2 Zebrafish as a Good Model Organism

For centuries, powerful model organisms, such as nematode and fruit fly, have helped us to discover many biological and developmental events in cell-fate decisions, pattern formation and genetic pathways. However, there are still many remaining questions with

regard to chordate development could not be simply answered by these invertebrate animals. In recent years, the zebrafish (*Danio rerio*) has emerged as a new genetic model organism to help us decipher the miracles of life.

1.2.1 Advantages of Zebrafish

The zebrafish is a small vertebrate that is easy to raise and breed in the laboratory. Although about 30 years ago, the legendary zoologist, Curt Kosswig, proclaimed that "smaller fish species provide by far the best material, at least among the vertebrates, for studying inheritance" (Kosswig, 1973), it was until recently that this small animal became the adored "pet" for developmental and genetic research. Comparing to other vertebrate organisms, zebrafish has many features that can be easily exploited in the laboratory. Firstly, natural weekly mating generate large and synchronous batches of embryos that are fertilized externally, allowing them to be easily collected and analyzed with assays used in mutagenesis screens. Secondly, its embryonic development is spectacularly fast: it generates a typical vertebrate body plan, with a neural tube, muscles, a vascular system, and a beating heart, within 24 hours of fertilization. During this process, tissue formation and organogenesis can be visualized through the transparent fish body under the light microscope. Finally, the small size and the short time required for its sexual maturation (3-4 months) permit the large numbers of animals to be maintained in relatively small facilities. All these advantages make zebrafish a suitable model organism for genetic screening.

1.2.2 Genetic Screening

Genetic screening has long been a staple for identification of new genes that regulate embryogenesis and adult organ functions. Mutant analyses of model systems, such as *Drosophila* and *Caenorhabditis elegnas*, have helped us identify many key molecules in

different genetic pathways. However, these invertebrate model systems cannot be utilized to address the development and function of vertebrate-specific features such as kidney, multi-chambered heart, multi-lineage hematopoiesis, notochord and neural crest cells. Hence, zebrafish, as a vertebrate genetic model system, have born the important task of elucidating the vertebrate development.

1.2.2.1 Large-Scale Genetic Screening

In 1993, Nusslein-Volhard, the pioneer of modern genetic study of fly and zebrafish, planned to recapitulate the *Drosophila* screen using chemical mutagen N-ethyl-N-nitrosourea (ENU) for embryonic pattern mutations in a vertebrate at the Max Planck Institute in Tubingen, Germany (Haffter et al., 1996). At the same time, Mark Fishman established a parallel effort in Massachusetts General Hospital, USA (Driever et al., 1996). After 2 years of screening, ~2000 embryonic lethal mutant phenotypes were recovered between Tubingen and Boston. Along with the construction of zebrafish genome database and genetic linkage maps with the high-resolution of markers by the Sanger Center (UK) and National Institute of Health (USA), through positional and candidate cloning strategies, the cloning of these zebrafish mutant corresponding genes would be feasible and fast. In addition to chemical mutagenesis approach, insertional mutagenesis screens using a retroviral system have also been carried out by Nancy Hopkins (Amsterdam et al., 1999). More than 300 stable insertion lines have been isolated from this approach and most of their corresponsive genes are orthologs of those known to be critical in *Drosophila*, mouse or human development. Although the efficiency of retroviral-based insertional mutagenesis is relatively low compared to that of ENU mutagenesis, disrupted gene sequences could be easily and rapidly cloned by inverse-polymerase chain reaction (PCR) based sequencing, thus providing a new powerful screening method in zebrafish.

1.2.2.2 Specific "Target" Screening

The morphology-based screening can identify numerous mutants with defects during embryogenesis, whereas detailed developmental processes sometimes cannot be visualized just by eye. Hence, "target" screens have been created to dissect the particular developmental program or specific organogenesis. Examples are whole mount *in situ* hybridization (WISH)-based genetic screening have been conducted by us and others to isolate mutants in T-cell development and thymus organogenesis (Trede et al., 2001); mutants with non-morphology defects of the digestive organ were identified using a fluorescent reporter to visualize enzymatic activity in live embryos (Farber et al., 2001); and recently, through behavior screening that monitor behavior in response to a visual stimulus, Neuhauss *et al.* uncovered mutants with genetic disorder of vision (Neuhauss et al., 1999; Baier, 2000). Thus, by using these creative designs of genetic screening, we can understand particular aspects of vertebrate development in more depth.

1.2.2.3 Mutants as Human Disease Model

With elegant experimental designs and incessant endeavors, mutagenesis screens allow us to identify plenty of molecules involved in various developmental pathways. These mutants provide researchers with an array of resources to analyze different aspects of vertebrate embryonic development, and some also resembled human disease states, and thus served as a useful tool for investigating the corresponding pathophysiology. Till now, many zebrafish models for human diseases have been established, encompassing different disorders involved in many tissue and organ development, including hematopoiesis, cardiovascular genesis and kidney (Dooley and Zon, 2000). Recently, the generation of zebrafish p53 mutants also provides a unique platform to elucidate the genetic pathway in tumorigenesis (Berghmans et al., 2005). Hence, through the studies in mutants, the mechanisms of many biological events could be uncovered, and their

potential on clinical research may help us to find drugs or new therapy methods to treat these disorders in human.

1.2.3 Molecular Techniques

Along with the generation of mutants, subsequent positional cloning of the genes responsible for the phenotypes are just the first steps to identify the molecules that are involved in the developmental processes. Molecular techniques are essential for in-depth studies to elucidate the mechanisms behind these processes. As more and more developmental biologists switch their interests to zebrafish, many well-established techniques are adopted to this animal and some new approaches specifically for zebrafish have also been developed. All these advancement on technology allow the study of this model to be more comprehensive.

1.2.3.1 Microarray

Gene expression profiling is one of the most useful tools to identify new genes and pathways. Microarray techniques have been used for many years to fulfill the gene expression analysis. Recently, three different kinds of microarray chips, cDNA chip, oligo chip and Affymetrix chip, have been created for the study of zebrafish. Through the application of cDNA microarray, Lo *et al.* compared the gene expression profiles from six different embryonic stages and confirmed that the coordination of gene expression is important for myogenesis (Lo et al., 2003); whereas, our group and others used Affymetrix and oligo arrays to identify many novel hematopoietic and vascular related genes by comparing gene expression between wildtype and *cloche*, a hematopoietic deficient mutant (Qian et al., 2005; Sumanas et al., 2005; Weber et al., 2005). More fascinatingly, Weinholds *et al* identified tissue specific expressed microRNAs (miRNAs) by using microarray and inferred their functions in tissue differentiation and maintenance

(Wienholds and Plasterk, 2005; Wienholds et al., 2005). All these examples illustrate that microarray technology is a powerful tool to find new genes, to build up gene expression profile database, and in turn to delineate the molecular events in vertebrate development.

1.2.3.2 Morpholino "Knock-down"

As more and more novel genes are identified through microarray and genomic analyses, their roles in development remain obscure. Gene-targeting technology has been well established in mouse to study the functions of genes of interest. However, in zebrafish, such approach is not available due to the limitations in embryonic stem (ES) cell culture (Ma et al., 2001). Fortunately, targeted gene 'knockdown' strategy with antisense morpholino (MO) has provided an effective and specific way to transiently interfere with RNA processing or inhibit translation of individual genes in zebrafish. MOs are chemically modified antisense oligonucleotides that are stable *in vivo* and have base-stacking abilities similar to those of native RNA molecules (Summerton and Weller, 1997; Heasman, 2002). Since MO effects can last up to 10 days, the functions of the genes in early development can be evaluated through knockdown experiments (Nasevicius and Ekker, 2000). Furthermore, the synergetic or counteractive effects of different genes can be easily investigated by co-injecting two or more corresponsive MOs into a single embryo. Hence, the combination of using gene transcript microarrays to identify candidates and producing antisense molecules in zebrafish for functional screening of these candidates is a quick way to identify genes with central roles in vertebrate development. This strategy was neatly applied by Catherine Verfaillie and colleagues (Eckfeldt et al., 2005), who identified HSCs specific genes using human Affymetrix array and subsequently defined their functions by using MOs to knock down their orthologes in zebrafish.

1.2.3.3 TILLING

Although MO knockdown have been widely applied for the functional studies of zebrafish genes of interest and proved to be very specific, however, MOs may sometimes introduce non-specific phenotypes and conceal the real ones due to toxicity. Hence, in addition to this transient method, “targeting-induced local lesions in genes” (TILLING) has brought permanent gene inactivation to the zebrafish field (Wienholds et al., 2003). Like standard mutagenesis, the adult zebrafish is firstly mutagenized by ENU and served as founder fish to generate F1 progeny. In the F1 population, mutations on a specific “target” gene of interest can be identified by genomic sequence analysis. Through TILLING, it is possible to create an allelic series of mutations in a gene of interest to facilitate the identification of critical functional regions or to provide information about gene function in cases where a null allele is lethal. Using this approach, a series of 15 *rag1* mutations were found ranging from silent, intronic region to premature stop codon (Wienholds et al., 2002). A truncated protein produced by the premature stop was shown to be incapable to performing V(D)J recombination, suggesting that the C-terminal of the *rag1* gene is critical for its function. Despite other missense alleles of *rag1* mutants have not been well characterized, their hypomorphic features may be useful for genetic studies such as suppressor/enhancer screens.

1.2.3.4 Transgenic Fish

Transgenic approach is another powerful tool for the analysis of gene function during development. Microinjection of DNA constructs has been proven to be a reliable means of producing transgenic zebrafish. In the zebrafish, tissue-specific promoters driving the expression of the fluorescent reporter protein such as GFP (green fluorescence protein) or DsRed have been used to observe the dynamic regulation of gene expression in specific cell lineages of transparent living embryos. GFP transgene controlled by *gata1*

promoter helped us to monitor the erythroid cell early development (Long et al., 1997), and the *flk1* promoter driven GFP limned a beautiful frame of zebrafish blood vessels (Jin et al., 2005b). As hundreds of embryos can be microinjected within a single day, the temporal and spatial patterns of gene expression can be analyzed quite rapidly. Identification of regulatory elements on the zebrafish *scl* promoter demonstrated that transgenic fish is a very useful tool to find *cis* elements in promoter or enhancer study (Jin et al., 2005a). Other than cell fate mapping or promoter study, transgenic fish has also been used to create human disease models. Kalev-Zylinska *et al* transiently expressed human RUNX1-CBF2T1 transgene (product of the t(8;21) translocation in acute myeloid leukemia) in zebrafish embryos, resulting in disruption of normal hematopoiesis, aberrant circulation, internal hemorrhages and cellular dysplasia (Kalev-Zylinska et al., 2002). These phenotypes mimic the human leukemia caused by RUNX1 deficiency as a result of t(8:21) chromosome translocation. Conditional transgenic fish have also been created by using Cre-loxP system recently, in which the expression of cre is controlled by a heat shock promoter (Thummel et al., 2005). To avoid the early tumorigenesis in the rag2-EGFP-mMyc transgenic fish, Langenau DM *et al* generated the rag2-loxP-dsRED2-loxP-EGFP-mMyc transgenic fish, in which tumor can be induced only at the presence of Cre expression (Langenau et al., 2005). Hence, transgenic fish has emerged as one of the most important tools for developmental biology study.

1.2.4 Genomics and Zebrafish Community

Zebrafish has 25 chromosomes and its genome consists of approximately 15 billion base-pairs, compared to mammalian genome sizes of approximately 30 billion base-pairs. Although it is currently unknown how many genes there are in the zebrafish, based on the gene prediction program, the total number of zebrafish genes will be very close to the one expected for mammalian genomes. With the high homology between

zebrafish and human and mouse genes, studies from zebrafish provide a powerful means to elucidate the complexities of higher vertebrates' development.

1.2.4.1 Gene Duplication

During evolution, like many other fishes, the zebrafish undertook the genome duplication or large-scale gene duplication, which is commonly given as the explanation for the increase in complexity via the acquisition of new functions (Lynch and Conery, 2000). The best evidence for this duplication event is from the studies on Hox genes. The function of Hox genes is to specify cell fate in the anterior-posterior axis of animal embryos. Invertebrate chordates have one Hox cluster, but mammals have four, whereas, the discovery of seven Hox gene clusters in zebrafish (Amores et al., 1998), almost twice as many as human and mouse, suggests that genome duplication occurred just before the teleost radiation.

Although the gene duplication makes the analysis of zebrafish genes function more complicated, the diverse functions of one single gene that has multiple activities in mammals can be easily dissected. One example is the Flk1 gene, which plays an important role in the development of hematopoietic stem cells and vascular endothelium cells in mammal (Shalaby et al., 1995). An initial report of zebrafish *flk1* mutant showed that the *flk1* gene is essential for angiogenesis, but not for angioblast cell specification in zebrafish, suggesting differences in function compared to mammalian Flk1 (Habeck et al., 2002). However, recent work has shown that there is a second zebrafish ortholog of flk1 and introduction of the morpholino of this gene in the *flk1* mutant leads to a more complete loss of angioblasts analogous to the phenotype of Flk1-knockout mice (unpublished data, Schulte-Merker,S.). These two clusters of *flk1* gene allow us to define its miscellaneous functions in vasculorgenesis and angiogenesis, and also indicate that

the gene duplication of zebrafish genome is one of the unique features to help us define genes functions more scrupulously.

1.2.4.2 Genomic Database

As genomic information is very important for genetic mapping of mutants, the National Insititutes of Health (NIH) launched the Trans-NIH Zebrafish Initiative to map the zebrafish genome and develop other genomic tools (http://www.ncbi.nlm.nih.gov/genome/guide/zebrafish/index.html). Subsequently, the Wellcome Trust Sanger Institute initiated the zebrafish genome-sequencing project. With these continuous endeavors, to date, about 60% of the zebrafish genome has been fully sequenced. Combined with expeditious increment of expression sequence tags (ESTs) and full-length clones, these genome sequence information are assembled and a very comprehensive zebrafish genomic infrastructure in Ensembl (http://www.ensembl.org/Danio_rerio/index.html) is built (Ashurst et al., 2005). Recently, this sequencing project is expanded to Zebrafish Models for Human Development and Disease (ZF-MODELS) project (Bradbury, 2004), whose aim is to combine the advantages of the zebrafish in developmental biology with recent advances in functional genomics and with the zebrafish genome sequence to harvest large data sets on gene functions. This project provides us invaluable knowledge and avant-garde technology to create disease models, to explore the pathways of gene regulation and also to discover drug targets applicable to human diseases. All the information, including genomic sequences, mutants and newly developed expression pattern database, can be accessed from the online zebrafish information center, http://zfin.org (Sprague et al., 2001). The website provides not only the prolific information about zebrafish but also serves as a unique platform to share and exchange experiences among researchers in the zebrafish community.

1.3 Hematopoietic Study in Zebrafish

The zebrafish offers a unique opportunity to discover and study novel genes required for the control of normal vertebrate hematopoiesis. This lower vertebrate is a more accessible model than the higher organisms as blood formation is established within 24 hr and circulating blood cells can be visualized under the light microscope. In addition, unlike the early lethal phenotypes of most blood deficient mutants in mouse, the bloodless mutants in zebrafish can survive for more than 7 days and develop quite normally in other non-hematopoietic tissues, providing good exemplars to specifically study the blood formation during early vertebrate development.

1.3.1 Hematopoiesis Program in Zebrafish

The hematopoiesis program is highly conserved during evolution. In zebrafish, this blood formation process can produce all kinds of blood cells, including the cells of the erythroid, thrombocytic, myeloid, and lymphoid lineages (Figure 1.1). Like other vertebrate models, the zebrafish also have two waves of hematopoiesis, the primitive and definitive hematopoiesis, which contribute to the embryonic blood cells formation and adult blood cells formation. In addition, the orthologues of the most critical mammalian hematopoietic transcription factor genes have been identified in zebrafish (Figure 1.2). Given the extensive similarities in hematopoiesis between zebrafish and mammals, an understanding of blood cell development from zebrafish provides insights into the ontogeny of hematopoiesis program in the higher vertebrates.

1.3.1.1 Primitive Hematopoiesis in Zebrafish

As we have discussed in section 1.1.2, the primitive hematopoiesis occurs in the extra-embryonic yolk sac in mammals and birds. In contrast, the primitive hematopoiesis in zebrafish is found in two intra-embryonic locations: the intermediate cell mass (ICM)

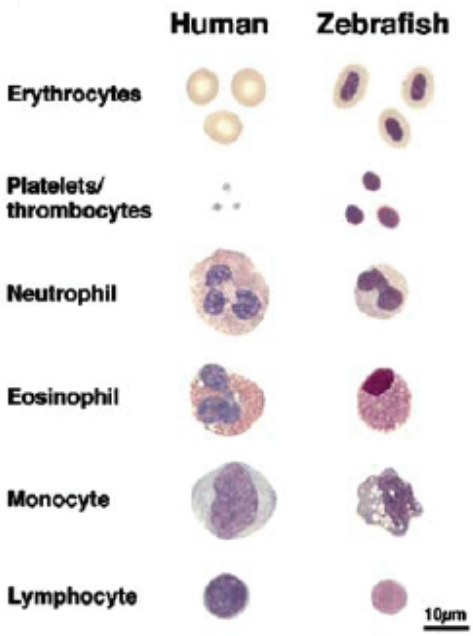

Figure 1.1 Comparison of Human and Zebrafish Mature Peripheral Blood Cells Stained with Wright Giemsa. (Adopted from Davidson and Zon, 2004)

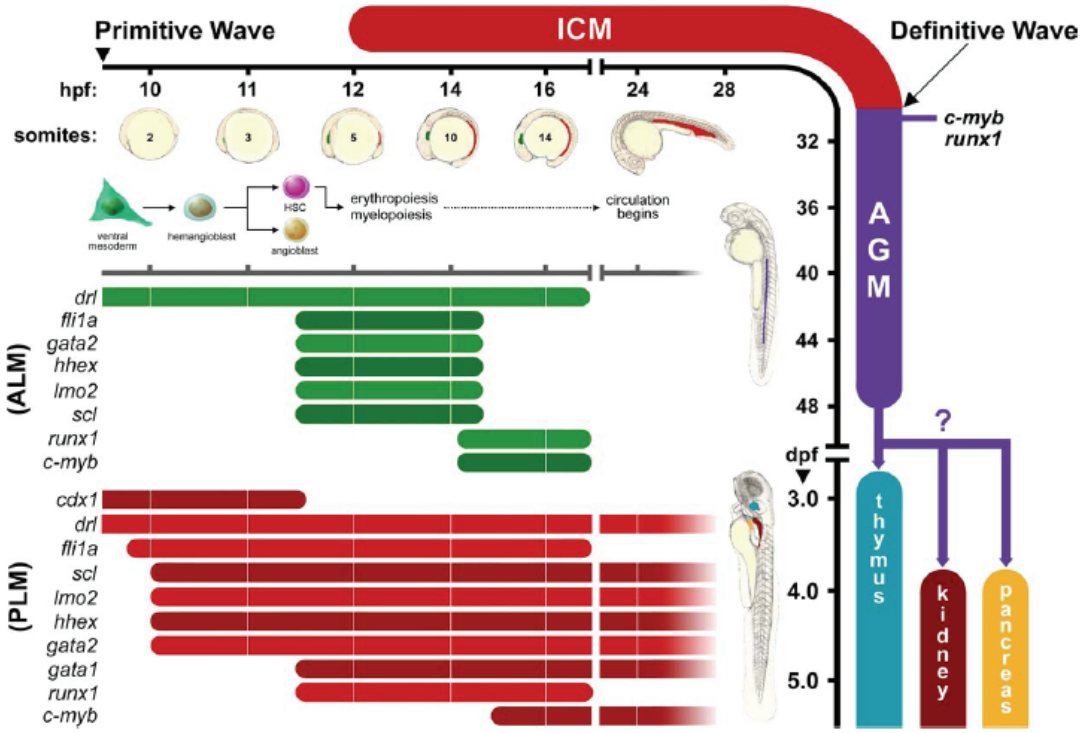

Figure 1.2 Hematopoietic Program in Zebrafish. (Adopted from Hsia and Zon, 2005) ALM: anterior lateral mesoderm; PLM: posterior lateral mesoderm; AGM: aorta-gonads-mesonephros; ICM: intermediate cell mass.

located in the trunk ventral to the notochord, and the rostral blood island (RBI) arising from the cephalic mesoderm. The origin of the ICM cells is the bilateral stripes of cells in the posterior mesoderm. At around 18 hours post fertilization (hpf), these mesoderm derived cells migrate to the trunk midline and differentiate into “primitive” proerythroblasts and endothelial cells of the trunk vasculature. Concurrently, the embryonic myeloid cells appear in the second anatomical site of primitive hematopoiesis, the RBI region (de Jong and Zon, 2005).

Many orthologues of the transcription factors that are involved in mammalian hematopoiesis are found in zebrafish. Gene expression analyses indicate that their temporal and spatial expression patterns are comparable to their mammalian counterparts. In zebrafish, the stem cell leukemia (*scl*) gene has been demonstrated to be a vital factor for the formation of HSCs and angioblasts (Dooley et al., 2005; Patterson et al., 2005). At 2-somite stage, the first primitive hematopoietic progenitors are marked as bilateral stripes with *scl* expression in the posterior mesoderm. At the same time, these cells also co-express *lmo2, gata2* and *fli1a*, supporting the fact that these factors form a multimeric complex and regulate the blood and vascular formation in an interactive way (Valge-Archer et al., 1994; Wadman et al., 1997). The presence of this complex in RBI at 3~5-somite stage suggests the idea that the common spatial and temporal characteristics of blood and vascular development are features shared by both rostral (RBI) and caudal (ICM) sites of hematopoiesis. One interesting question is whether these early *scl*$^{+}$ cells are hemangioblast cells or they are heterogenic cells comprising both HSCs and angioblasts. Although many factors are co-expressed in these cells, the answer for this question is still controversial.

At about 4-somite stage, a subset of *scl*$^{+}$ cells express erythroid-specific transcription factor *gata1*(Detrich, III et al., 1995). These first committed erythroid cells differentiate sequentially in a rostral to caudal direction. The number of these *gata1*$^{+}$ erythroid

precursors increases as they migrate towards the midline. By the time blood circulation begins between 25-26 hpf, the ICM is comprised of at least 300 proerythroblasts (Long et al., 1997) that express genes required for red blood cell function and membrane stability, such as embryonic *globin* genes, *urod* and *band3* etc (Wang et al., 1998; Brownlie et al., 2003; Paw et al., 2003). Over the next 4 days, the circulating proerythroblasts synchronously mature into flattened elliptical erythrocytes, but they are clearly distinguishable from adult zebrafish erythrocytes that have a characteristic large elongated nucleus and smaller amount of cytoplasm. The first cluster of ICM-derived blood cells persists as the only circulating cells for at least 4 days. This result is demonstrated by transfusion of fluorescently labeled blood cells from 36hpf donor embryos into the sinus venosus of the recipient embryos (Weinstein et al., 1996). The proportion of blood cells in the circulation which are contributed by the donor does not decline significantly until approximately 6dpf. After 5dpf, both the proportion and number of donor blood cells decline gradually, reaching approximately 50% of their starting values by 10 dpf. At 10 days, labeled transfused erythrocytes are noticeably smaller in size than many unlabelled erythrocytes, indicating the emergence of a morphologically distinctive new erythrocyte cell population. These results indicate that primitive erythrocytes are a single population of blood cells originating from the ICM, which are formed and matured during the first 5 days of development in zebrafish embryos.

The first macrophages are identified in the lateral mesoderm of the head at the 3-somite stage (Herbomel et al., 1999; Bennett et al., 2001; Lieschke et al., 2002). Like erythroid cell differentiation in the ICM, the development of myeloid cell in the RBI is also marked by some myeloid-specific factors. At 11~15-somite stage, a subset of these anterior cells expresses *pu.1*, a member of the ETS family of transcription factors essential to the development of myeloid cells (Lieschke et al., 2002). This subset of *pu.1*$^{+}$ cells represents the early myeloid cells, including macrophages and granulocytes, which

migrate rostrally and then laterally across the yolk sac around 22-24 hpf. Although *pu.1* expression levels in these macrophage precursors decline after the 18-somite stage, additional molecular markers including *c/ebp1, fms, l-plastin,* and *lysozyme-c* are expressed at this time (Herbomel et al., 1999; Bennett et al., 2001; Lyons et al., 2001; Herbomel et al., 2001; Liu and Wen, 2002; Lieschke et al., 2002). These early macrophages has been observed to be in action as early as 26 hpf in the ducts of Cuvier, where macrophages can be seen 'interrogating' and engulfing apoptotic erythroblasts from bloodstream (Herbomel et al., 1999). These macrophages express *l-plastin* and are distributed throughout the embryo by 28-32 hpf. Primitive immune function of macrophages is also evident as they migrate to the site of an infection with *Escherichia coli* or *Bacillus subtilis* and phagocytose the offending organisms, and they can clear microinjected carbon particles from the circulation as early as 2 dpf (Herbomel et al., 1999; Lieschke et al., 2001). Another population of RBI-derived myeloid cell is the granulocyte. The expression of the granulocyte-specific marker myeloperoxidase (*mpo*/*mpx*; encoding an enzyme abundant in the granules of mature neutrophils and eosinophils) is first detected at 18 hpf in presumptive neutrophilic precursors within the caudal ICM and co-localized with some *pu.1*$^{+}$ myeloid progenitors (Bennett et al., 2001). Soon after this stage, *mpo*$^{+}$ cells also appear scattered on the anterior yolk sac. Although very few *mpo*-expressing cells co-localize with *l-plasin,* consistent with these two populations representing distinct granulocyte and macrophage lineages, both of these two markers are also expressed in the caudal ICM region, indicating that the ICM also gives rise to a small population of myeloid progenitors.

1.3.1.2 Definitive Hematopoiesis in Zebrafish

The definitive HSCs in mammals are first identified in the intra-embryonic AGM region. In zebrafish, the AGM counterpart is also found in the ventral wall of the dorsal aorta,

where definitive HSCs marker gene *runx1* is expressed between 24~48 hpf (Kataoka et al., 2000; Burns et al., 2002; Kalev-Zylinska et al., 2002). The expression of other transcription factors including *c-myb*, *ikaros*, *lmo2*, and *scl* also support the hypothesis that these AGM-derived cells are definitive HSCs (Thompson et al., 1998). Around 4~5 dpf, the location of blood formation shifts to the kidney where the lifelong definitive hematopoiesis is established (Willett et al., 1999; Galloway and Zon, 2003). In the adult zebrafish, hematopoietic cells are found intercalated between the renal tubules in the kidney marrow, much like mammalian adult hematopoiesis that takes place in and around the fat and stroma of the bone marrow. Like mammals, the zebrafish definitive hematopoiesis also gives rise to all the erythroid, thrombocytic, myeloid, and lymphoid lineages (Traver et al., 2003b).

The definitive erythropoiesis is postulated to begin around 5dpf, as the recovery of circulating red blood cells in primitive erythropoiesis deficient mutant *bloodless* is around this stage (Liao et al., 2002). Like other higher vertebrates, globin switching from primitive embryonic globin chains to the adult globin chains is the hallmark of definitive red blood cell formation (Chan et al., 1997; Brownlie et al., 2003). The zebrafish thrombocytes are nucleated blood cells equivalent to mammalian platelets, which function to maintain hemostasis by facilitating clot formation (Jagadeeswaran et al., 1999). Although the ontogeny of these thrombocytes is not well understood, the adhesion and aggregation of these cells in response to ristocetin, collagen, thrombin, ADP, and arachidonic acid suggest that they have similar function as mammalian platelets (Hill and Rowley, 1996; Jagadeeswaran et al., 1999; Gregory and Jagadeeswaran, 2002). At 7dpf, myeloblasts and neutrophilic granulocytes are readily observed within the pronephros. At this time, both macrophage marker *lysozyme-c* and granulocyte marker *mpo* are expressed in these myeloid progenitor cells (Willett et al.,

1999; Liu and Wen, 2002), however, whether these cells are from primitive myeloid cell or they are representation of a second wave of myelopoiesis is still largely unknown.

The most significant difference between primitive and definitive hematopoiesis is the evidence of lympoid lineage cells. In zebrafish embryos, a combination of histological and gene expression analyses have identified the thymus, pancreas, and pronephros as sites of lymphopoiesis. Like mammals and other vertebrates, zebrafish possess an adaptive immune system containing T and B lymphocytes. The T cell maturation takes place in the zebrafish thymus, as it does in mice and human. The pharyngeal epithelium between the third and fourth pharyngeal pouches outgrowth form the bilateral thymic primordial, where the first immature lymphoblasts are populated around 65 hpf (Willett et al., 1997a; Willett et al., 1997b; Willett et al., 1999). The origin of the lymphoid progenitors that first populate the thymus rudiment is not known. Given the timing when these cells appear, their progenitors must not originate in the kidney marrow, because HSCs are not found there until 5-6 dpf. In mouse, the T-cell precursors originate from the splanchnopleural mesoderm (from which the AGM region is derived), thus, it has been proposed that in zebrafish, the lymphoid progenitors that seed the thymus descended from AGM-HSCs generated between 24 and 48 hpf. This hypothesis is supported by the evidence that *ikaros*-expressing cells can be detected both in the AGM region as well as throughout the pharyngeal arches at 48 hpf (Willett et al., 2001). Relative to T lymphopoiesis, B-cell formation initiates later in zebrafish development. The first immunoglobulin (Ig) gene rearrangements are detected by polymerase chain reaction (PCR) at 4 dpf, whereas transcripts for the membrane form of IgM appear at 7 dpf. Whole mount *in situ* hybridization of *rag1* genes shows that the initial site of B lymphopoiesis is likely to be the region of the pancreas primordium of 4 dpf larva (Danilova and Steiner, 2002). However, lymphocytes labeled with GFP are not detected in the pancreas of larval *rag2*^{gfp} or *lck*^{gfp} transgenic zebrafish (Langenau et al., 2004).

While the reason for this discrepancy is unknown, it is clear that the pronephros becomes an active and major site for B lymphopoiesis starting at 19 dpf, consistent with its role as the mammalian bone marrow equivalent (Danilova and Steiner, 2002).

1.3.2 Methods of Studying Hematopoiesis in Zebrafish

As we have discussed in section 1.2.3, while the forward and reverse genetic methods have been widely employed on hematopoiesis study in zebrafish, recent methodological advances on cell sorting and transplantation intensively enhance the hematopoiesis study in zebrafish. These techniques provide means to evaluate the cell autonomous requirement of mutant genes, assay of leukemic transformation, test for HSC activity, and to examine cell migration and homing.

In mouse, cell sorting is the most important advancement for comprehensive understanding of the hierarchical development of blood cells. Recently, Traver D. and colleagues successfully applied this technique to isolate the major blood lineages from whole-kidney marrow (WKM) in zebrafish (Traver et al., 2003b). Using combined profiles of forward scatter (FSC, cell size) and side scatter (SSC, cellular granularity), the blood cells can be separated into 4 groups: mature erythroid cells, myelomonocytic cells, lymphoid cells and immature precursors. Although the lack of specific antibodies for different lineages markers in zebrafish prevent further classification of these cells, the generation of transgenic fish under gene specific promoters allow us to isolate different blood lineage cells in detail. Analysis of WKM isolated from transgenic zebrafish expressing enhanced GFP (EGFP) under the control of *gata2* promoter showed that the GFP^+ cell are predominantly myeloid cells, further morphological analysis revealed that the majority of these cells are eosinophils. Similarly, lymphocytes and erythrocytes have been isolated from $rag2^{eGFP}$ *and* $gata1^{eGFP}$ transgenic fishes, respectively. The isolation of different lineage cells by cell sorting not only differentiate erythroid, myeloid and

lymphoid cells in normal wildtype fish, but also provides cell biology evidence to characterize hematopoietic cells in mutants. The blood mutant *retisna* (*ret*) has mutation in the gene, *anion exchanger 1* (*slc4a1*) (Paw et al., 2003). It presents the phenotype of gradual decrease in blood counts throughout the larval stages as a result of failure in membrane integrity. Cell sorting on heterozygous *ret* mutants displayed mild anaemia with a concomitant twofold increase in the precursor scatter population. Further sorting of the precursor fraction showed predominance of immature erythroid cells. This observation indicates the erythrocytes require a full dosage of *slc4a1* for normal development. Cell sorting also provides the opportunity to generate lineage specific cDNA libraries, when combined with microarray technology, can define the molecular signatures of different hematopoietic cells (Traver et al., 2003a).

With the establishment of cell sorting techniques, the hematopoietic cell transplantation, an important clinical and research approach used in other vertebrate hematopoietic studies, has also been developed in zebrafish. In the embryos of zebrafish *gata1* mutant *vlad tepes*, transplantation of wild-type kidney marrow cells (carrying a $gata1^{gfp}$ transgenic reporter) is sufficient to rescue a small fraction of mutants for at least 8 months (Traver et al., 2003b). To assess the distribution of HSCs in WKM, Traver *et al* transplanted the lymphoid, erythroid, precursor and myeloid fraction of WKM in $gata1^{eGFP}$ transgenic fish into wildtype 48hpf embryos and revealed that only the lymphoid fraction contains long-term reconstituting HSCs and is capable of long-term $EGFP^{+}$ erythrocyte generation within 6 months time after transplantation. In addition, Langenau *et al* recently discovered the homing properties of zebrafish lymphocytes using the lck^{gfp} transgenic fish (Langenau et al., 2004). Transplantation of lck^{gfp} cells from adult kidney marrow into 2dpf embryos allowed the visualization of T-cell homing to the thymus by 3 days of age, indicating the embryonic thymus expresses receptors or chemoattractants that facilitate the migration of mature T cells to the thymus. Hence, the combination of

cell sorting and transplantation provide a useful tool to dissect the developmental processes of different hematopoietic lineage cells and their functions in the normal hematopoiesis as well as in the diseased condition.

1.3.3 Hematopoietic Mutants and Disease Model

Genetic screenings in zebrafish have generated many mutants with hematopoietic defects. To date, more than 40 mutants, consisting of 26 complementation groups, are identified in the large-scale chemical mutagenesis screenings in Boston and Tubingen (Weinstein et al., 1996; Ransom et al., 1996). These mutants were initially identified by the absent or decreased blood circulation in early embryos and were later characterized by the gene expression analysis of known hematopoietic transcription factors, such as *gata1* and *scl*. These mutations fall into three groups: HSCs deficient mutants, early erythroid development mutants and late stages erythroid mutants. Many of these mutants represent models of human disease.

1.3.3.1 HSCs Mutants

There are three mutants in this group: *cloche* (*clo*), *spadetail* (*spt*), and *kugelig* (*kgg)*. The *clo* mutant was initially identified because of the enlarged heart and lack of blood circulation after 24hpf (Stainier et al., 1995). Further histology and gene expression analyses showed that the endocardium and all blood lineage cells are lost in this mutant, whereas adjacent tissues formed normally, indicating that the *clo* defect is specific to the hematopoietic and vascular lineages, most likely, the hypothetical hemangioblast cells (Liao et al., 1997; Thompson et al., 1998; Liao et al., 1998). As the *clo* gene is located at the telomere, the positional cloning of the corresponding gene has not been fulfilled yet. The second mutant, *spt,* is caused by a defect in *tbx16*, encoding a T-box transcription factor (Griffin et al., 1998). In *spt*, at gastrulation stage, the cells that would normally

contribute to the trunk somites accumulated in the tailbud instead, indicating the *tbx16* gene is involved in regulating proper cell migration during gastrulation. Although the RBI-derived myeloid cells and pronephric duct precursors are relatively normal, the absence of erythroid cells suggested defects in ICM-HSCs in *spt* mutants (Thompson et al., 1998; Oates et al., 1999). The *kgg* mutant was first characterized by a shortened tail and reduced yolk tube extension (Haffter et al., 1996; Hammerschmidt et al., 1996). Similar to *spt* mutant, the *kgg* embryos are severely anaemic and hematopoietic defects are also seen in the ICM-derived erythroid cells but not in RBI-derived myeloid cells. Through positional cloning, the corresponsive gene for *kgg* is *cdx4*, which belongs to the *caudal*-related homeobox transcription factor family (Davidson et al., 2003). In vertebrates such as mouse, frog and chick, members of the *cdx* family have been implicated in AP patterning of the embryonic body axis by acting as 'master regulators' of the *Hox* genes, another family of homeobox transcription factors (Lohnes, 2003). In the *kgg* mutant, *hox* genes expressed in the anterior trunk exhibit expanded expression domains towards the posterior, while more caudally expressed *hox* genes are reduced or absent expression. Concomitant with these perturbations in *hox* expression domains, there is a severe reduction in ICM-HSCs but not in the adjacent angioblasts population. These observations suggest an additional and more specific requirement for *hox* genes in the specification of ICM-HSC fate (Davidson et al., 2003).

1.3.3.2 Early Bloodless Mutants

Mutants in this group include *vlad tepes* (*vlt*), *moonshine* (*mon*) and *bloodless* (*bls*), which possess defects in the development of erythroid progenitor cells. Mutation in *vlt* corresponds to the well-known erythroid-specific transcription factor *gata1* (Lyons et al., 2002). Like gata1 knockout mouse (Pevny et al., 1991), *vlt* retains normal hematopoietic progenitors, myeloid cells and lymphoid cells. However, the lack of functional *gata1*

makes the hematopoietic progenitors unable to differentiate down to the erythroid lineage. This phenotype strongly suggests that the *gata1* gene is specifically involved in both primitive and definitive erythroid cell differentiation. Mutations in the *mon* mutant cause a disruption in both primitive embryonic and definitive adult hematopoiesis, resulting in a severe loss of erythroid cells (Ransom et al., 1996). Although the erythroid progenitor cells in *mon* mutants are initially present, they fail to express normal levels of hematopoietic transcription factors and eventually undergo apoptosis. Transplantation studies showed that the defects in *mon* mutants are in a cell-autonomous manner during the differentiation of erythroid precursors. Ultimately, positional cloning revealed that the *mon* gene encodes the zebrafish orthologue of the mammalian transcriptional intermediary factor 1 γ (TIF1γ) (Ransom et al., 2004). The last mutant *bls* was originally isolated as a spontaneous mutation and was inherited in an autosomal dominant fashion with incomplete penetrance (Liao et al., 2002). The mutant embryos have no visible circulation until approximately 5 dpf when hemoglobinized cells begin to appear, coincident with the onset of definitive hematopoiesis. In *bls* adult, the kidney marrow hematopoiesis appears normal, indicating that only primitive erythropoiesis is affected. Cell transplantation experiments showed that cells derived from *bls* mutant donors can differentiate into blood cells in a wild-type host, but wild-type donor cells fail to form blood in the mutant host. These observations demonstrate that the *bls* gene product is uniquely required in a non-cell autonomous manner for primitive hematopoiesis. Given that *bls* is the only primitive hematopoietic deficient mutant in the vertebrate, positional cloning of *bls* corresponding gene will provide us indispensable information in the understanding of the difference between primitive and definitive hematopoiesis in vertebrate development.

1.3.3.3 Late Stage Erythrocyte Mutants

While the above two groups of zebrafish hematopoietic mutant help us to comprehend the nature of blood development from the initial HSCs to the final lineage cells, the mutants in this group establish some very useful disease models that mimic the human anaemia. Based on the different types of human anaemia, these mutants can be classified into three categories: hemolytic anaemia, hypochromic anaemia and erythropoietin porphyria. The hemolytic anaemia mutants, including *cabernet* (*cab*), *chablis* (*cha*), *grenache* (*gre*), *merlot* (*mot*), *riesling* (*ris*), *retsina* (*ret*) and *thunderbird* (*tbr*), have a phenotype of decreasing number of blood cells after apparently normal blood development in the first 2 dpf (Ransom et al., 1996; Weinstein et al., 1996). The progressive anaemia phenotype of these mutants suggests that these mutations affect the erythroid cell expansion or the stability of mature red cells. Most of the corresponsive genes for these mutations have been cloned and their functions are found to be involved in the construction of red blood cell framework, such as maintenance of membrane structure (*mot, cha* and *ris*) (Liao et al., 2000; Shafizadeh et al., 2002) and segregation of chromosome (*ret*) (Paw et al., 2003). These results indicate that the main reason of human hemolytic anaemia is instability of red blood cell cytoskeleton. In the second category, mutants such as *chardonnay* (*cdy*), *chianti* (*cia*), *clear blood* (*clb*), *frascati* (*frs*), *sauternes* (*sau*), *weissherbst* (*weh*), and *zinfandel* (*zin*), are shown to have hypochromic microcytic anaemia characterized by a reduced number of primitive erythrocytes, which are pale and small in size (Ransom et al., 1996; Weinstein et al., 1996). This phenotype indicates that the defect lies in the production of hemoglobin. Genetic identification of these mutations revealed that the corresponsive genes for these mutants are involved in different processes of hemoglobin production, including regulation of iron metabolism (*weh*, *cdy* and *cia*) (Donovan et al., 2000; Donovan et al., 2002; Wingert et al., 2004) and

the *de novo* synthesis of heme and globin (*sau* and *zin*) (Brownlie et al., 1998; Brownlie et al., 2003). The last category of photosensitive mutants consists of *dracula* (*drc*), *desmodius* (*dsm*), *freixenet* (*frx*), and *yquem* (*yqe*) (Ransom et al., 1996; Weinstein et al., 1996). These mutants produce normal numbers of erythrocytes, but the cells autofluoresce and lyse when exposed to ambient light. This phenotype is analogous to the human congenital erythropoietic porphyries, which is due to defects in heme biosynthesis pathway. The genes responsible for mutants *yqe* and *drc* have been positional cloned as *uroporphyrinogen decarboxylase* (*UROD*) (Wang et al., 1998) and *ferrochelatase* (Childs et al., 2000), respectively.

1.3.3.4 Transgenic Fish As Disease Models

Other than using mutants as disease models, the transgenic approach can be used to simulate some hematopoietic disease, e.g. leukemia. In addition to chromosome translocation model in RUNX1-CBF2T1 transgenic zebrafish (section 1.2.3.4), Langenau *et al.* generated a transgenic model of Myc-induced T-cell acute lymphoblastic leukemia (T-ALL) (Langenau et al., 2003). The zebrafish *rag2* promoter was used to drive lymphoid expression of murine *c-Myc*, an oncogene known to participate in the pathogenesis of mammalian lymphoid malignancies. Approximately 5% of the F0 founder fish developed lymphoblastic leukemia with aggressive infiltrations in the intestine, gills, skeletal muscle, and fins within 30-131 days. To further aggrandize the study of this disease model, *rag2-myc* transgene was injected into *rag2gpf* transgenic embryos, and then these fluorescent labeled leukemia cells can help us visualize the disease onset and the spread of lymphoblasts from the thymus in living animals. In addition, this inducible line of leukemia-prone fish can be used as founder to perform “second-hit” screening to find mutations that influence the development of the leukemic

phenotypes, as well as to provide a resource for the discovery of compensating mutations or chemicals that would prevent leukemia development.

1.4 Objective of the Study

We took advantage of zebrafish as a good vertebrate model system to study the early development of hematopoiesis. Both genetic and functional genomics approaches have been conducted to identify key molecules in this program. Firstly, we carried out forward genetic screen using T-cell specific gene *rag1* as a marker. Through this *in situ* based screen, we hoped to identify genes involved in T-cell early development and thymus organogenesis. Secondly, we used microarray techniques to compare the gene expression profiles between wild-type and zebrafish early hematopoietic and vasculature deficient mutant *cloche.* The affected genes identified from microarray analysis could help us decipher the molecular pathways in the early hematopoiesis.

Chapter II: Material and Methods

2.1 Zebrafish

2.1.1 Fish Maintenance

Zebrafish (*Danio rerio*) AB strain obtained from Tubingen was used as wild-type line for daily crossing and mutagenesis. Fish were maintained in central fish facility in IMCB according to standard methods described by Westerfield (Sprague et al., 2001).The *clo*^{s5} allele and *flk1* promoter driven EGFP transgenic fish were generously provided by Dr. Didier Y. R. Stainier (Jin et al., 2005b). The *mon*^{tg234} was kindly provided by Artemis Pharmaceuticals GmbH (Germany).

2.1.2 Stages of Embryonic Development

For developmental studies, the accurate staging of the embryos is very important for defining the timing of various developmental events. To obtain synchronized embryonic stages of zebrafish embryos, male and female fish were separated by a divider in the crossing tank the day before crossing day. On the morning of the crossing day, the divider was removed to let the male and female fish mate. The fertilized eggs were collected in a petri dish containing egg water (0.03% sea salt in distilled water) 15 min after the female fish started to spawn and raised at 28.5°C. The desired stages were determined under stereomicroscope (LEICA) according to Kimmel's description (Figure 2.1, Kimmel et al., 1995).

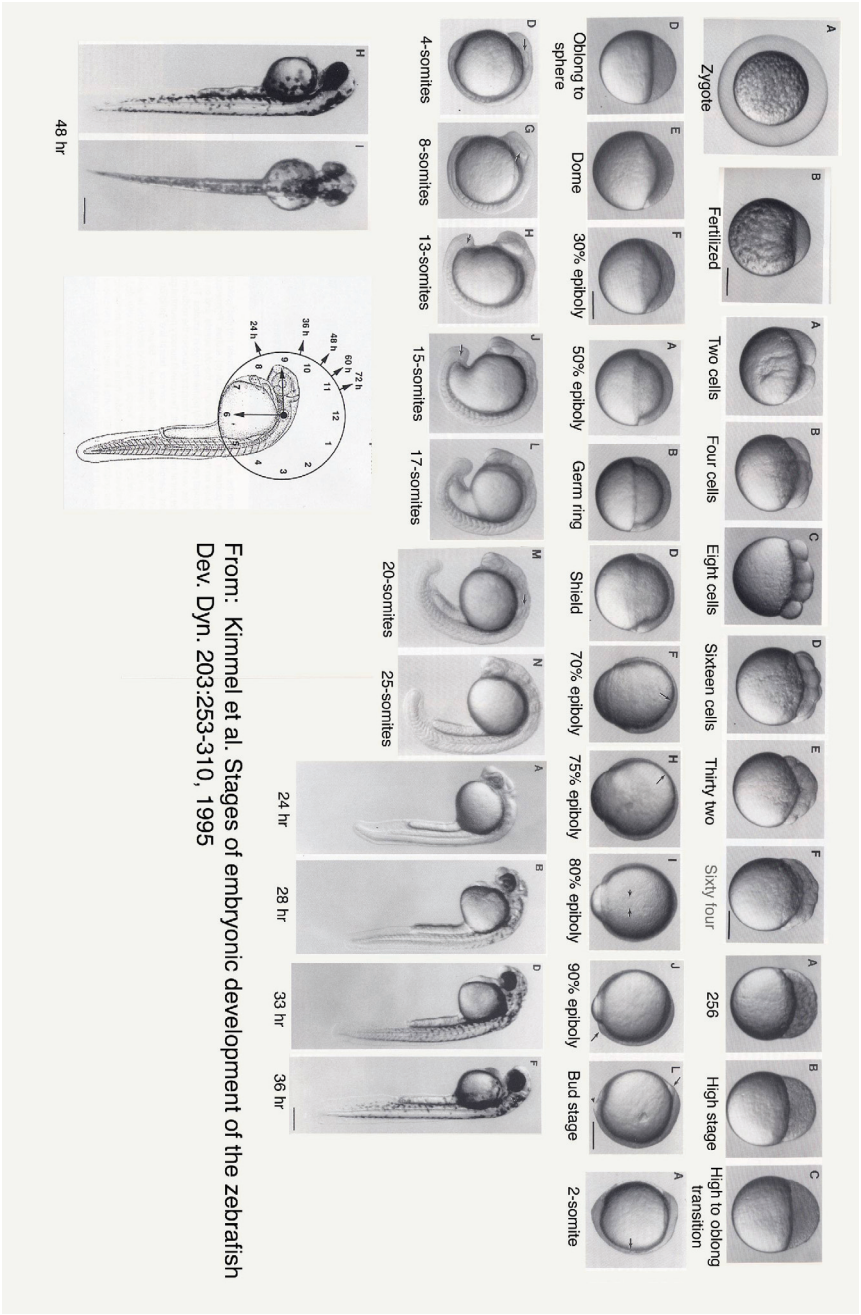

Figure 2.1 Stages of Embryonic Development of the Zebrafish. (Adopted from Kimmel et al., 1995)

2.1.3 General Manipulation for Zebrafish

2.1.3.1 Microinjection

The samples for injections were diluted in nuclease-free water to the desired concentration. Equal volume of phenol red (0.1% in DPBS, Sigma) was mixed with the injection sample to facilitate monitoring of the injection process. Before 1 cell stage, 0.5-1nl of each sample was injected into the middle of embryo yolk by using gas microinjector (PLI-100, HARVARD APPARATUS). The injected embryos were then raised in incubator at 28.5°C.

2.1.3.2 Whole Embryo Staining for *Globin* Expression

o-Dianisidine staining was used to study the expression of hemoglobin (Detrich, III et al., 1995). Live embryos after 36 hrs post-fertilization (hpf) were dechorionated by pronase (0.5mg in 1ml egg water) treatment, followed by a brief wash in phosphate buffered saline (PBS, 58mM NaH_2PO_4, 2.7mM KCl, 10.1mM Na_2HPO_4, 1.8mM KH_2PO_4). The embryos were then placed in the staining buffer, which contains *o*-dianisidine (0.6mg/ml), 0.01M sodium acetate (pH 4.5), 0.65%H_2O_2, and 40% (v/v) ethanol, in dark for 15 min. The *o*-dianisidine staining was then observed under the light microscope.

2.1.4 Genetic Screen in Zebrafish

2.1.4.1 ENU Mutagenesis

The mutagenesis process was carried out with chemical mutagen ENU according to the standard protocol with minor modifications (Mullins et al., 1994; Solnica-Krezel et al., 1994). Male fish were crossed with females the night before mutagenesis. The male fish that gave fertilized offsprings were selected and transferred to a 5-liter container with fish water (50% tap water, 50% RO water) at 22°C in the morning. 6 to10 fishes were placed

in an 800ml plastic cylinder with fine mesh bottom, and then dunked in 300ml of ENU working solution (3mM ENU in 10mM sodium phosphate buffer) at 22.5°C. After one hour's treatment, the fish were transferred to the cylinder with fresh fish water and left for 6 hr before transferring into a 5-liter container with 28°C fish water for the night. This process was repeated 3 times within 1 to 3 weeks. The ENU working solution were mixed with equal amount of 2X inactivation solution (20% sodium thiosulfate, 1% NaOH) and incubated overnight to inactivate the ENU before discard.

2.1.4.2 Generation of F1 and F2 Family

The ENU treated male fish were mated with untreated female fish two days following the last mutagenesis treatment. These male fish were unable to produce viable embryos. They need to be out-crossed at least twice before they can produce normal embryos weekly. These mutagenized males (F0) that were able to produce fertilized embryos were selected and out-crossed with wild-type females to generate F1 fish. Each F0 male generated about 100 F1 progeny. When the F1 fish matured, siblings were mated with each other to raise the F2 families. Each F2 families consisted of at least 40 fish. After the generation of F1 fish, the F0 male fish were stored at -70°C to preserve their DNA for positional cloning in the future.

2.1.4.3 *rag1* Screen

The F2 fish matured after about 3-4 months and could be used to set up in-cross for F3 screening. Ideally, each F2 family should have about 10 successful crosses. On Mondays and Thursdays of the week, approximately 200 pairs of fish from different F2 families were mated. Embryos from successful crosses were collected on the next day and the F2 parents were maintained in the system in each individual tank with appropriate tracking number. The dead embryos were removed next morning and the

egg water was changed to PTU water (0.003% 1-phenyl-2-thiourea in egg water) to prevent pigmentation. After 4 days, about 40 surviving embryos from each cross were subjected to whole mount *in situ* hybridization (WISH) using *rag1* as a probe in specially designed boxes (Figure 2.2A, see section 2.4.2). A F2 pair was selected as potential mutant candidate should about one quarter of the embryos have dramatic decrease or negative *rag1* signal. Each mutant was re-confirmed by repeating the WISH at least twice.

2.2 General DNA Application

2.2.1 PCR and Cloning

To examine the expression pattern of Affymetrix target genes, we generated clones with partial sequences of responsive genes based on Affymetrix target sequence. First strand cDNA was synthesized from 1μg of 18hpf or 24hpf fish total RNA by using oligo dT as primer. The synthesized cDNA template was then diluted 2.5 times with 1X TE (10mM Tris.HCl, 1mM EDTA). PCR reactions were performed using 2μl of the diluted cDNA template in 25μl reactions containing 200nM of forward and reverse primers (Table 2.1A), 200μM of each dNTPs, 1X Advantage2™ buffer ,0.5μl Advantage2™ polymerase (Clontech) and sterilized double distilled water (DDW). Thermocycling parameters consisted of an initial denature step of 1 min at 94°C followed by 30 or 35 cycles of 94°C for 5 sec, 58°C for 10 sec, 72°C for 1 min and a final extension of 10 min at 72°C. The PCR products were analyzed on 1% agarose gel (Invitrogen) and subsequently ligated into T/A vector pGEM®-T Easy Vector (Promega) or pDrive Cloning Vector (Qiagen). After 1 hr fast ligation at room temperature (RT), 2μl of ligation products were incubated with 50μl DH5α competent cells for 40 min on ice, followed by a 50-sec heat-shock on the 42°C heat block. The heat-shocked competent cells with ligated plasmid were put back on ice immediately and recovered on ice for 10 min. 20μl X-gal (Promega) were

A

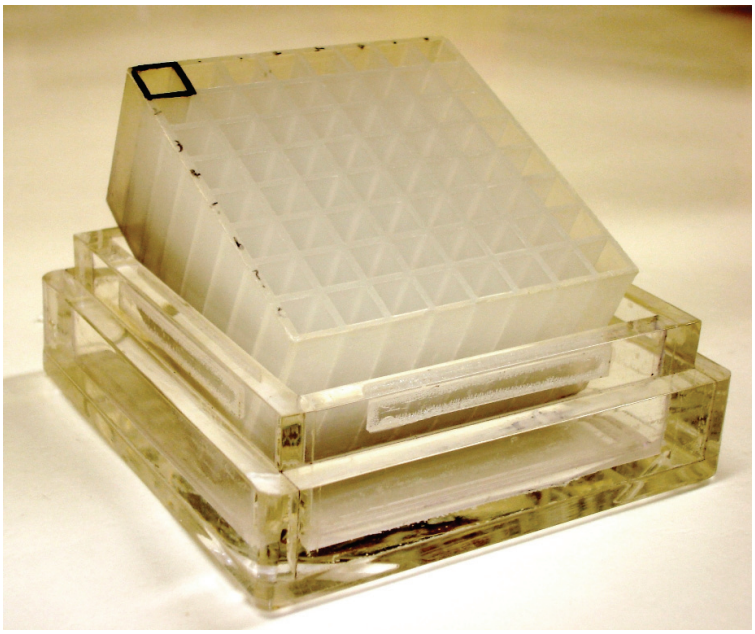

B

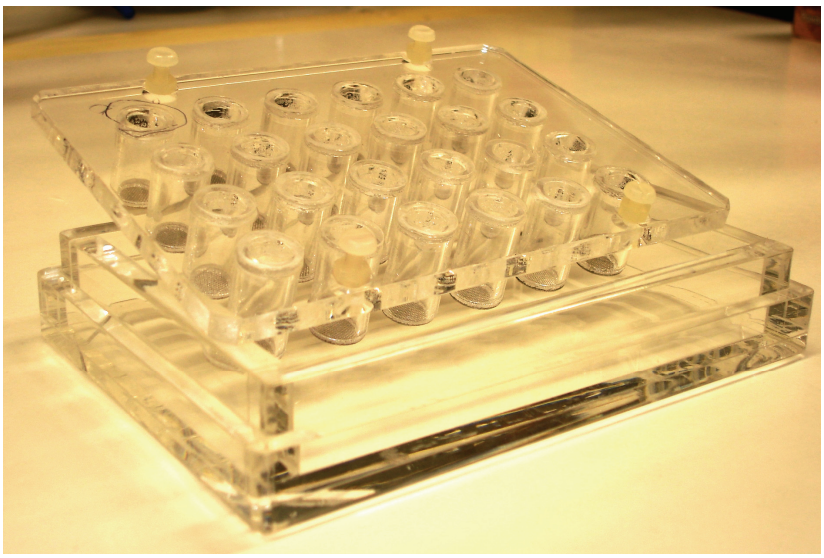

Figure 2.2 Specially Designed Multi-well Boxes for WISH Screening. A: 8X8 *in situ* box for simultaneous detection of multiple samples. B: 4X6 *in situ* box for simultaneous detection of different probes.

added to the competent cells to facilitate blue/white selection before spreading the bacterial cell onto LB plate containing ampicillin (100μg/ml). After an overnight incubation at 37°C, colonies were picked and subjected to colony PCR to further screen for the desired clones. White colonies were randomly picked from the plate using the tips of toothpicks, followed by stirring each tip in individual reaction mix and then in a PCR tube that was labeled correspondingly with 50μl of LB containing ampicillin. The tubes with LB were incubated at 37°C for future large culture. Each 20μl colony PCR reaction consisted of 2μl 10x buffer, 0.4μl Taq polymerase, 0.4μl M13 Forward and Reverse primers (10μM), 0.4μl dNTPs mix (10mM) and 16.4μl DDW. The colony PCR program was set up as 10 min 94°C initial denaturation, followed by 35 cycles of 94°C for 10 sec, 55°C for 15 sec, 72°C for 1 min, and a final extension of 5 min at 72°C. Colonies that showed correct predicted size of PCR products on the 1% agarose gel were selected as potential accurate clones. The corresponding 50μl LB culture was topped up to 2-3ml LB containing ampicillin and cultured at 37°C for plasmid extraction the next day.

2.2.2 Plasmid DNA Extraction

To extract small amount of plasmid DNA, single colony was picked from LB plate and inoculated in 2-3ml LB medium containing appropriate selective antibiotic. The cultures were incubated overnight at 37°C with vigorous shaking. On the next morning, 200μl of the overnight culture was mixed up with 200μl of 50% glycerol and stored at -80°C to be used as stock for future use. The remaining bacterial culture was spun down at full-speed for 3 min in a bench-top centrifuge (Eppendorf), The supernatant was discarded and the plasmid was extracted from the pellet using Miniprep column kit (Qiagen) according to the manufacturer's protocol. Generally, approximately 20μg of plasmid could be recovered from a 2ml culture. Midi or Maxi columns (Qiagen) were used to extract larger amount of DNA.

2.2.3 DNA Sequencing

A standard 20µl DNA sequencing reaction contained 8µl BigDye™ (V3.1) (ABI), 1µl appropriate primer (10µM), 100-200ng plasmid DNA and DDW. Thermocycling parameters for sequencing consisted of an initial denaturation step of 3 min at 95°C followed by 35 cycles of 95°C for 30 sec, 52.5°C for 10 sec and 60°C for 4 min. The PCR cycled sequencing reactions were sent to the IMCB Central Sequencing Facility for clean-up and sequencing analysis.

2.2.4 DIG DNA Probe Labeling

PCR method was used to synthesize DIG labeled DNA probe for Northern blotting or Virtual Northern blotting analysis. The PCR reaction mixture composing of 0.5µl Taq polymerase (Qiagen), 2.5µl 10X PCR buffer, 0.5µl of gene specific forward and reverse primers (10mM), 2.5µl PCR DNA DIG Labeling Mix (Roche), 2-5ng plasmid or PCR products as template, was topped-up to 25µl with DDW. A normal PCR reaction was set up as a control at the same time. After the PCR reaction, 2µl of labeled and control products were analyzed on 1% agarose gel and the yield was estimated by comparing to the fluorescence density of 1Kb ladder (NEB).

2.2.5 Virtual Northern Blotting

To assess the quality of cDNA after PCR amplification, I developed the Virtual Northern blotting based on the principles of Southern blotting method (Joseph Sambrook, 2001). Firstly, 5µl of amplified cDNAs were run on a 1% agarose gel along with 50ng of 1Kb ladder on a separated lane. After 1-2 hr of electrophoresis, the gel was first examined under UV light and treated for blotting with brief rinse between each step: 10 min in depurination solution (250mM HCl); 15 min in denaturation solution (0.5M NaOH, 1.5M NaCl); 15 min in neutralization solution (0.5M Tris-HCl, 1.5M NaCl, pH adjusted to 7.5).

After a brief rinse in DDW, the cDNAs on the gel were transferred onto a nylon membrane (Hybond N+, Amersham Bioscience) by the vacuum blotter (Bio-Rad) with 6XSSC (0.9M NaCl and 0.09M Sodium Citrate, pH adjusted to 7.0). After 2 hr of transfer, the membrane was placed face up on a plastic sheet and auto-crosslinked twice in a UV crosslinker (Stratagene). The membrane was pre-hybridized with DIG-Easy Hyb buffer (Roche) for at least 1 hr at 42°C. 100-200ng DIG labeled probe was diluted in 5ml DIG-Easy Hyb buffer and incubated with the membrane overnight at 42°C. On the following morning, the probe was carefully removed and stored at -20°C for reuse. The membrane was rinsed with 2XSSC and followed by a series of washing with vigorous shaking: primary washing buffer (2XSSC, 0.1%SDS) for 2x15 min at RT; secondary washing buffer (0.2XSSC, 0.1%SDS) for 2x15 min at 50°C; washing buffer (0.1M Maleic Acid, 0.15M NaCl and 0.3% Tween20, pH adjusted to 7.5) for 5 min at RT. After all the washes, the membrane was submerged in Blocking Solution (Roche) for at least 45 min at RT with gentle shaking, followed by incubation with anti-DIG-AP Ab (1:10000 dilution in Blocking Solution) for 30 min at RT. The membrane was then rinsed with washing buffer for 15 min at RT, and subsequently equilibrated with detection buffer for 3 min. Chemiluminenscent substrate, Ready-to-use CDP-Star (Roche), was applied drop-wise over the surface of the blot until the entire surface was evenly soaked and incubated for 5 min at RT. Excess substrate was removed and the membrane was exposed to an X-ray film at RT for 5 min to a few hrs depending on the signal intensity.

2.2.6 Semi-Quantitative RT-PCR

With the exception of *βe1-globin and elf1a*, which were amplified for 23 cycles and served as positive and negative control respectively, semi-quantitative RT-PCR was performed for either 30 or 35 cycles at 95°C for 10 sec; 55°C for 20 sec; 72°C for 1 min.

Primers were designed according to the sequence provided by Affymetrix except *lmo2, scl, flk1, gata1* and *βe1-globin* and *elf1a* (Table 2.1A).

2.3 General RNA Application

2.3.1 RNA Extraction from Embryos or Tissue

Fish embryos or tissue were homogenized in TRI Reagent (Molecular Research Center) using 1ml syringes with 24 gauge needles. With the standard TRI Reagent RNA isolation protocol, about 50μg total RNA can be extracted from 100 1dpf fish embryos. These RNA were directly used for Northern Blotting analysis. For reverse transcription or microarray analysis, RNA was treated with DNAse I and further purified by using RNeasy Mini Column (Qiagen) to eliminate the contamination of genomic DNA.

2.3.2 5' and 3' RACE (Rapid Amplification of cDNA Ends)

5' and 3' RACE were performed by using SMART RACE cDNA Amplification Kit (Clontech) according to the manufacturer's instructions. RACE primers for genes *zvsg1* and *ncf1* were listed in Table 2.1B. The RACE products were cloned into pGEM®T-Easy Vector (Promega) for sequencing. Full-length sequences were aligned by program Seqman (DNASTAR Inc.).

2.4 Whole Mount *in situ* Hybridization (WISH)

2.4.1 RNA probe synthesis

Plasmid DNAs were linearized by using the appropriate restriction enzyme (Table 2.2) and purified using the PCR purification kit (Qiagen). A 20μl RNA probe synthesis reaction contained 1μl RNA polymerase (Stratagene), 1μl RNAsin (Roche), 2μl 10X DIG or FLU RNA labeling mix (Roche), 4μl 5X reaction buffer, 1μg linerized plasmid DNA and nuclease free water. The reaction mix was incubated in a 37°C water bath for 2 hr. 1μl

DNase I (Roche) was then added to the reaction and further incubated at 37°C for 20 min. The synthesized probe was further purified using a Millpore microcon (Millipore). An aliquot (0.5µl) of purifed probe was loaded onto a 1% agarose gel to determine its quality and quantity. Finally, the probe was diluted to a final concentration of 0.5µg per ml of WISH hybridization buffer (50% formamide, 5XSSC, 0.92mM citric acid, 0.1% Tween20, 50µg/ml heparin and 500µg/ml tRNA) and stored at -20°C.

2.4.2 Compact WISH Protocol for *rag1* Screening

4dpf fish embryos were fixed in 4% paraformaldehyde dissolved in PBS (PFA) either overnight at 4°C or 2 hr at RT. All washes were carried out at room temperature unless specified. Embryos were then washed 3x10 min in PBST (PBS with 0.1%Tween 20), followed by equilibrating in methanol for 5 min and stored in 100% methanol at -20°C for at least 20 min. At this stage, embryos can be kept for later use. To recover embryos stored in 100% methanol for *in situ* hybridization, they were washed in 50% and 30% methanol in PBST for 5 min each followed by 2x5 min washes in PBST. The methanol treated embryos were permeabilized by digestion with proteinase K (10µg/ml) for 20 min. After a brief wash in PBST, the embryos were subsequently fixed in 4% PFA for 20 min followed by 3x10 min washes in PBST. The embryos were pre-hybridized in WISH hybridization buffer (Hb) for at least 1 hr at 60°C. The pre-Hb was replaced with DIG-labeled *rag1* RNA probe (0.5µg/ml in WISH Hb) and the embryos were incubated overnight at 60°C. On the next morning, the RNA probe was removed and stored at -20°C. These RNA probes could be reused for 3-4 times without notable decrease in hybridization signal. The embryos were washed 1x10 min in 2XSSCT at 60°C, then 1x10 min in 0.2XSSCT at 60°C, and finally 1x10 min in PBST at RT. After post-hybridization wash, the embryos were blocked in 10% BCS/PBST at RT for 1 hr and then probed with anti DIG-AP antibody (Roche) at 1:2000 dilution in 10% BCS/PBST for 2 hr at RT. The

antibody was collected and stored at 4°C for reuse. Finally, the embryos were washed 2x10 min in PBST, 2x10 min in buffer 9.5T (100mM Tris, 5mM $MgCl_2$, 0.1%Tween20, pH adjusted to 9.5), and incubated with NBT/BCIP color substrate solution (one NBT/BCIP tablet (Sigma) in 10 ml DDW with 0.1% Tween20) in the dark at RT. The *rag 1* signal could be seen after 1-2 hr of staining.

2.4.3 High-Resolution WISH Protocol

We applied a high-resolution WISH protocol from http://zfin.org to study temporal and spatial expression patterns of genes obtained from the microarray analysis. Fish embryos were collected at desired stages and dechorionated by pronase treatment. All washings were carried out at room temperature unless specified. The chorions were removed and the embryos were washed briefly in PBST before fixing in 4% PFA in multi-wells *in situ* box (Figure 2.2B), which was specifically designed for *in situ* hybridization with different probes at same time. The fixed embryos were washed 2x5 min in PBST, 1x5 min in 100% methanol, and then stored in fresh 100% methanol at -20°C for at least 20 min. These dehydrated fish were re-hydrated with a series of methanol/PBST solutions (3:1, 1:1, 1:3) for 5 min each, and subsequently 2x5 min wash in PBST. Embryos were permeabilized by digestion with proteinase K (10µg/ml) for an appropriate time (Table 2.3). After a brief washing in PBST, the embryos were re-fixed in 4% PFA for 20 min. The fixed embryos were washed 3X10 min in PBST before equilibrating in WISH Hb for 5 min at 60°C, and then changed into fresh WISH Hb and pre-hybridized for at least 1 hr at 60°C. Specific RNA probe (0.5µg/ml in Hb) was denatured at 68°C for 8 min, and cooled down on ice. The pre-Hb was discarded and the embryos were incubated in Hb with probe overnight at 60°C. On the next morning, the Hb with probe was recovered and stored at -20°C. The embryos were then washed as followed: 2x30 min in 2X50%formamide/2XSSCT at 60°C, 3x20 min in 2XSSCT at 60°C, 2x30 min in

0.2XSSCT at 60°C, and 2x 5min in PBST at RT. After the washes, the embryos were incubated in blocking buffer (2% lamb serum in PBST) for at least 1 hr at RT, and followed by anti-DIG-AP antibody solution (1:2000 dilution in blocking buffer) overnight at 4°C. After the overnight antibody incubation, the embryos were washed with PBST 6x20 min at RT, and equilibrated with buffer 9.5T 2x10 min before detection. The embryos were incubated with NBT/BCIP substrate solution in the dark. Staining time could vary from 1/2 hr to overnight at 4°C depending on the probe used. The color reaction could be stopped by washing the embryos twice with PBST for 10 min each, followed by fixing with 4% PFA for 1 hr at RT. After 4x15 min wash with PBST, the embryos could be stored in 70% glycerol at 4°C for up to 1 month. For bright and clear signal, images of the embryos should be taken as early as possible.

2.5 Microscopy and Photography

LEICA MZ75 stereomicroscope was used for daily injection and embryo development monitoring. *In situ* or live fish pictures were captured by Spot Insight QE digital camera under LEICA MZ16 stereomicroscope. *flk1*-GFP transgenic fish was visualized under LEICA MZ FLIII fluorescence microscope, which a Nikon DXM1200F digital camera was attached to for fluorescence photography. For *in situ* stained embryo earlier than 10 somites stage, the embryos' bodies were separated from yolk, and then flat-mounted on the glass slides for holistic view.

2.6 Single Embryo cDNA Library Construction

2.6.1 RNA Extraction from Single Embryo

Zebrafish embryos were collected from crossing one pair of wild-type or mutants crossing. At the stage of interest, single embryo was collected and put into individual 1.5ml tube. Total RNA from each single embryo was prepared using the RNeasy Micro

Kit (QIAGEN) according to the manufacturer's instructions. Typically, the final elution volume was about 10µl and contained 100-200ng total RNA.

2.6.2 PCR Amplification

Single Embryo cDNA library was constructed by using SMART PCR cDNA Synthesis Kit (Clontech). Firstly, RNA sample was transferred to a PCR tube and spun dry in an Eppendorf Concentrator. Reverse transcription reaction was set up in this PCR tube, which contained 1µl 3'SMART CDS Primer IIA, 1µl SMART II A Oligonucleotide (Table 2.1C) and 3µl RNase Free water. The reaction mix was denatured on Perkin-Elmer thermal cycler 9700 at 72°C for 2 min and then cooled down on ice for 2 min. The tube was spun briefly to collect all the contents at the bottom, and the following reagents were added: 2µl 5X First-Strand buffer, 1µl DTT (20mM), 1µl 50XdNTP (10mM) and 1µl PowerScript Reverse Transcriptase. The reaction mix was incubated at 42°C for 60-90 min on the thermal cycler. After the reverse transcription, the mix was diluted by adding 40µl of 1X TE and was ready for PCR amplification. The Long-Distance (LD) PCR reaction for cDNA amplification composed of 10µl 10X Advantage2™ PCR buffer, 2µl dNTPs mix (10mM), 2µl 5'PCR Primer IIA, 2µl Advantage2™ polymerase mix, 10µl first strand cDNAs as template and 74µl DDW. The LD PCR condition was 95°C 1 min followed by 15 cycles of 95°C 5 sec, 65°C 5 sec and 68°C 6 min. In order to determine the optimal number of PCR cycles for linear amplification of products, the PCR sample was removed after 15 cycles, and 20µl of the PCR reaction was aliquot into 4 PCR tubes (5µl in each tube), while the remaining 80µl was kept on ice. The 4 aliquoted PCR reactions were put back to the thermal cycler to continue the PCR amplification. At cycles 18, 21, 24, 27(15+3, 6, 9, 12), one PCR tube was taken out from thermal cycler and kept on ice. A total of 5 PCR samples from cycles 15-27 were analyzed on a 1% agarose gel to determine optimal number of PCR cycles. Good amplification products

should display a moderately strong smear of cDNA from 0.5 to 6kb, which means the amplification is in the exponential phase (Figure 2.3). In this case, the optimal cycle number was about 17-19. After amplification, semi-quantitative PCR or virtual Northern blotting was applied to verify the quality of amplified cDNA.

2.7 Affymetrix Array and Data Analysis

2.7.1 Sample Preparation

For a non-amplified sample, the standard RNA extraction method as described in section 2.3.1 was used for the RNA preparation. The quality of the RNA extracted was examined by a spectrophotometer (NanoDrop). The ratio of Ab_{260}:Ab_{280} should be between 1.8-2.2, and the ratio of Ab_{260}:Ab_{230} should be above 2 for good quality of RNA. For an amplified sample, Single Embryo cDNA Library Construction approach was employed with the difference that SMART-T7-Anti-Sense Primer (Table 2.1C) was used instead of 3'SMART CDS Primer II A. 200µl of amplified PCR reaction was purified by PCR purification column (Qiagen), and the final yield of purified cDNA was about 2µg in RNase-Free water. A total of 10µg of non-amplified RNA or 1.5µg of single-embryo amplified cDNA were labeled with ENZO BioArray High Yield T7 RNA Transcript Labeling Kit (Enzo Life Sciences).

2.7.2 Affymetrix Array

The Zebrafish Genome Array (Affymetrix), containing 14,900 *Danio rerio* transcripts, was used as the chip for microarray. Array hybridization was performed according to the manufacturer's instructions and the raw data was analyzed by using the Microarray Suite 5.0 software. Spots with a ratio of greater than 1.5-fold (log ratio>0.6) were scored as positive. The results were in xls format and the detailed description of each clone could

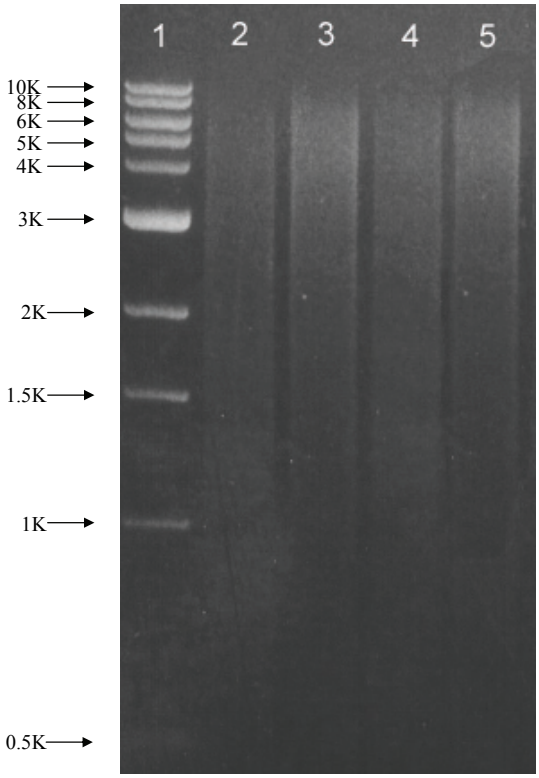

Figure 2.3 Electrophoresis of Amplified cDNA from Single Embryo. A total of 5µl amplified single embryo cDNA (lanes 2,3,4,5) was examined on 1% agarose gel. Compared to the 1Kb ladder (lane 1), ethidium bromide staining displayes an evenly distributed smear of DNA from high molecular weight (8Kb) to low molecular weight (1Kb).

be found from netaffx analysis center in Affymetrix website (https://www.affymetrix.com/analysis/netaffx/index.affx).

Table 2.1 List of Primer Sequences

A.

Primers for cloning and semi-quantitative RT-PCR		
Gene	Forward Primer	Reverse Primer
gata1	5'-actacaacactatggagacgc-3'	5'-acaacataatttacaagcttcg-3'
lmo2	5'-ctgtgacctctgcggctg-3'	5'-acatttattgcaattgtgttac-3'
flk1	5'-actcctcctctgaaatatatcagacc-3'	5'-acaggaaatgtgaatctctgaatgacc-3'
scl	5'-acactgacggtatggaggtcag-3'	5'-aaagacgttgagctgcgccatc-3'
βe1-globin	5'-acttcgccaagtttggaaacc-3'	5'-actgtcttcccagagcggac-3'
actin	5'-accaccggtattgtgctggatgc-3'	5'-acagatccttacggatgtcaatgtc-3'
elf1a	5'-cttctcaggctgactgtgc-3'	5'-ccgctagcattaccctcc-3'
cld g	5'-ggcctctcgagctatccttgtcat-3'	5'-caaagacgatctcagacagacatt-3'
mmp13	5'-atcaaaggtgagaaggtttgggct-3'	5'-ctcggattcttcttcaggcggtaa-3'
yrk	5'-ctggaagctcaactagtttgcgtt-3'	5'-gctcagtgtaatagattggcacaa-3'
copIII	5'-gatctgaccgaaggagaaaactca-3'	5'-caacagcactgtgctcgactcag-3'
znfl2	5'-cgagcccgtgcacagcgaactgaa-3'	5'-cctggtgaactcctccatcatctc-3'
dusp5	5'-gccatcatctcgcccaattttagc-3'	5'-caggcgctgataggcagaacatca-3'
aqp8	5'-ctctggtcactgtcagcattgtga-3'	5'-gcgaagagacatttaagcatcagg-3'
cahz	5'-ctgatcttctaaaactgtctgcgt-3'	5'-cctcttgatgaaaaaggaatcact-3'
Dr.11977	5'-cggaaatgccttcaactgttgcca-3'	5'-catatttgcagaccaatatggcct-3'
Dr.14448	5'-gccttcagaccgactctagatgct-3'	5'-gcagcacaatatcttacagcaact-3'
Dr.14553	5'-ccagtcctaaagaggtggttcaca-3'	5'-gaaaagggatgatcaaagggtctg-3'
Dr.16206	5'-caagcagtacagtgtgattgctcc-3'	5'-cactggtaacatgcagcaatatga-3'
Dr.1870	5'-cttgttttcatgctgggctgcctt-3'	5'-cacatccagctcttcaacatgagg-3'
Dr.2973	5'-ctcctgtttagcccagaacctgtt-3'	5'-gcatacttaagtagcctattgctg-3'
Dr.25630	5'-ctgaattaggttattcctgaattg-3'	5'-ccattttgaaagcatgtgacagat-3'
Dr.25117	5'-ctggagagagtctgattggctgga-3'	5'-ctgtggtgattctgatcatgcaat-3'
Dr.6885	5'-gacctgtgagtcatgggcctacaa-3'	5'-gtgcccaaagaaattagaactaga-3'
Dr.9665	5'-cggacgctgtgtttctgagtatct-3'	5'-ggtcaataagaccagcagatacat-3'

B.

Primers for 5'and 3'RACE		
zvsg1	3'-race-1	5'-ggggtcttaaaatgtgcttaaatggga-3'
	3'-race-2	5'-gactacatttcatgtatctgctggtct-3'
	5'-race-1	5'-tcccatttaagcacattttaagacccc-3'
	5'-race-2	5'-tcagaaacacagcgtccggccttgaga-3'
ncf1	5'-race-1-560R	5'-gccttgtcaagccaagtcgtctatggt-3'
	5'-race-2-377R	5'-tttcagtgcagcgctccagaatgagct-3'

C.

Primers for SMART cDNA Amplification	
3'SMART CDS Primer IIA	5'-AAGCAGTGGTATCAACGCAGAGTACT(30)VN-3' (N = A, C, G, or T; V = A, G, or C)
SMART II A Oligonucleotide	5'-AAGCAGTGGTATCAACGCAGAGTACGCGGG-3'
SMART-T7-Anti-Sense Primer	5'AAGCAGTGGTATCAACGCAGAGTACGGCCAGT GAATTGTAATACGACTCACTATAGGGAGGCGGT (24)VN-3' (T7 promoter is underlined.)

Table 2.2 List of Constructs for WISH RNA Probes

AFFX GENE ID	GENE	Vector	Cutting Site	RNA Polymerase
Dr.8153.1.S1_at	cldn g	pDrive	Sal I	T7
Dr.10314.1.S1_a_at	mmp13	pCS2+	EcoRI	T7
Dr.6834.1.A1_at	cpoIII	pDrive	BamH I	Sp6
Dr.3201.1.S1_at	znfl2	pGEM-Teasy	NcoI	Sp6
Dr.5365.1.A1_at	dusp5	pGEM-Teasy	Sal I	T7
Dr.2973.1.A1_at	Dr.2973(ncf1)	pGEM-Teasy	NcoI	Sp6
Dr.916.1.S1_at	aqp8	pCS2+	EcoRI	T7
Dr.450.1.S1_at	cahz	pGEM-Teasy	Sal I	T7
Dr.9655.1.A1_at	Dr.9655(zvsg1)	pGEM-Teasy	NcoI	Sp6

Table 2.3 Duration of Proteinase K Permeabilization for Zebrafish Embryo

Stage of Embryo (dpf)	Proteinase K Treatment (min)
<1	0
1-2	5
2-3	10-15
3-4	15-20

Chapter III: Genetic Screen of *rag1* Deficient Zebrafish Mutants

3.1 Background

Thymus plays an important role for T-cell development. T-cell lymphopoiesis and thymic organogenesis are crucial interdependent processes for the establishment of a functional vertebrate immune system. In mouse, lymphopoiesis starts from the pluripotent HSCs, which firstly home in the fetal liver and then migrate to the thymus for further proliferation and differentiation (Keller et al., 1999). With the interaction with the thymic epithelial cells (TECs), the immature lymphoid progenitors differentiate from double negative ($CD4^-CD8^-$) cells to double positive ($CD4^+CD8^+$) cells; subsequently, these $CD4^+CD8^+$ cells undergo positive and negative selection and finally become mature T lymphocytes (Douagi et al., 2002). The thymic development requires the inter-communication from all the three embryonic germ layers: ectoderm, mesoderm and endoderm (Manley, 2000). Thymic developmental process can be separated into two stages: formation of the thymic rudiment and the interaction between T cells and thymic epithelial cells (TECs). In the first stage, neurectodermally derived neural crest cells (NCCs) from the sixth hindbrain rhombomere migrate to the third and fourth pharyngeal pouches, where they interact with endoderm to induce the formation of thymic rudiment. In the second stage, after the entry of T-cell precursors, blood vessels develop in the thymic rudiment, and subsequently the thymic epithelial cells differentiate into a three-dimensional interdigitating to form the mature thymus. Only in this mature thymus microenvironment, the T lymphocyte precursors further proliferate and differentiate into mature T-cells (Manley, 2000).

Although many important factors or pathways involved in T-cell lymphopoiesis and thymic development have been uncovered, the genetic programs defining the early steps in these processes and TEC-T-cell interactions are poorly understood. To better understand the mechanism of the T-lymphoid program and thymic organogenesis during vertebrate development, we used zebrafish as the model organism to carry out forward genetic screen. Recombination activating gene (*rag*) 1 was selected as marker for this screen. The main function of RAG1 protein is to catalyze the V(D)J recombination of the immunoglobulin and T cell receptor (TCR) genes in immature B and T lymphocytes, respectively (Mombaerts et al., 1992). No mature T cell and B cell can be found in the rag1 knock-out mouse. *rag1* is highly conserved across different species. The zebrafish Rag1 protein shares ~60% identity to mouse and human orthologues, and is specifically expressed in B and T cells (Willett et al., 1997a). Consistent with the mouse, the V(D)J recombination was impaired in the zebrafish *rag1* mutant (Wienholds et al., 2002). Thus the zebrafish *rag1* gene, having similar function as the mammalian counterpart, is required for B and T lymphocyte development. Given the fact that the expression of *rag1* can be easily detected by WISH in the thymus after 72hpf of zebrafish development (Willett et al., 1997b), it serves as an excellent genetic screen marker for mutations affecting development of thymus or its constituent lymphocytes.

Through our *in situ* based genetic screen of 540 mutagenized zebrafish genomes, a total of 86 *rag1* deficient mutant families were initially isolated. Considering the criterions of general development, blood circulation and thymus rudiment marker *foxn1* expression, 13 mutants were selected for future study.

3.2 Results

3.2.1 ENU Mutagenesis and Family Generation

The ENU-based mutagenesis protocol was shown to be the most effective mutagenic method in zebrafish. Through this protocol, point mutation in the zebrafish spermatogonia stem cells would be induced by alkylation on the genomic DNA (Deutsch et al., 1981). Since the frequency of ENU-induced mutations is dosage-dependent and the increment of ENU concentration from 2.0 to 3.0mM results in a significant increase in the mutation frequency, hence, we used 3.0mM ENU to achieve the high efficiency of mutagenesis. Forty healthy male wild-type AB fish were selected and treated with ENU as described in section 2.1.4.1. After three rounds of mutagen treatments, only 8 fish survived and one of them was sterile, which could be the result of high lethality rates caused by application of high ENU concentration. Hereafter, we were left with 7 founder fish to generate F1 progeny (Table 3.1). The mutagenesis efficiency was calculated by the frequency of induced pigmentation mutations by crossing the founder fish with pigmentation deficient mutant *albino*. This test should be done prior to the generation of F1 fish. However, in order to raise more F1 fish carrying more mutations, we performed this test after the generation of F1 fish, and the mutagenesis efficiency was found to be $2/10^3$, which was within the normal mutagenesis rates of $0.9\text{-}3.3X10^{-3}$ (van Eeden et al., 1999). Considering the high mutagenesis efficiency existed even after the clearance of mutagenized sperm through the generation of F1, we assumed that the efficiency of our mutagenesis was possibly higher than $2/10^3$. The mutagenized male fish were crossed with wild-type AB females to generate F1 progeny. To reduce the risk of raising progeny from spermatogonial clones, the number of F1 fish raised from each founder was limited to 150 fish, and hence, about 700 F1 fish were generated (Table 3.1). In order to save

space and reduce workload, we inter-crossed the F1 fish derived from different founders, and 330 F2 families were generated for genetic screen.

3.2.2 *rag1* Screen

3.2.2.1 *rag1* Whole Mount *in situ* Hybridization

To screen for mutants affecting thymus formation or T lymphocyte development, we used *rag1* as a marker gene to visualize the embryonic thymus by WISH. The 3 prime sequences, from nucleotides 1426 to 2944, of the zebrafish *rag1* gene (NM_131389) were cloned into pBluescript II KS (+) vector. The DIG labeled anti-sense RNA probes were generated by *in vitro* transcription. Newly synthesized probes were tested to ensure a robust thymic expression of *rag1* is displayed in every wild-type 4dpf fish (Figure 3.1) before being used for the screen. In general, about 20μg of *rag1* probe was sufficient for each round of WISH to simultaneously screen 128 clutches of embryos and could be re-used at least 3 times. When the *rag1* signal appeared slightly weaker than the previous screen, new probes was added to the old probe solution to maintain the strong and clear *rag1* staining in the next round of screen.

The forward genetic screen is a time and labor consuming process and requires a lot of space. In addition, the WISH based screen further complicates issues. In general, for our screen, the thymic expression of *rag1* was best observed in at least 4dpf embryos and the normal WISH protocol took 3 days to complete; so taken together, the whole procedure lasted more than one week. In order to reduce the time and workload and maximize the available resources, we simplified the WISH protocol. As described in section 2.4.2, the post-hybridization washes and post-antibody washes were reduced, so the WISH took only 2 days, one day less than the standard protocol, to complete while retaining the strong intensity of the *rag1* signal. Furthermore, we designed 64 and 96 wells *in situ* box (Figure 2.2A), which made it possible to examine multiple samples

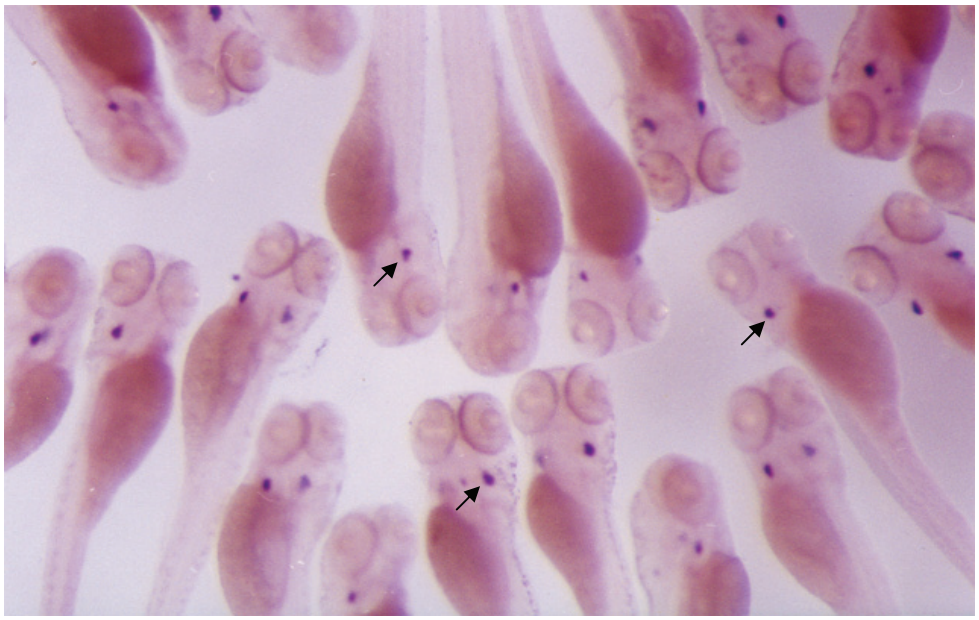

Figure 3.1 Thymic Expression of *rag1* Gene in Zebrafish Embryos. 4dpf wild-type embryos were hybridized with DIG-labeled *rag1* anti-sense probe. *rag1* expression was observed in bilaterally symmetric spherical regions posterior to the eyes.

simultaneously. Through these optimizations, we could screen more than 100 F2 families within one week.

3.2.2.2 The Primary Screen of *rag1* Expression Deficient Mutants

The general scheme of zebrafish genetic screen was illustrated in Figure 3.2. F3 offsprings of each F2 family were screened for recessive mutations altering *rag1* expression in the thymus. Each F2 family constitutes sibling fish that share a gene pool of two mutagenized haploid genomes from each F1 parents and half of the fish in each F2 family are heterozygous for any particular mutation. Hence, sibling crosses within each F2 family will match two carriers of a mutation in a quarter of the matings ($^1/_2X^1/_2$), and a recessive mutant phenotype will be displayed by 25% of the F3 offsprings. The probability to identify a recessive homozygous mutation can be calculated using the formula $1 - 0.75^n$, where n is the number of successful cross. Theoretically, if 4 successful crosses are screened in one F2 family, the chances to isolate this particular mutant will be about 70%. Therefore, we had set the criteria that at least four successful crosses should be screened in each F2 family (Table 3.1). Since the rate of success for crossing was about 40% in our fish, hence, to achieve 4 successful crosses, we had to set up at least 10 crosses from each family. After 3 months of primary screen, a total of 1551 successful crosses from 270 F2 families had been screened and the average successful cross number achieved for each F2 family was 5.74. Applying this number to the formula $1 - 0.75^n$, the average probability to identify one mutation in our screen was 81%. For the rest of the 60 F2 families, we could not successfully achieve enough crosses due to sex bias of the F2 offsprings. Through the primary round of screens, we identified 422 potential mutants that were distributed in 180 F2 families. This result corresponded to 1.64 mutants per screened family.

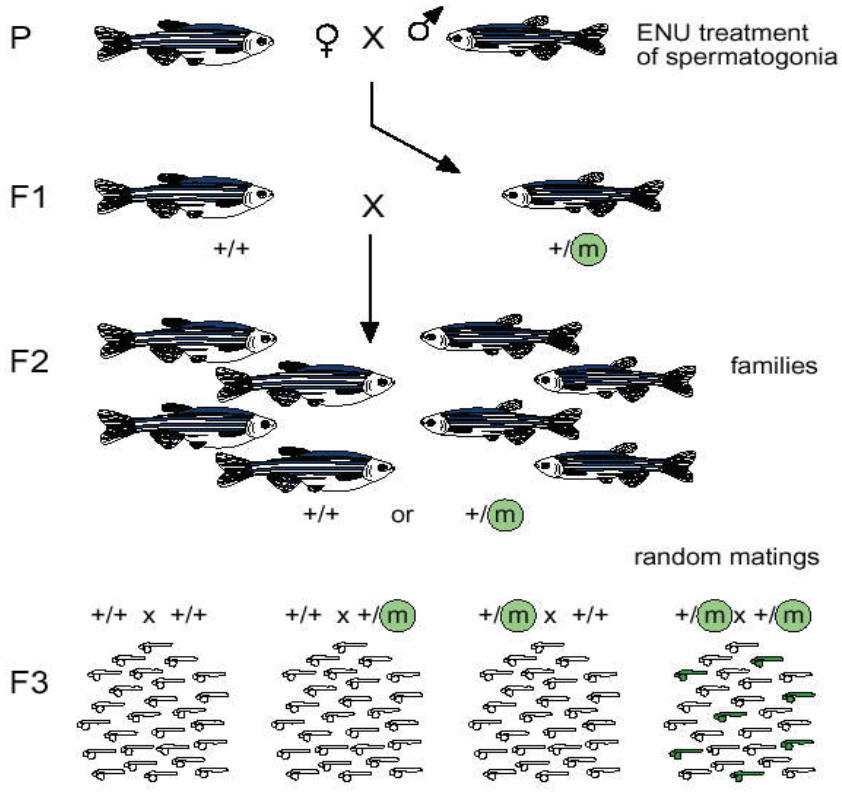

Figure 3.2 Scheme of Forward Genetic Screen in Zebrafish.(Haffter et al., 1996) Males mutagenized with ENU were mated to wild-type females to generate the F1 progeny. F2 families were raised from sibling matings. A mutation **m** present in one of the F1 parents was shared by 50% of the fish in the F2 family. Eggs were collected from a number of matings between sibling fish. If both parents were heterozygous for **m,** expected in ¼ of the crosses, ¼ of the eggs will be homozygous and show the mutant phenotype. For simplicity, a mutation carrier F1 fish mated with a wild type fish is shown here. In our experiment, both were heterozygous for a mutagenized genome. Therefore, the number of mutagenized genomes per family scored was two.

3.2.2.3 Re-screen and Out-cross

Rescreening of the 422 mutants identified from the first round of screens were of absolute necessity as the absence of *rag1* signal observed might be due to spurious development abnormalities. Two additional rounds of screens were carried out to weed out false positive mutants. During the re-screens, mutant phenotypes were confirmed by at least two observers, and their *in situ* images and other morphological phenotypes were recorded in a mutant management database (see section 3.2.2.4). After two rounds of rescreens, 140 mutants from 110 families were confirmed. Although inter-cross between two F2 mutants could generate more heterogeneous F3 progenies, however in practice, the viability and vigor of fish resulting from inbreeding was very much reduced compared to outbred fish. This was also true in the next generation, and therefore outcrossing to independent AB wild-type was performed to generate F3 families. The generation of F3 families was not only for the maintenance of mutants, but also to further expurgate the genetic background of each mutant. The offsprings from each F3 family were re-screened from at least 8 successful crosses and an additional 24 families were abandoned due to problems such as sterility, sex bias or absence of the mutant phenotype. The remaining 86 mutant families were confirmed to have reduced or absence of *rag1* signal and were subjected to further, more detailed characterization.

3.2.2.4 Data Management

Genetic screening is a time, labour and resource-consuming task. To maximize benefits that we can reap from this screening, we collaborated with Dr Jinrong Peng whose group is interested in the study of liver development. While we carried out the *rag1* screening in the embryos at 4dpf, Dr Peng's group screened for their liver deficient mutants at 3dpf. Hence, we had to divide the embryos from each clutch of embryos among two groups. More than often, the embryos from a single cross was only enough for one group's

screen and it was necessary to set up a new cross for this pair of fish on the following week. There were also incidents that a certain pair of mutants was identified to be carrying mutations of interest to both groups, and we needed to negotiate how we could assign this mutant for future characterization. Therefore, management of resources (such as fish and space) during genetic screen was a challenging but important issue. To deal with difficulties and complications arising from the screening procedure efficiently, a database management tool for data input was required to facilitate the mutant management and characterization. I developed a fish-screen/mutant management database by using File Maker Pro 5.0 (Filemaker Inc.) to assist us with the characterization and organization of our mutants. As illustrated in Figure 3.3, the database consisted of 3 features of each mutant: I) basic information of each mutant, which included the origin of founder, the birth of the mutants, the family number, the number of screens and the time of out-cross; II) morphological phenotype under microscope, which included general development status, the length of the body, the brain, eye and heart development etc.; III) other lineage markers test, which included blood circulation and *foxn1* expression. All the parameters of each mutant were searchable to subgroup them, which made it easy for us to trace each pair of mutants during the screening.

3.2.3 Initial Characterization of Mutants

The thymus organogenesis requires the cross-talks of different cell types from all three germ layers and multiple factors are involved in this process. As shown in Figure 3.4, besides the *rag1* deficiency, a large portion of the mutants also displayed many defects in other tissues or organs. Some mutants, like those in Figure 3.4 F,L,O, which had severe growth retardation or disorganization of body order, appeared to have multi-organ development defects which might in turn affect the normal development of the

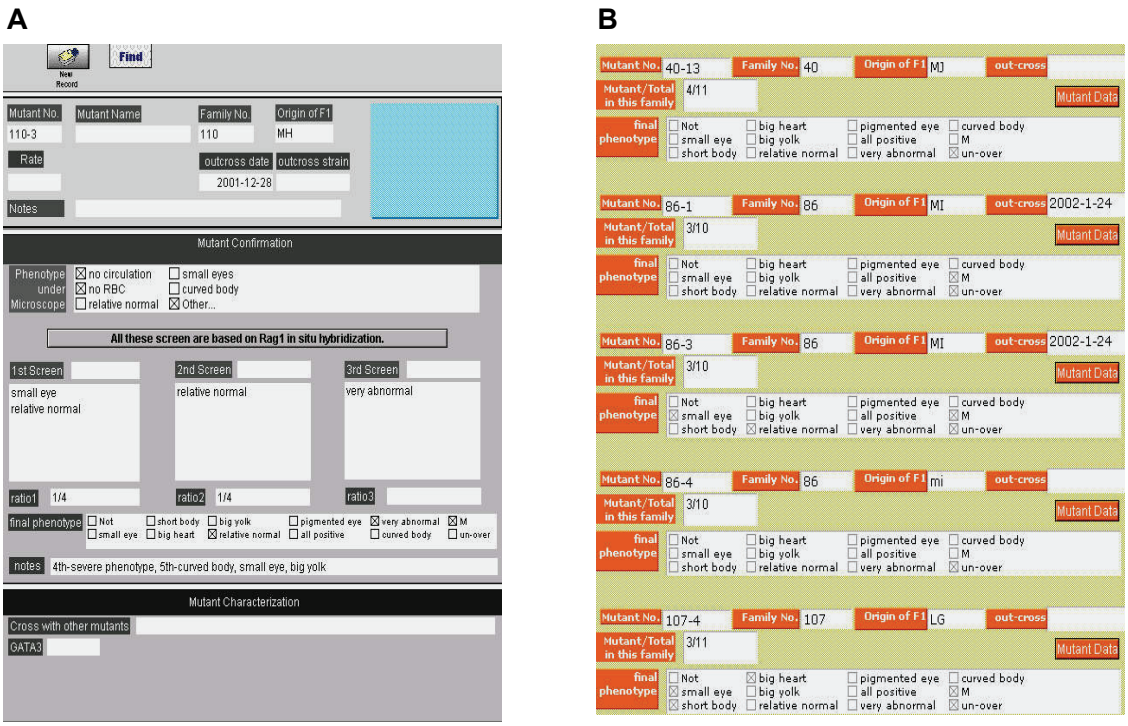

Figure 3.3 Database Management of *rag1* Screen. A fish screen/mutant management database was created by using File maker Pro 5.0. Panel A shows an example of a full data input built up during screen for a mutant. Panel B shows the summarized screen-shot of the database in a compact format.

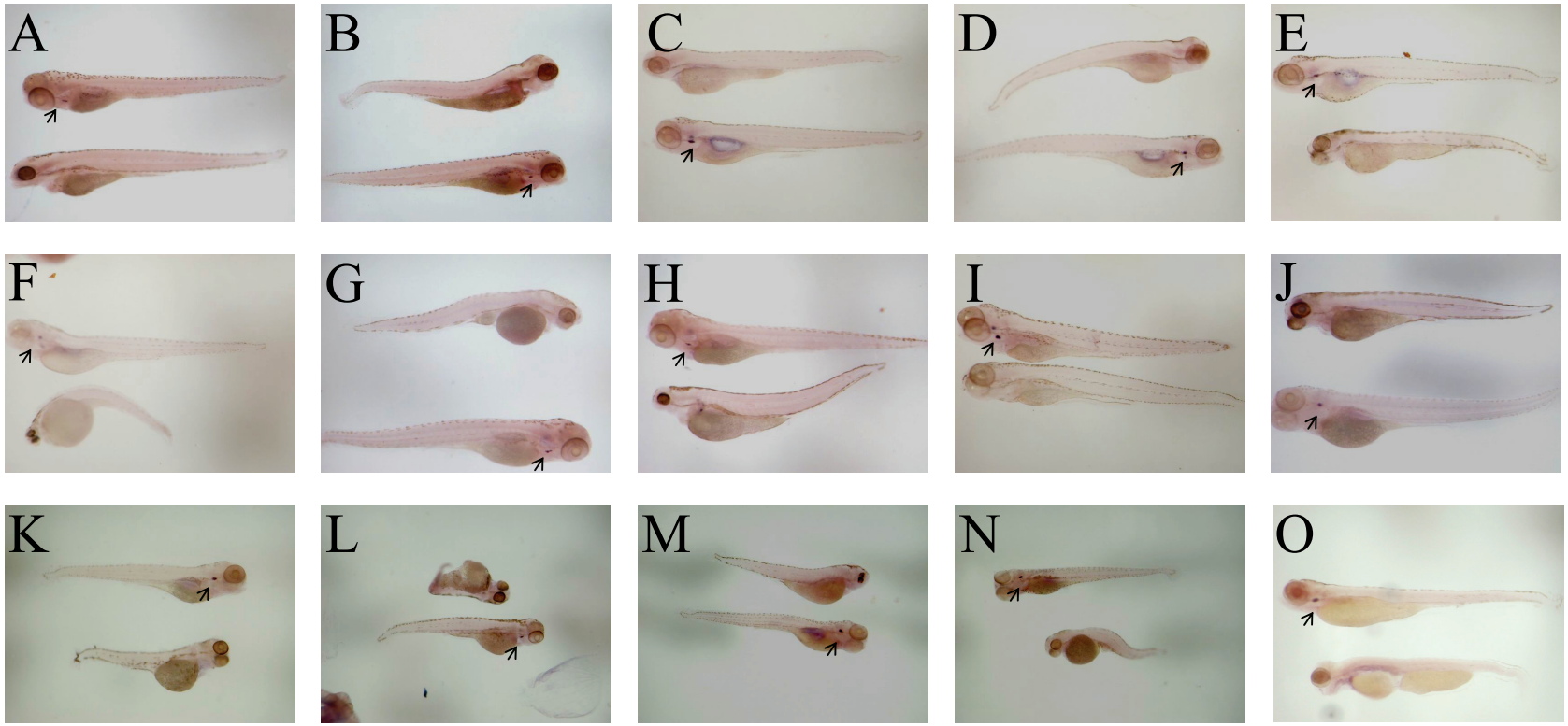

Figure 3.4 Morphological Phenotypes of Different *rag1* Deficient Mutants at 4dpf. After two rounds of re-screens, a total of 86 *rag1* deficient mutants have been confirmed based on WISH. Panel A to O illustrate the different severity of morphological phenotypes exhibited by the *rag1* deficient mutants (no thymic *rag1* staining) compared to the wild-type siblings (arrows show *rag1* staining in wild-type thymus).

thymus. We are not interested in performing further analyses on these mutants with general defects. Based on careful considerations and stringent selections, we chose 1 early blood defect mutant (260) and 12 morphologically relative normal mutants (180-3, 193-1, 213-3, 174-6, 179-2, 161-6, 116-3, 262-3, 244-11, 194-2, 147 and 370) to carry out detailed investigations (Figure 3.5). Given the complexity and peculiarity of thymus and T cell development, we attempted to classify these 13 mutants into two groups: mutants with (I) thymic rudiment anomaly and (II) lymphoid lineage deficiency.

We took advantage of *in situ* hybridization using transcription factor *foxn1/whnb* to help us identify mutants with thymic rudiment anomaly. It has been shown in mouse that the lack of *foxn1/whnb* causes a differentiation arrest and colonization failure in pro-thymocytes (Wortis et al., 1971; Nehls et al., 1994). WISH staining of *foxn1* in zebrafish showed that the expression is also mainly localized in the thymic rudiment (Schorpp et al., 2002), indicating a similar function by zebrafish *foxn1* to that of mouse. We examined all the 13 mutants and found that although the expression patterns of *foxn1* appeared to be in a condensed manner in the thymic rudiments in some mutants (Figure 3.6), all 13 mutants maintained the *foxn1* transcripts. This result suggested our mutants have normal thymus epithelial cell development and the *rag1* deficiency phenotype should be attributed to the hematopoietic lineage cell abnormality.

Based on our preliminary characterization by the presence of intact thymic rudiments in the mutants, all 13 mutants are categorized under group II. The mutations affecting the group II mutants could result in defects in the hematopoietic stem cells, common lymphopoietic progenitor (CLP), or T-cell lineage cells. To determine if the mutants had defective hematopoietic stem cells, we examined defects in the erythroid lineage by visualizing the blood circulation in the mutants at 2dpf under stereomicroscope. One mutant, 260, has dramatically decreased blood circulation. This phenotype was further

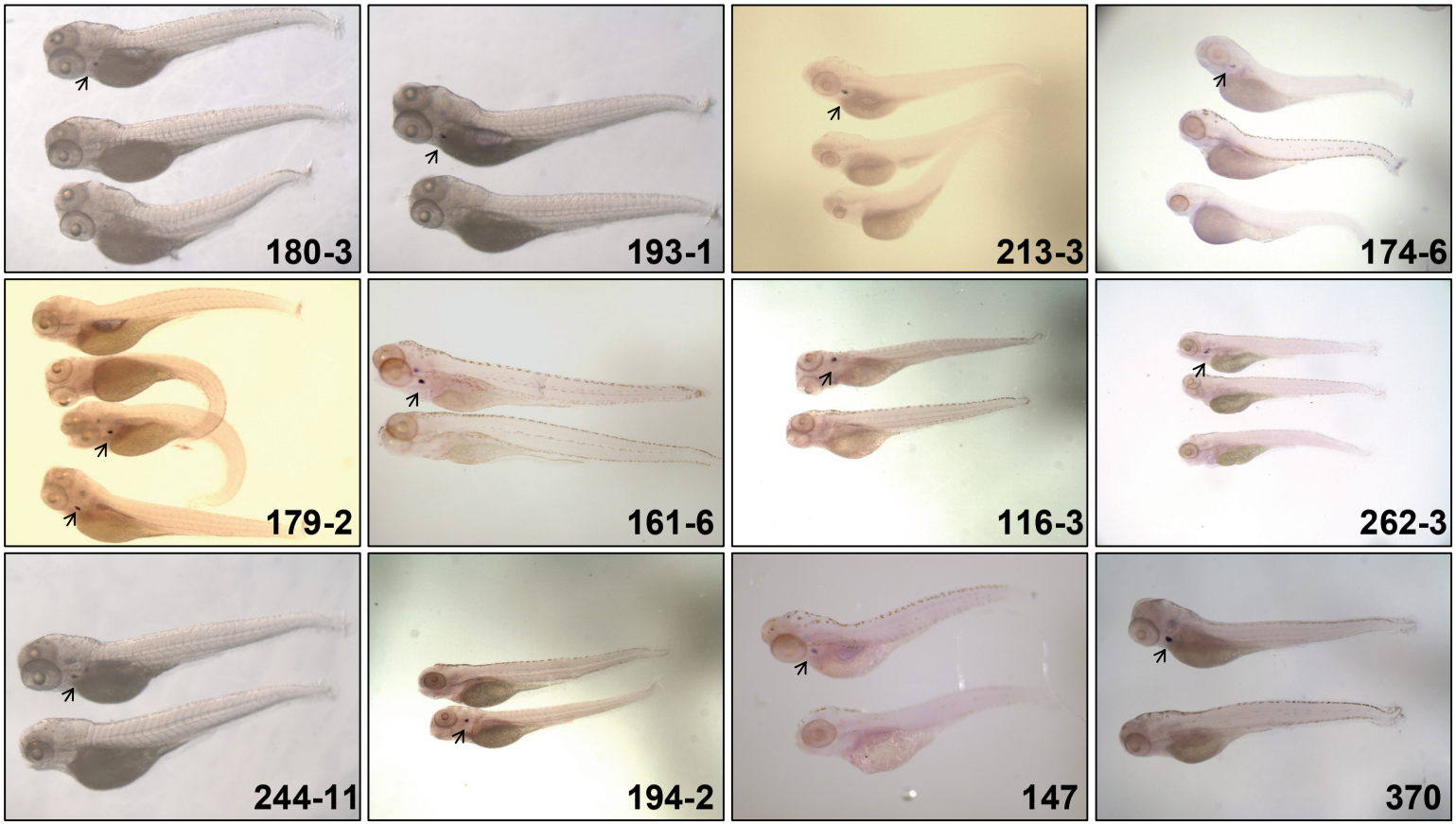

Figure 3.5 Twelve Morphologically Normal-looking *rag1* Deficient Mutants Maintained. Mutants (180-3,193-1,213-3,174-6,179-2,161-6,116-3,262-3,244-11,194-2,147 and 370) are chosen for maintenance and future studies based on their relatively normal phenotypes. Each panel consists of 4dpf WT fish (arrows show *rag1* staining in thymus) and *rag1* deficient mutant(s).

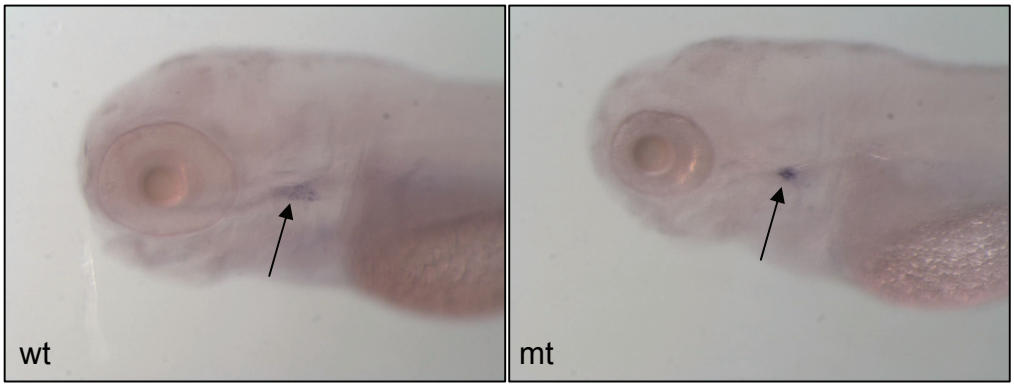

Figure 3.6 *foxn1* Expression in Wild-Type and Mutant. RNA whole mount *in situ* hybridization on 5dpf wild-type embryo shows that the *foxn I* expression is located in the thymus (left panel). Although all 13 mutants exhibited the *foxn1* staining, the expression pattern in some mutants is in a condensed manner (right panel).

confirmed by *o*-dianisidine staining (Figure 3.7), which reacts with mature hemoglobin protein to produce a red coloration (Detrich, III et al., 1995). The lack of red blood cells indicated that this mutant has deficiency in both erythroid and lymphoid lineage cells and strongly suggested that the mutation causes defects at the hematopoietic stem cell level. Positional cloning revealed that the responsible gene for this mutation encoded a novel gene with unknown function (unpublished data, Liu Y.M.). The remaining 12 mutants have seemingly normal development of erythroid lineage cells based on the red blood circulation suggesting that their mutations cause deficiencies in the CLP or the lineage cell migration.

3.3 Discussion

Our genetic screen was designed for isolating T-cell or thymus defective mutants based on whole mount *in situ* hybridization of *rag1* expression in the zebrafish thymus region. As *rag1* expression in immature thymocytes required both normal development of T cell precursors and an appropriate microenvironment for the thymus anlage, our *rag1* deficient mutants were expected to possess defects in T-lymphoid cell development or thymus formation.

Through our genetic screen, 86 mutants were confirmed both in the F3 and F4 generation. However, many of them were accompanied by developmental retardation. Since the thymic development requires the contribution of tissues from all three germ layers, thus, any defects in endoderm, mesoderm and ectoderm development may also affect the body formation as well as normal development of thymus. Hence, some of our mutants may have general defects in germ layer formation and may not have specific functions in thymogenesis. Based on this criterion, 12 morphologically normal mutants (180-3, 193-1, 213-3, 174-6, 179-2, 161-6, 116-3, 262-3, 244-11, 194-2, 147 and 370) were finally selected and maintained for future study. In addition, we chose to keep a

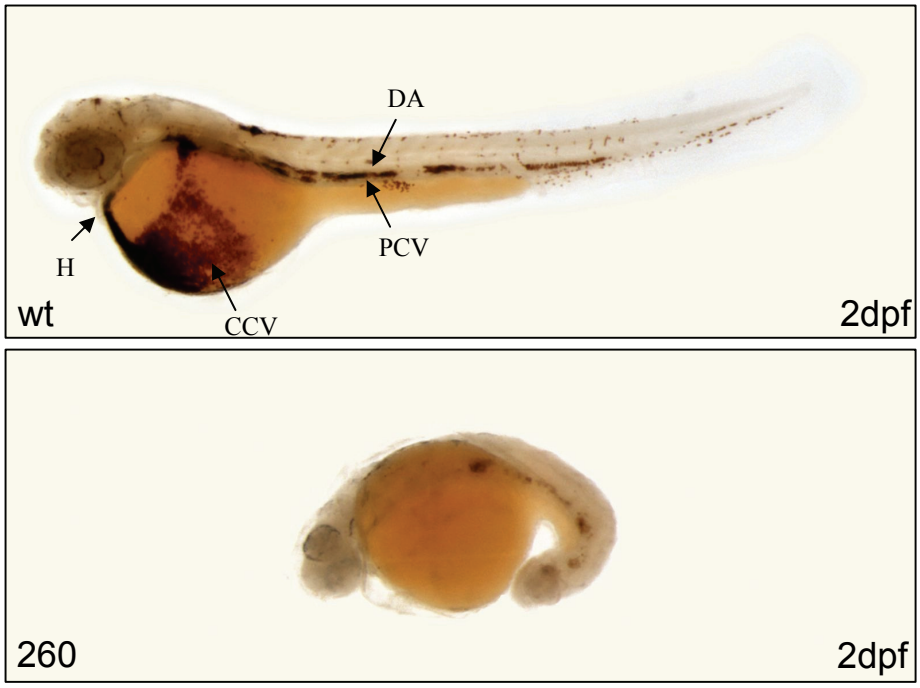

Figure 3.7 *o*-dianisidine Staining on 2dpf Wild-Type and Mutant 260. The *o*-dianisidine stains the erythroid cell containing hemoglobin and develops brown coloration. In wild-type embryo, the stained erythroid cell can be seen to be distributed in the heart (H), common cardinal vein (CCV), posterior cardinal vein (PCV) and dorsal aorta (DA) (upper panel). In mutant 260, the erythroid cells are dramatically decreased as indicated by weak brown color staining (lower panel).

mutant, 260, as it has dramatic decrease in the number of the primitive erythroid cells (Figure 3.7), making it a potential HSCs deficient mutant, despite its severe phenotype during early development.

Although *foxn1* expression, a thymus epithelial cell marker, was positive in all the mutants, its expression in some of the mutants appeared to be smaller and condensed. This phenotype was similar to the *foxn1* expression in HSCs deficient mutant *cloche* (Schorpp et al., 2002), suggesting the thymus rudiment formation in these mutants are normal, but failed to further expand due to the absence of T cell precursors. In addition, the normal morphology of the 12 mutants also suggested that the pharyngeal epithelial cells could develop normally and form the thymus rudiment. Thus, the initiation of the thymus rudiments in our mutants were not affected, and the main defects could be either on the T lymphocyte precursors or the migration of these precursor cells.

Through the observation of blood circulation, we have shown that with the exception of mutant 260, the 12 morphologically normal mutants have normal primitive blood cell development, which indicate their defects could be specifically in the lymphoid lineage cells. However, we did not examine the blood circulation after 5dpf when the definitive red blood cells start to proliferate (Weinstein et al., 1996). Therefore, although the primitive blood formation is normal in these 12 mutants, they may have defects in both definitive erythropoiesis and lymphopoiesis. Most of our mutants died within 10dpf, which may be due to developmental failure in other organs. This early lethal phenotype makes it impossible for us to examine the mutation in B lymphocyte development since B lymphocytes in zebrafish are first detected in kidney by *rag1* expression on 21dpf (Willett et al., 1999). Considering the zebrafish *rag1* mutant can survive to adulthood without special attention (Wienholds et al., 2002); the early lethal phenotype of our mutants exclude the possibility that their corresponding genes for the mutations are *rag1* itself.

3.4 Conclusions and Future Work

13 mutants, comprising one HSCs mutant and 12 lymphoid precursor mutants, are selected for future analysis. Since the 12 lymphoid precursor mutants are morphological normal and similar, complementation test should be fulfilled before detailed characterizations and positional cloning are carried out. In addition, it is also important to further characterize these mutants using other molecular approaches. Histological section can help us define the disrupted cell population in the mutant thymus, whereas lymphoid cell migration and homing can be examined by cell transplantation. Studies from these mutants will provide invaluable information about the early T cell development.

Table 3.1 Summary of *rag1* Genetic Screen

	Number
Founder Fish	7
F1 Fish	~700
F2 Families	330
Screened F2 Families	270
Successful Crosses	1551
Successful Crosses per Family	5.74
Primary Identified Mutants	422
Identified Mutants Family	180
Rescreen Confirmed Mutants	140
Rescreen Confirmed Mutants Family	110
Identified F3 Mutants Family	86
Final Maintained Mutants	13

Chapter IV: Microarray Analysis of Gene Expression Profiles in Zebrafish *cloche* Mutant

4.1 Background

Zebrafish serves as an excellent model organism for the study of early hematopoiesis development in vertebrate. So far, more than 30 hematopoiesis-defected zebrafish mutants have been isolated (Ransom et al., 1996; Weinstein et al., 1996), of which the *cloche* (*clo*) mutant has one of the most interesting phenotypes (Stainier et al., 1995). The zebrafish *clo*^{m39} mutant was originally isolated from an Indonesian fish farm in search for spontaneous mutations affecting early development, and till now, 2 more alleles (*clo*^{s5}, *clo*^{m378}) were identified by Stainier and Driever's group. Molecular and genetics studies showed that *clo* acts upstream of stem cell leukemia (*scl*) and endothelial growth factor (VEGF) receptor *flk-1*, and is required for the development of both hematopoietic and endothelial lineage cells (Liao et al., 1998; Thompson et al., 1998), implying that the *clo* mutation affects development of the hemangioblast, a common progenitor of hematopoietic and vascular endothelial cells. Hence, cloning of the *clo* gene and identification of its downstream targets will shed light on our understanding on the molecular basis underlying the initiation and differentiation of hematopoietic and endothelial lineages as well as subsequent specification of the distinct blood cell types. With the availability of zebrafish cDNA Microarray and Affymetrix array, gene expression profiling analysis would be a powerful approach to identify downstream target genes perturbed in *clo* mutants. Since most of early hematopoietic events occur before 24 hr in zebrafish and it was hard to differentiate *clo* mutant from wild-type sibling based on morphology before 24 hpf, isolating large numbers of *clo* homozygous mutant embryos at the early stage became a big obstacle

for early gene profiling analysis. To overcome this restriction, I developed a method using amplified cDNA probes derived from single embryo for gene expression comparative analysis on the 18-somite *clo* mutant and wild-type sibling embryos. The study resulted in identification of the 13 *clo* downstream target genes that have not been reported previously. We further showed that this amplified cDNA approach is comparable and complementary to that of the conventional unamplified method using large numbers of pooled embryos, demonstrating that it is well suited for zebrafish embryo gene expression profiling analysis.

4.2 Results

4.2.1 Single Embryo cDNA Library Construction

The method for the single embryo cDNA library construction was adapted from SMART (switching mechanism at the 5' end of the RNA transcript) technology (Clontech), which takes advantage of the template-switching activity of Moloney Murine Leukemia Virus (MMLV) reverse transcriptase to synthesize and anchor first-strand cDNA in one step (Zhu et al., 2001). The strategy for this method is illustrated in Figure 4.1. The first-strand cDNA synthesis is carried out in the presence of two oligonucleotides: a "lock-docking" primer that contains a universal sequence and oligo-d(T), and an SMART II A oligonucleotide that contains the universal sequence. When reverse transcriptase reaches the 5'end of the mRNA, the enzyme's terminal transferase activity adds additional nucleotides (predominantly dCTP) that are not encoded by the template. The SMART II A oligonucleotide contains three consecutive rG nucleotides at the 3' end to serve as a second template for reverse transcriptase. When reverse transcriptase reaches the 5' end of the mRNA, the complementary interaction of the r(G)3 stretch at the 3' end of the SMART II A oligonucleotide and dC-rich extended sequence of the cDNA promotes template switching. Reverse transcriptase then transcribes the

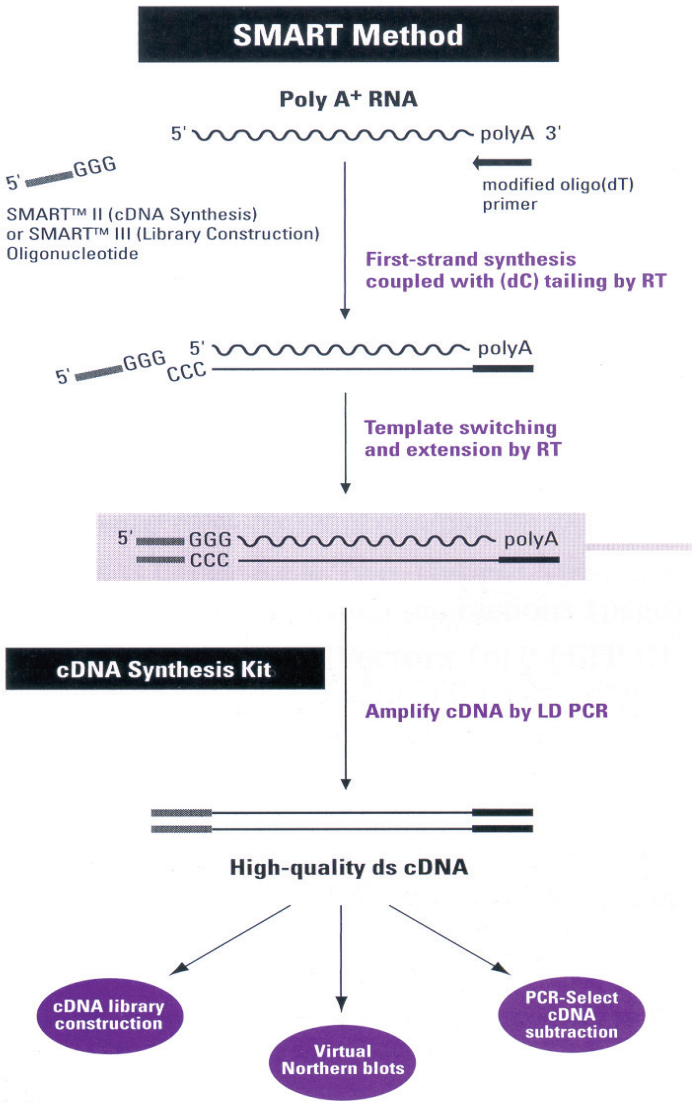

Figure 4.1 Scheme of the SMART cDNA Library Construction Method. (Adopted from SMART™ PCR cDNA Synthesis Kit User Manual, Clontech, 2001)

oligonucleotide, adding the universal sequence as an anchor to the end of first-strand cDNA. The resulting full-length, single-stranded (ss) cDNA contains the universal sequence at both the 5' and 3' ends. This anchor sequence is then used as priming sites for end-to-end cDNA amplification by long-distance PCR to generate the amplified single embryo cDNA library. To ensure each sample was amplified properly, cDNA within the exponential phase was examined by electrophoresis and result showed that each amplified sample yielded an evenly distributed smear of DNA (Figure 2.3). Virtual northern by using low-abundance marker *gata1* and large size marker *flk1* (4.6kb) also ascertained that the cDNA library was well constructed (Figure 4.2).

4.2.2 Isolation of 18hpf *clo* Homozygous Mutant Embryos

Previous studies by whole-mount *in situ* hybridization analysis have shown that many early hematopoiesis-specific genes, such as *scl*, *gata1* and embryonic *globins*, appear to express more abundantly from 18hpf to 24hpf in wild-type fish, but be down-regulated in *clo* mutant (Thompson et al., 1998). We therefore chose to compare the gene expression profile of the 18-somite *clo* mutant and wild-type/heterozygous sibling embryos in the hope of increasing the possibility of identifying potential target genes involved in early hematopoiesis. One difficulty, however, was to isolate large numbers of the 18-somite stage *clo* homozygous mutant embryos due to their indistinguishable morphology from the wild-type/heterozygous siblings before 24hpf. To solve this problem, 18hpf single embryo was randomly collected from mating of two heterozygous *clo* adult fish and homogenized to extract total RNA. To distinguish the *clo* mutant from wild-type sibling embryos, each RNA sample was 'genotyped' by examining the expression of *flk1*, *scl*, *lmo2*, *gata1* and *βe1-globin* that are known to be either absent or greatly reduced in *clo* mutant at this stage. As shown in Figure 4.3, semi-quantitative RT-PCR assays showed that several samples, such as samples e4, e7 and e9, lacked expression of *flk1*,

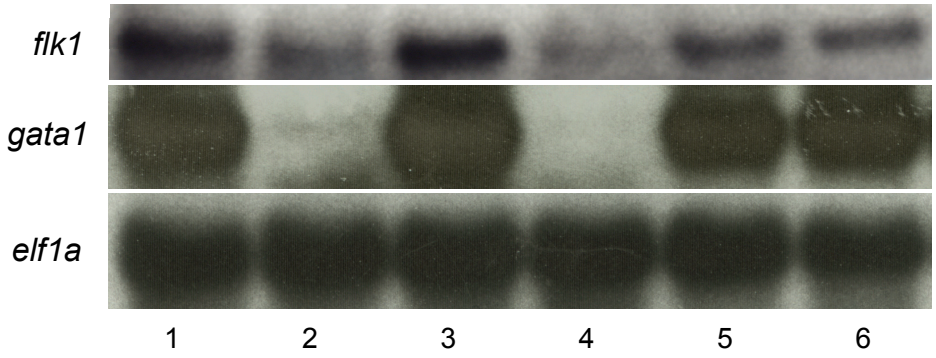

Figure 4.2 Quality Examination of Single Embryo cDNA Library by Virtual Northern. Amplified cDNAs from single embryo were transferred to the Hybond-N^+ membranes. Virtual Northern was used to examine the quality of each constructed cDNA library using *flk1* and *gata1* as probes, while *elf1a* was used as loading control. The strong detection of large size transcript *flk1* and low abundant gene *gata1* indicated the good quality of amplification. The absence of *flk1* and *gata1* bands in lanes 2 and 4 indicated these two embryos were *clo* mutants.

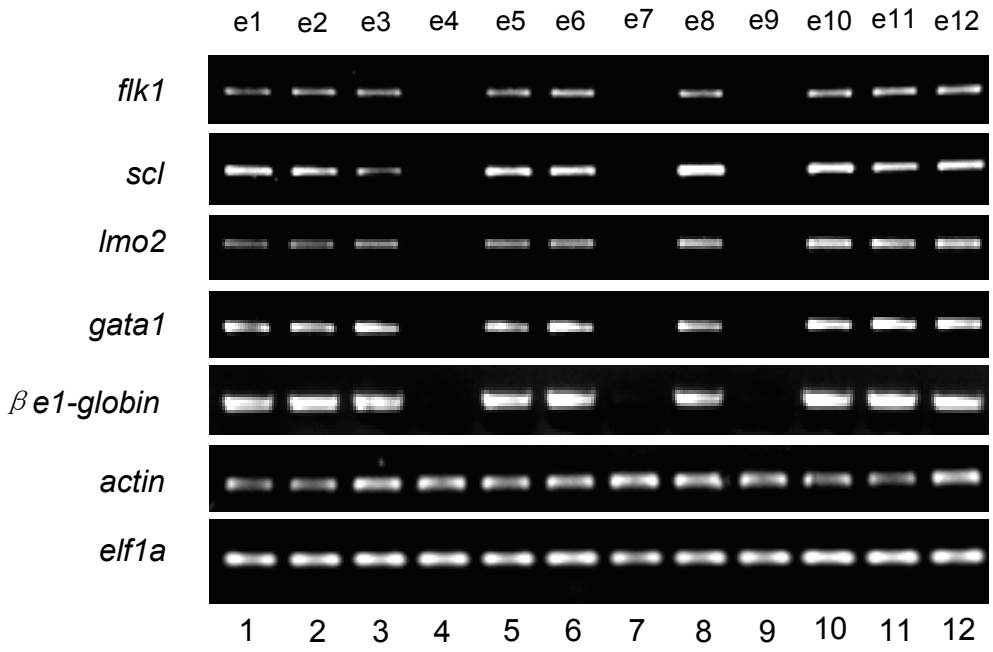

Figure 4.3 "Genotyping" of the 18-Somite *clo* Homozygous and Wild-Type/Heterozygous Sibling Embryos by Semiquantitative Reverse Transcriptase-Polymerase Chain Reaction (RT-PCR). Equal amount (1/10) of cDNA from the randomly selected single 18-somite embryo was subjected to semiquantitative PCR analysis with specific primers for zebrafish *flk1*, *scl*, *lmo2*, *gata1*, and *βe1-globin. actin* and *elf1a* were used as control to indicate the amount of cDNA used. Lanes 4, 7, and 9 are *clo* mutants, whereas the other lanes (lanes 1,2,3,5,6,8,10,11 and 12) represent wild-type or heterozygous sibling embryos.

scl, *lmo2*, *gata1* and *βe1-globin*. In fact, of the 96 samples examined, 23 lacked expression of the five mentioned genes. This number is close to the expected Mendelian segregation ratios. Subsequently, cDNAs from potential *clo* or sibling single embryo were amplified by single embryo cDNA library construction method. After that, each constructed cDNA library was qualified by DNA electrophoresis and virtual northern blot assay (Figure 4.4). The virtual northern results confirmed that the RNA samples deficient in *flk1*, *scl*, *lmo2*, *gata1* and *βe1-globin* expressions were indeed derived from the *clo* homozygous mutant embryos, whereas others represented the wild-type/heterozygous sibling embryos, and the amplified cDNAs were of good enough quality for further Microarray analysis.

4.2.3 Affymetrix Array Using Amplified Approach

In order to reduce the variation of the microarray analysis, five of the single embryo cDNAs from the *clo* mutant embryos or wild-type/heterozygous siblings were pooled together and subjected to PCR amplification. A pair of modified universal primers, in which a T7 promoter sequence was inserted in the 3' primer (Table 2.1C), was used for PCR amplification so that probe labeling could be carried out by in vitro transcription with T7 RNA polymerase. To ensure each sample was amplified properly, DNA within the exponential phase was examined by electrophoresis and result showed that each amplified sample yielded an evenly distributed smear of DNA (Figure 4.4A). Virtual Northern blot analysis confirmed that *flk1*, *gata1* and *βe1-globin* transcripts remained either undetectable or greatly reduced in the *clo* mutant samples after amplification (Figure 4.4B), indicating that the amplified cDNA samples were well constructed. The amplified cDNAs were then biotin-labeled by *in vitro* transcription with T7 RNA polymerase and applied on the Affymetrix chip representing ~14,900 zebrafish unique EST clusters. The intensity of each fluorescent dye hybridized on a single spot was

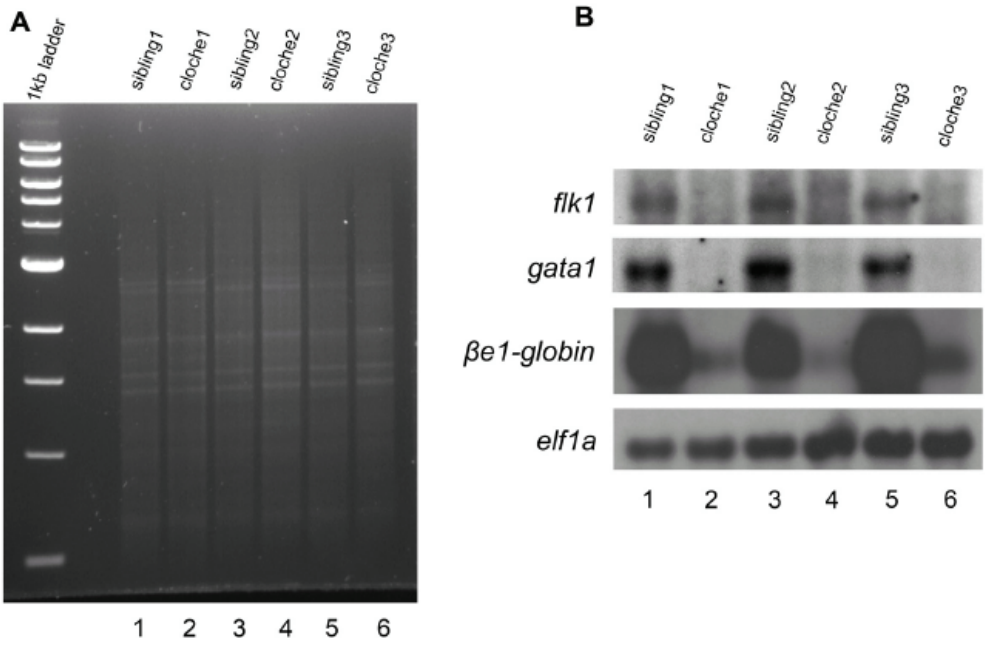

Figure 4.4 Analysis of Amplified cDNA Quality. **A:** DNA electrophoresis analysis. 100ng of each amplified cDNAs derived from the single 18-somite *clo* homozygous mutants (lanes 2, 4 and 6) and wild type or heterozygous sibling (lanes 1, 3 and 5) was separated on 1% agarose gel. Ethidium bromide staining shows an evenly distributed smear of DNA in each lane. **B:** Virtual Northern analysis. cDNAs of (A) were transferred to a Hybond-N^+ membrane and probed with digoxingenin-labeled *flk1*, *gata1*, *βe1-globin* and *actin*. While *elf1a* transcript was maintained at a similar level in all the samples, expression of *flk1*, *gata1* and *βe1-globin* were either absent or drastically reduced in *clo* mutant embryos (lanes 2, 4 and 6).

calculated using Affymetrix Microarray Suite 5.0 Software (MAS 5.0) and the spots with a ratio of greater than 1.5-fold were scored as positive. Three sets of independent experiments were performed and those clones scored positive in at least two of the three experiments were selected as potential differentially expressed targets. In total, 37 potential down-regulated targets were identified. Among these clones, 18 of them (listed in Table 4.1 under category I) are well-known early hematopoiesis- and endothelial-related genes arrayed on the Affymetrix chip. There was no obvious up-regulated clone found from the Affymetrix arrays. To evaluate the reproducibility of Affymetrix array, R^2 values of any two experiments were calculated. The consistent results, 0.9830, 0.9777, 0.9859 from each comparison, indicated that our Affymetrix array results were reproducible.

4.2.4 Affymetrix Array Using Conventional Approach

To further evaluate the result obtained by the amplified approach, we sought to compare, in parallel, with the standard method using large numbers of pooled embryos. Fortunately, we have generated a heterozygous *clo* line carrying the homozygous EGFP transgene under the control of the zebrafish *flk1* promoter (Jin et al., 2005b), in which the 18-somite *clo* homozygous embryo can be distinguished from wild-type and heterozygous sibling based on alteration of the EGFP expression under the stereomicroscope (Figure 4.5). Total RNA was prepared from one hundred 18-somite *clo* homozygous embryos or the wild-type/heterozygous siblings, labeled with biotin according to the manufacture's protocol and applied onto the Affymetrix chip. Similar to the single embryo method, three sets of experiments were conducted. Through software analysis, we found 39 potential targets, among which included 22 well-known early hematopoiesis- and endothelial-related genes. The R^2 values of each two experiments

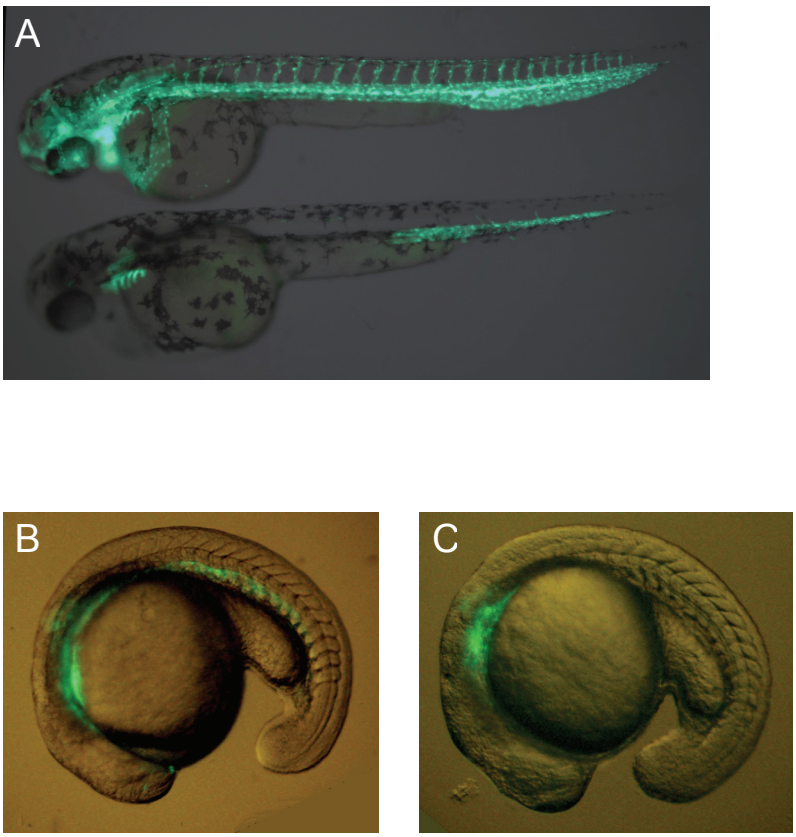

Figure 4.5 Vascular Expression of *Tg*(*flk1:EGFP*) in Wild-Type and *clo* Mutant at 2dpf and 18-somite stage. In 2dpf wild-type *flk1* promoter driven transgenic fish (upper fish in panel A), EGFP expression can be visualized in all the blood vessels, whereas in the *clo* mutant (lower fish in panel A), only part of the vessels in the gill and tail regions have EGFP expression. At 18-somite stage, both anterior lateral mesoderm (ALM) and posterior later mesoderm (PLM) have EGFP expression in wild-type embryo (panel B), while in the *clo* mutant embryo (panel C), EGFP is expressed only in ALM region.

are 0.9921, 0.9835 and 0.9761, evidently demonstrated that our conventional method is as reproducible as single embryo methods when applied on Affymetrix arrays.

4.2.5 Affymetrix Results Validation

Although Affymetrix array showed a total of 49 genes down-regulated in *clo* mutant from both methods, the validity of these results need to be corroborated by other approaches. We examined the expression level of these potential clones by semi-quantitative PCR, and found that 84% (31/37) and 90% (35/39) of the clones from the amplified and conventional methods, respectively, were indeed differentially expressed in *clo* mutant and wild-type/heterozygous sibling (Figure 4.6). Further comparison between the PCR confirmed clones from both methods revealed that 26 of the 31 clones identified by the amplified approach overlapped with those obtained by the conventional unamplified method. In summary, 40 clones were found to be down-regulated in *clo* mutant (Table 4.3).

4.2.6 Amplified Vs Conventional Approach

To collate the Affymetrix results from amplified and conventional methods, firstly, we investigated the standard array quality metrics, including Raw Q, Background, Scaling Factor, Percent Present Call, GAPDH 3'/5' ratio and actin 3'/5' ratio. As shown in Table 4.2, these parameters were all comparable and within the appropriate range, indicating that both approaches gave rise to similar array quality. Next, we examined the Signal Intensities of any given two experiments obtained within each approach and results showed that their patterns and R^2-values (0.9830 and 0.9921 for amplified and unamplified methods, respectively) were comparable (Figure 4.7), affirming that the reproducibility of the amplified approach was similar to that of the standard unamplified method. In fact, semi-quantitative RT-PCR, which showed that 26 of the 31 clones

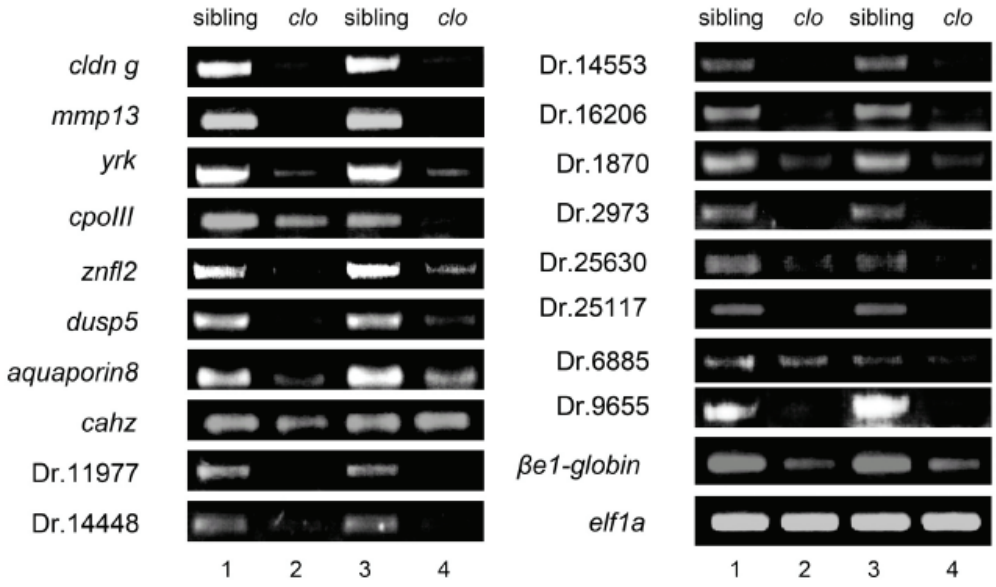

Figure 4.6 Verification of Target Clones by Semi-Quantitative RT-PCR. 1**µ**g of total RNA sample (20 embryos/each) derived from the wild type sibling (lanes 1 and 3) and *clo* mutant embryos (lanes 2 and 4) were reverse transcribed and subjected to PCR analysis with specific primers corresponding to each of the perspective target genes. PCR products were electrophoresed on 1% agarose gel and stained with ethidium bromide. *βe1-globin* and *elf1a* were used as internal controls.

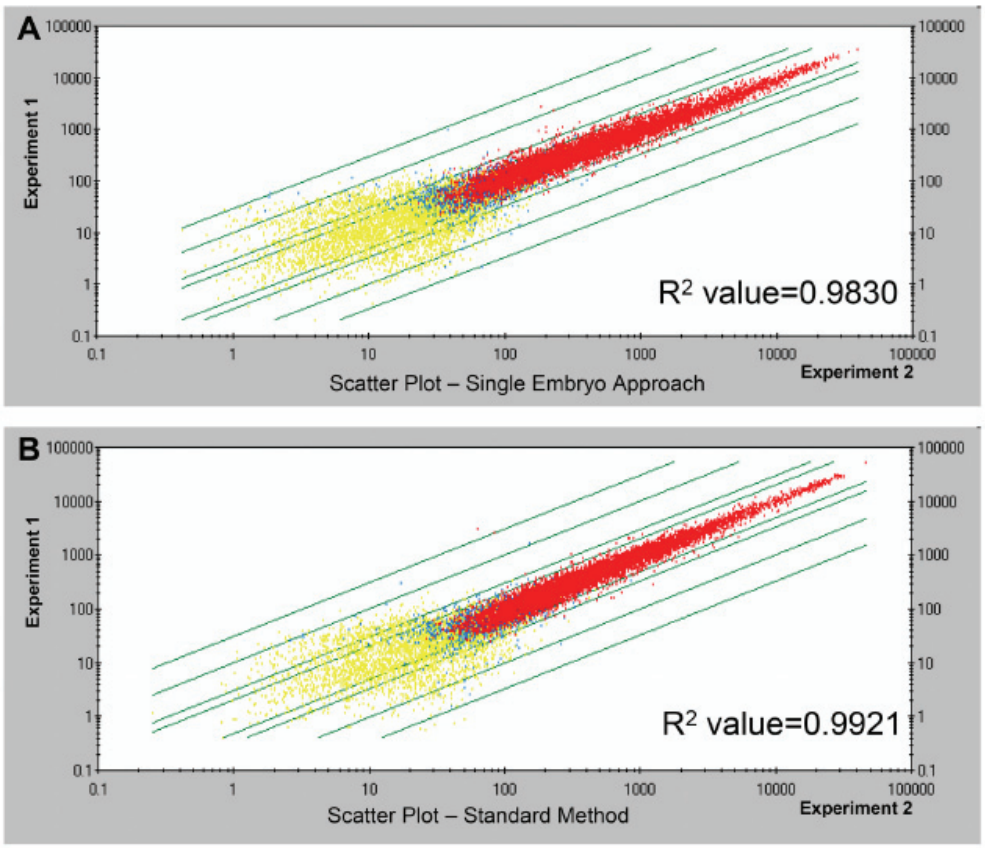

Figure 4.7 Reproducibility of Affymetrix Arrays. The scatter plots of signal intensity were generated to assess the reproducibility of duplicated samples. A-B**:** Comparison of any two experiments of either the approach with limited embryos (A) or standard unamplified method (B) shows that the scatter plot patterns and R^2-values between two experiments of each approach are similar with the majority of the present spots (red spots) within a narrow range. The R^2-value is indicated at the bottom right-hand side.

identified by the amplified approach were common among those of the 35 clones from conventional method, also gave similar conclusion. These results clearly demonstrated that the amplified approach is comparable to the conventional method. Remarkably, although majority of positive clones were detected by both method, there were still 14 clones uncovered only by one method (5 from amplified method and 9 from conventional method), suggesting that the amplified approach is also complementary to that of the conventional unamplified method.

4.2.7 Gene Expression Analysis

After microarray analysis and semi-quantitative PCR confirmation, a total of 40 clones showed absence or dramatic decrease in expression in *clo* mutant. Among these 40 clones, 22 of them are well-known early hematopoiesis- and endothelial-related genes. Since the involvement of a gene during development could be indicated by its expression pattern, temporal and spatial expressions of the remaining 18 differentially expressed clones were investigated by whole-mount *in situ* hybridization analysis. WISH results showed that nine target genes, coproporphyrinogen oxidase (*cpo*), carbonic anhydrase (*cahz*), claudin g (*cldn g*), zinc finger-like gene 2 (*znfl2*), neutrophil cytosol factor 1 (*ncf1*), matrix metalloproteinase 13 (*mmp13*), dual specificity phosphatase 5 (*dusp5*), aquaporin 8 (*aqp8*) and *Dr.9655* (Dailey, 2002; Peterson et al., 1997; Kollmar et al., 2001; Yoda et al., 2003; Volpp et al., 1989; Leeman et al., 2002; Kwak and Dixon, 1995; Sudol et al., 1993; Yang et al., 2005) were predominantly expressed in hematopoietic and vascular endothelial cells.

As shown in Figure 4.8, *znfl2*, *cldn g*, *cpo* and *cahz* are erythrocyte-specific. *znfl2* was first detected at 3-somite stage as a single pair of stripes in the posterior lateral mesoderm (Figure 4.8A). The two stripes subsequently extended anteriorly and posteriorly and finally merged along the midline in the ICM region at around 18- to 20-

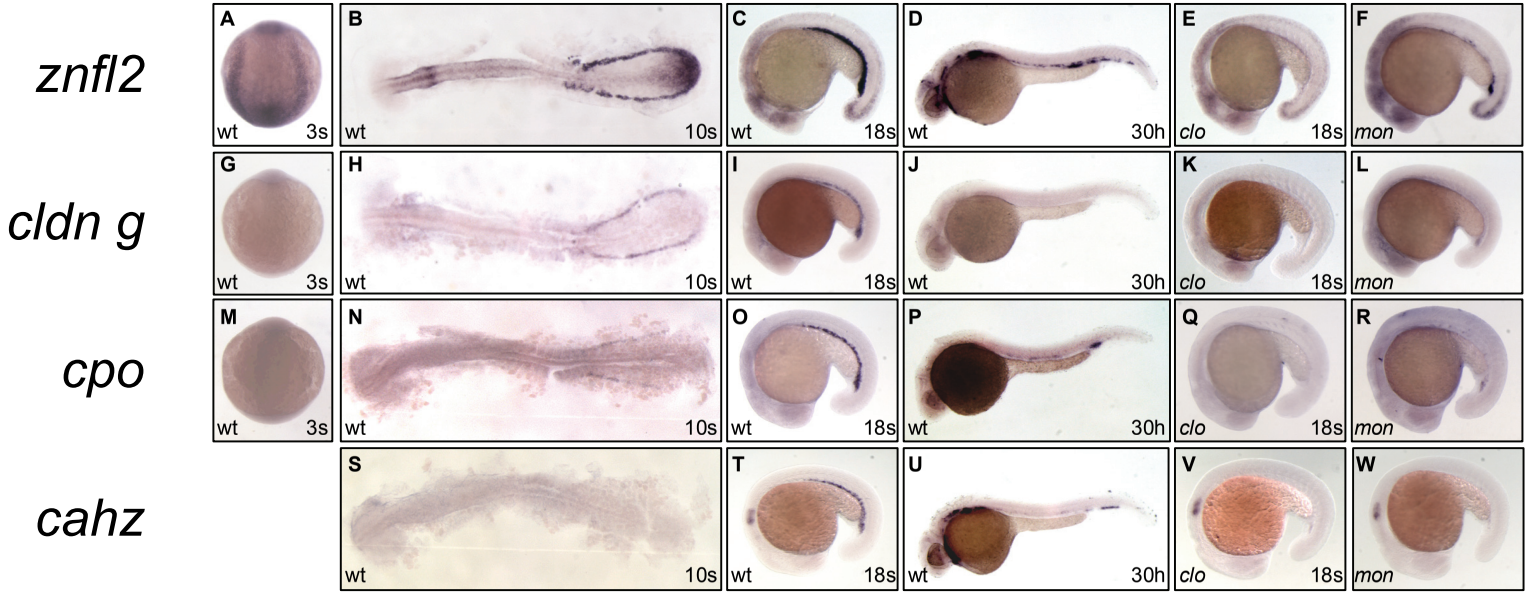

Figure 4.8 Erythroid-Specific Affymetrix Target Genes. *znfl2*, *cldn g*, *cpo* and *cahz* are specifically expressed in the erythroid cells. Panels A to D show the expression of *znfl2* in 3s, 10s, 18s and 30h wild-type embryos. Panels H to J show the expression of *cldn g* in 10s, 18s and 30h wild-type embryos. Panels N to P show the expression of *cpo* in 10s, 18s and 30h wild-type embryos. Panels T and U show the expression of *cahz* in 18s and 30h wild-type embryos. The expression of these four genes in the *clo* mutants (panels E,K,Q,V) and *mon* mutants (panels F,L,R,W) are dramatically decreased or completely lost. 3-somite (3s) embryos are dorsal view (panels A,G,M), while the 10-somite (10s) embryos are flat-mounted in dorsal view (panels B,H,N,S). The rests of the embryos are lateral view.

somite stage (Figure 4.8 B,C). Its transcript was clearly reduced by 30hpf (Figure 4.8D). This expression is similar to the pattern of the early erythrocyte marker *gata1* (Detrich, III et al., 1995), suggesting that *znfl2* is expressed in erythrocyte. The *cldn g*, *cpo* and *cahz* transcripts emerged later at around 10- (*cldn g* and *cpo*) to 14-somite stage (*cahz*) as two stripes in the posterior lateral mesoderm, extended toward both anterior and posterior directions and fused at around 18- to 20-somite stage (Figure 4.8 H,I,N,O,T). Similarly, their transcripts were reduced in the ICM region by 30hpf (Figure 4.8 J,P,U), a pattern more similar to that of embryonic *globin* (Brownlie et al., 2003). As expected, expressions of *znfl2*, *cldn g*, *cpo* and *cahz* were either absent or greatly reduced in the *clo* and erythrocyte-deficient *moonshine* (*mon*) (Ransom et al., 2004; Ransom et al., 1996; Weinstein et al., 1996) mutant embryos (Figure 4.8 E,F,K,L,Q,R,V,W). Taken together, these observations demonstrate that *znfl2*, *cldn g*, *cpo* and *cahz* are predominantly expressed in erythroid lineage cells. Notably, in addition to the ICM, the *cahz* transcript was also detected in the otic capsule where its expression remained unchanged in the *clo* and *mon* mutant embryos (Figure 4.8 T,V,W). The biological meaning of this otic capsule expression, however, is unclear.

Both *mmp13* and *ncf1* appear to fall into the myeloid-specific group of genes (Figure 4.9). The *mmp13* transcript was first detected at around the 10-somite stage in the region close to the rostral blood island where the primitive myeloid lineage is believed to arise (Lieschke et al., 2002) (Figure 4.9A). At the 18-somite stage the number of *mmp13*-positive cells increased and scattered around the anterior region of the yolk sac (Figure 4.9B). By 36hpf a small number of *mmp13*-positive cells began to emerge in the posterior region of the ICM (Figure 4.9C). Thus, *mmp13* is expressed in a manner similar to that of the myeloid lineage marker *pu.1* from 10- to 18-somite stages (Lieschke et al., 2002) and *lysozyme-C* at 36hpf (Liu and Wen, 2002). The *ncf1* displayed an overlapping but slightly distinct expression pattern compared to *mmp13*. It emerged at

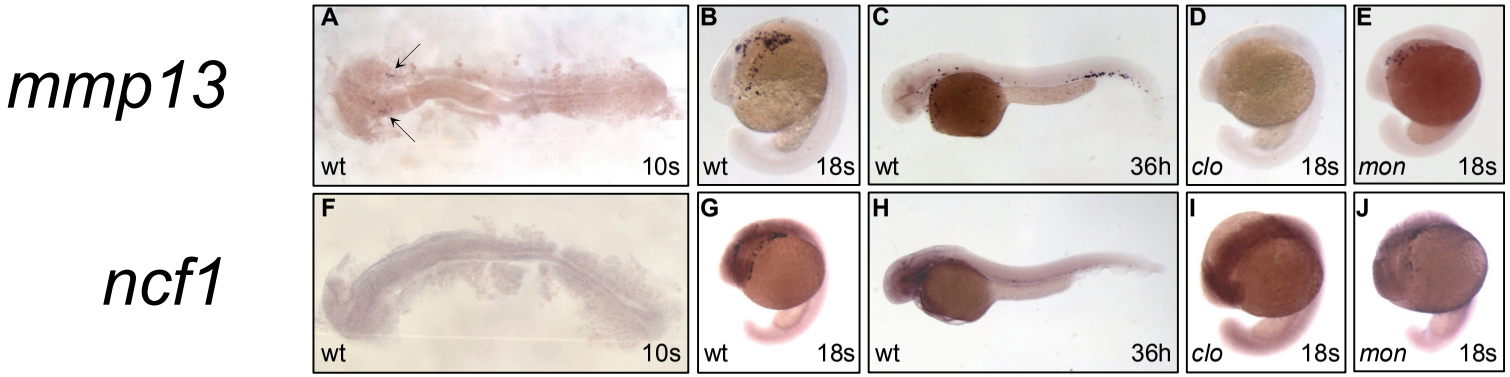

Figure 4.9 Myeloid-Specific Affymetrix Target Genes. *mmp13* and *ncf1* are specifically expressed in the myeloid cells. Panels A to C show the expression of *mmp13* in 10s, 18s and 36h wild-type embryos. Panels G and H show the expression of *ncf1* in 18s and 36h wild-type embryos. Although the expression of these two genes in the *clo* mutants (panel D,I) are completely lost, their expression in the *mon* mutants (panel E,J) are still normal. 10-somite embryos (10s) are flat-mounted in dorsal view (panels A,F), whereas the rests of embryos are lateral view.

around the 14-somite stage in the rostral blood island region, increased and scattered around the anterior region of the yolk sac at 18- to 20-somite stage (Figure 4.9G). However, by 36hpf the *ncf1* expression was almost undetectable (Figure 4.9H). Given it emerges from the region close to the rostral blood island and the mammalian counterpart is highly expressed in neutrophil (Heyworth et al., 2003), we believe zebrafish *ncf1* is also expressed in myeloid lineage cells. To provide additional evidence to support the argument that *mmp13* and *ncf1* are myeloid lineage-specific, whole-mount *in situ* was also carried out on the 18-somite stage *clo* and *mon* mutant embryos. Our result showed that, while expression of *mmp13* and *ncf1* was absent in the *clo* mutant embryos (Figure 4.9 D,I), their transcripts remained unchanged in the erythrocyte-deficient *mon* mutant embryos (Figure 4.9 E,J). These results show that both *mmp13* and *ncf1* are specifically expressed in myeloid lineage.

The last three genes, *dusp5, aqp8* and *Dr. 9655*, are vessel enriched genes. As shown in Figure 4.10, the transcript of *dusp5* was first detected at around 3-somite stage as two pairs of stripes, one in the head and another in the lateral mesoderm (Figure 4.10A). In the head region, the *dusp5*-expressing cells were mainly localized anteriorly and posteriorly to the eye (Figure 4.10B). Intriguingly, at around 6- to 8-somite stages, a third pair of stripes along the inner region of the lateral mesoderm stripes began to emerge (Figure 4.10B). The outer bilateral pairs of stripes, which appeared similar to the lateral mesoderm stripes representing the hematopoiesis-endothelial cells, extended anteriorly and posteriorly from 10-somite stage onward and converged in the midline at around the 18 to 20-somite (Figure 4.10C). By 24hpf, *dusp5* was mainly expressed in the trunk as two stripes where the dorsal aorta and axial vein forms (Isogai et al., 2001) (Figure 4.10D). This expression pattern is particularly similar to that of vascular endothelial marker *fli1* (Brown et al., 2000), suggesting that *dusp5* is likely to be expressed in vascular endothelial cells. This argument was further supported by the finding that the

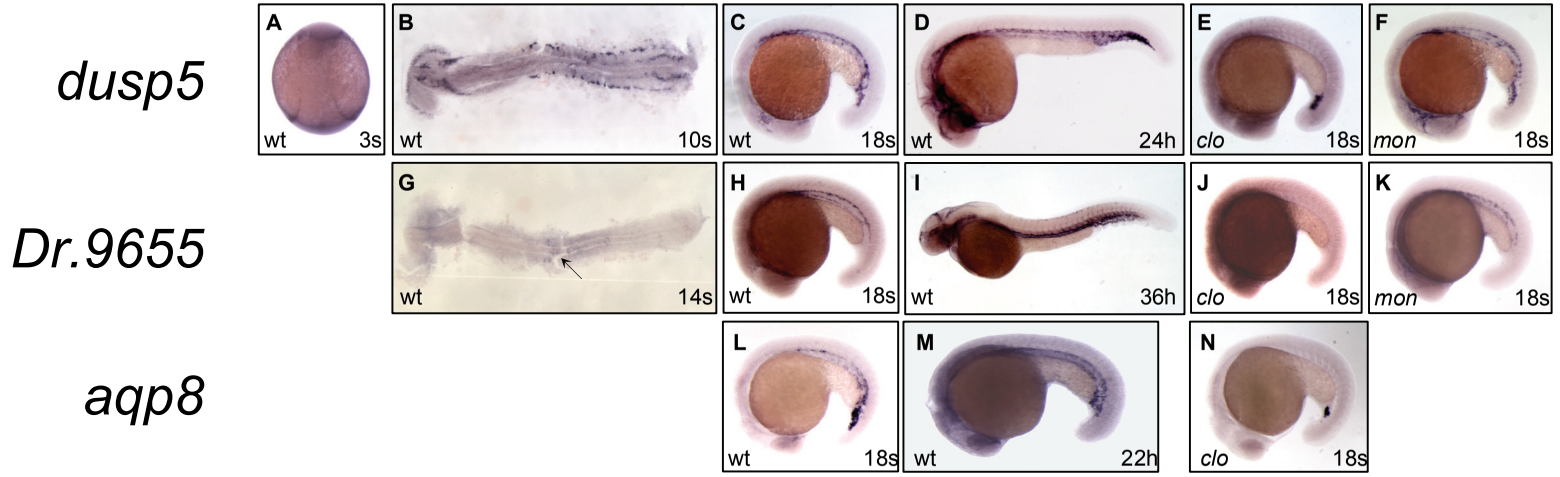

Figure 4.10 Vascular-Specific Affymetrix Target Genes. *dusp5*, *Dr.9655* (*zvsg1*) and *aqp8* are specifically expressed in the vascular cells. Panels A to D show the expression of *dusp5* in 3s, 10s, 18s and 24h wild-type embryos. Panels G to I show the expression of *Dr.9655* (*zvsg1*) in 14s, 18s and 36h wild-type embryos. Panels L and M show the expression of *aqp8* in 18s and 22h wild-type embryos. The expression of these three genes in the *clo* mutants (panel E,J,N) are dramatically decreased, while the expression of *dusp5* and *Dr.9655* (*zvsg1*) are normal in the *mon* mutants (panel F,K). 3-somite embryo (panel A) is dorsal view, while 10-somite (panel B) and 14-somite (panel G) are flat-mounted in dorsal view. The rests of embryos are lateral view.

dusp5 transcript was absent in the 18-somite stage *clo* but not erythrocyte-deficient *mon* mutant embryos (Figure 4.10 E,F). The inner lateral stripes behaved similarly to the *biklf*-enriched inner stripes (Kawahara and Dawid, 2000). It appeared at around 6- to 8-somite and soon diminished by 18-somite stage. As expected, the inner stripes were not affected in both *clo* and *mon* mutants, indicating that they might not be hematopoietic and endothelial lineage cells. In contrast to the broad temporal and spatial expression of *dusp5*, another two genes, *aqp8* and *Dr.9655*, in this group displayed an expression more concentrated in the blood vessel endothelial cells. At 18-somite stage, *aqp8* is expressed in the blood vessel endothelial precursors at ICM region, more substantially in dorsal aorta (Figure 4.10L). At 22hpf, both the dorsal aorta and posterior cardinal vein were stained with equal density of the *aqp8* transcripts (Figure 4.10M). This expression pattern of *aqp8* was very similar to that of the vascular endothelial marker *flk1*. The last gene, *Dr. 9655*, in this group began to express as a cluster of cells in the position between the third and fourth somite at 14-somite stage (Figure 4.10G). These *Dr. 9655*-positve cells extended posteriorly from 18-somite onwards and were subsequently detected in the dorsal aorta, choroidal vascular plexus and intersegmental vessel by 36hpf (Figure 4.10I). Similar to *dusp5*, *Dr.9655* transcript was absent in the *clo* mutant embryos but was not affected in the *mon* mutant embryos (Figure 4.10 J,K). In summary, the observations clearly show that *dusp5, aqp8* and *Dr. 9655* are specifically expressed in vessels and may play roles in vasculargenesis and angiogenesis.

Taken all together, the whole-mount *in situ* analyses demonstrate that the nine target genes (*cpo*, *cahz*, *znfl2*, *cldn g*, *mmp13*, *ncf1*, *dusp5, aqp8* and *Dr.9655*) are indeed down-regulated in the *clo* mutant embryos, which are in consistence with the semi-quantitative RT-PCR analyses. Thus, we believe that the remaining nine clones (*yrk*, *Dr. 6885*, *Dr. 11977*, *Dr. 25117, Dr.1870, Dr. 14448, Dr.14553, Dr.16206* and *Dr. 25630*),

although they fail to show specific expression pattern in whole-mount *in situ* hybridization, are also most likely to be down-regulated in *clo* mutant.

4.2.8 Sequence Analysis and Generation of Full-length cDNA Clone

To explore the genome structure and mammalian orthologue of these target genes, I blasted their sequences over two zebrafish genomic servers, NCBI (http://www.ncbi.nlm.nih.gov/genome/guide/zebrafish/index.html) and Ensembl (http://www.ensembl.org/Danio_rerio/index.html), which contain the latest and most comprehensive resources of zebrafish genome, ESTs and genes (Table 4.4). Through genomic blasting, all clones, except *Dr.25117*, were located on a certain lineage groups (Table 4.4). Moreover, 13 clones (*cld g, mmp13, yrk, cpo, znfl2, dusp5, aqp8, cahz, ncf1, Dr.11977, Dr.16206, Dr.9655, Dr.25117*) have full-length cDNA sequences in GeneBank, and their Gene IDs were listed in Table 4.4. To examine their functions from detailed sequence analysis, T-coffee multiple sequences alignment program was applied to achieve protein comparisons among different organisms (Poirot et al., 2004). As shown in Figure 4.11, 9 out of the 18 newly identified target genes, including *cpo, cahz, cldn g, znfl2, ncf1, mmp13, dusp5, aqp8* and *yes-related kinase* (*yrk*) are known genes that have high homology to their mammalian counterparts and have been reported in other vertebrate species, but the functions relating to hematopoiesis and vessel development for most of these genes have yet to be fully illustrated. In addition, clone *Dr.16206* is predicted similar to embryonic transglutaminase and with about 50% identity to mouse coagulation factor XIII; clone *Dr.25117* matches a mammalian cDNA sequence that is predicted to encode a hypothetical protein (FLJ13263), whereas clone *Dr. 11977* shares low similarity (35% identity) with a functional unknown human ELLP3030 cDNA. No mammalian homologues were found for the remaining six clones, *Dr.6885, Dr.9655, Dr.25630, Dr.1870, Dr.14448* and *Dr.14553*, suggesting that they either contain partial

sequences, probably a noncoding region in this case, or encode genes that are unique to fish. To further investigate these six genes, 5' and 3' RACE were carried out to generate the full length cDNA clones. So far, only one full length cDNA clone, *Dr.9655,* which contains 1910 nucleotides and encodes a protein of 410 amino acids, was obtained from RACE. Since there is neither mammalian homologue nor annotations from the zebrafish database, based on the expression pattern of this gene, we named it as *zvsg1*, acronym for *zebrafish vessel-specific gene 1*, and the sequence was submitted to Genbank with accession ID NM_001014364.

4.3 Discussion

4.3.1 Single Embryo Approach

With the wide, growing interest in large scale genomic research, robust and reliable methods to isolate and manipulate small amount of samples need to be developed. Although amplification processes through *in vitro* transcription or PCR have been described in tissue culture or laser ablation cells(Wang et al., 2000; Iscove et al., 2002), method suitable for zebrafish embryos has yet been reported. Here I described a method using amplified cDNAs from single embryo to compare the gene expression profiles of the 18-somite *clo* mutant with wild-type/heterozygous sibling embryos on Affymetrix DNA microarray. Our results show that this amplified approach is able to identify differentially expressed genes in a manner similar to that of the standard unamplified method.

Among the 37 potential clones from single embryo arrays, 31 of them were confirmed by semi-quantitative RT to be down-regulated in *clo* mutant compared to the wild-type/heterozygous sibling. Hence, the ratio of true positive clones is 84% of the potential candidates and this is comparable to that of conventional approach at 90% (35/39). Although, with the exception of *plexind I, band4.1, ikaros and hhex*, the amplified

approach had successfully identified 18 early well-known hematopoietic- and endothelial- related genes arrayed on the Affymetrix chip that served as positive controls and this largely assured the quality of the array results. Failure to detect the mentioned four genes could be due to a bias generated by the PCR amplification. However, the bias is low as it only eliminated a few of the positive signals. On the other hand, in comparison to the conventional approach, the PCR amplification method has rendered advantages by elevating the levels of low expression genes that are differentially expressed in the mutant and wild-type sibling so that they can be detected on the array. Indeed, from the gene expression analyses, we found that the *cahz* gene was expressed both in the ear and ICM region of the wild-type, whereas it's expression was lost in the ICM region in the *clo* mutant (Figure 4.8 T,V). This low level difference in expression was picked out by the amplified method but not by the conventional method. Similarly, the expression of *zvsg1* was very low at 18-somite stage but was notably expressed throughout the dorsal aorta, choroidal vascular plexus and intersegmental vessel at 36hpf (Figure 4.10 H,I) in the wild-type. Clearly, *zvsg1* is a vessel-specific gene and is absent in the *clo* mutant. However, the difference in *zvsg1* transcript level between the wild-type and *clo* mutant is too low at 18-somite and will fall below the statistically set ratio of 1.5-fold to be scored as positive when the conventional method is employed. Correspondingly, genes that are differentially expressed at very low levels in the wild-types and mutants that play potentially important roles in early developmental processes will not be identified by using the conventional method. Hence, the amplified method not only complements the conventional method but is more superior than the conventional method to uncover low level differentially expressed genes at early developmental stages. With an estimate of 100,000 predicted genes in the zebrafish genome (TIGR Zebrafish Gene Index), the present zebrafish Affymetrix array covers only ~1/6 of the predicted genes (14,900 unigenes). Along with the amazing speed of data mining and

growing unigenes repertoire, it is very likely that there will be more genes spotted on the Affymetrix array in the near future. This will render us a better tool to discover more low abundance genes that are essential for early developmental processes via the amplified approach.

As increasing number of zebrafish mutants have been identified through large scale genetic screening, microarray technology is one of the most powerful tools to study these mutants. However, to collect enough material for the analysis of early developmental processes is always the limiting factor to fulfill the microarray analysis, and the indistinguishable morphological phenotype between wild-type and mutant at desired stage excludes gene expression profiling by microarray as well. Although many transgenic fishes that displayed specific fluorescent reporter gene distribution were generated to facilitate the discrimination of mutant from wild-type sibling fishes based on a specific fluorescence characteristics, the generation of such transgenic lines take about 6 months and another 6-8 months to generate the mutant line carrying homozygous reporter transgene. In addition, the generation of a suitable reporter transgenic fish may not be applicable to every mutant to distinguish between the mutant and wild-type siblings at a desired developmental stage. Our single embryo approach described here bypasses the requirement of transgenic fish and can be applied on any mutants without any restrictions. The results demonstrated that differentially expressed target genes could be successfully identified through the single embryo approach, and the comparison between two methods show that the amplification method is not only a substitution, but also the reinforcement of traditional method.

4.3.2 Newly Identified Hematopoietic and Vascular Genes

From our microarray study, we confirmed that 22 previously known zebrafish hematopoietic and vascular endothelial cell genes and 18 newly identified hematopoietic

and vascular endothelial cell related genes were down-regulated in the *clo* mutant. Sequence and expression pattern analyses revealed that these novel genes are assigned to almost all different blood lineage cells, demonstrating the whole embryo microarray was nondiscriminatory and is a valuable tool to identify tissue specific genes. However, with a little surprise, we could not found any genes up-regulated in the *cloche* mutant. This result might favor the argument that the function of the *cloche* gene during hematopoiesis and vasculogenesis was transcriptional activation, and not suppression.

4.3.2.1 Erythroid Lineage

Genes in this group were *cpo, cahz, znfl2, cldn g* and *Dr.16206*. *cpo* is a mitochondrial enzyme that catalyze coproporphyrinogen III to protoporphyrinogen IX during heme synthesis (Ibraham et al., 1983); likewise, another gene *cahz* is an enzyme too, which is involved in carbon dioxide transportation (Henry and Swenson, 2000). Hence, the abundance of their expression in the red blood cells was indubitable. The third gene, *znfl2*, which contains six tandem zinc-finger motifs at the C-termius of the protein, falls into the kruppel-type zinc-finger (ZNF) –containing protein super-family known to play an essential role in cell differentiation, development, and tumorgenesis (Kaczynski et al., 2003). Although not closely related to either the zebrafish erythrocyte kruppel-like family (*eklf*) or blood island-enriched kruppel-like factor (*biklf*) (Kawahara and Dawid, 2001; Oates et al., 2001), nonetheless, its erythrocyte-restricted expression suggests that *znfl2* may be involved in erythroid lineage development. *cldn g* is a member of the large family of claudin proteins that has been shown to play a pivotal role in the barrier functions of tight junctions in epithelial and endothelial cellular sheets (Kollmar et al., 2001; Turksen and Troy, 2004). Interestingly, recent studies have suggested that claudin proteins are also implicated in regulation of cell adhesion and migration (Tiwari-Woodruff et al., 2001). Given its erythrocyte-enriched expression, we speculate that *cldn g* may participate in

cell adhesion and migration of erythrocyte during zebrafish erythropoiesis. The last gene, *Dr.16206*, did not exhibit specific expression pattern through our *in situ* hybridization examination. However, a sequence blast revealed that it shared about 50% identity to mouse coagulation factor XIII, which is an important substance for the blood clotting and maintenance of normal homeostasis. Therefore, the function of *Dr.16206* in zebrafish is very likely to be also involved in clotting process.

4.3.2.2 Myeloid Lineage

Two genes, *mmp13* and *ncf1*, displayed a myeloid specific expression pattern from WISH analyses. *mmp13* belongs to the collagenase subfamily of matrix metalloproteinase that can degrade the main protein components of extracellular matrix (Leeman et al., 2002). Recent studies on *mmp13*-null mice demonstrated that MMP13 played an important role in the development of growth plate cartilage and in endochondral ossification (Inada et al., 2004; Stickens et al., 2004). However, our result shows that *mmp13* is expressed specifically in the primitive macrophage during zebrafish early development, raising the possibility that it may be involved in the maturation and migration of primitive macrophage. Another gene, *ncf1*, as its name implied, is expressed in neutrophils and serves as a component of the NADPH oxidase complex, which is the key player in the phagocyte-mediated antimicrobial or proinflammatory events (Babior et al., 2002). The deficiency of this gene in human causes chronic granulomatous disease (Francke et al., 1990). Therefore, *ncf1* can be acted as an early neutrophil marker in zebrafish granulopoiesis.

4.3.2.3 Vascular Endothelial Cell

Genes, *dusp5, zvsg1, aqp8* and *yrk*, are potential candidates involved in vasculogenesis. *dusp5* is a member of dual specificity phosphatase or mitogen-activated protein kinase

phosphatase family that is capable of removing phosphate group on both tyrosine and serine or threonine residues on the same protein (Kwak and Dixon, 1995; Farooq and Zhou, 2004). Although recent study has indicated that human DUSP5 suppresses the growth of several types of human cancer cells in a p53-dependent manner (Ueda et al., 2003), its main substrate and physiological function is poorly defined. Our preliminary result shows that the *dusp5* may regulate vascular endothelial cell development. *zvsg1* is a vessel-specific gene that encodes a novel protein without any notable domain. Given the fact that no mammalian homologues of this gene can be found in GeneBank, we think it may be a gene exclusively expressed in zebrafish. Nevertheless, its late vessel-specific expression suggests that this molecule may play a role in angiogenesis. *aqp8* belongs to the major intrinsic protein superfamiliy of water-transporting channel (Koyama et al., 1998). In mammals, it is widely expressed in many organs, including gastrointestinal tract, testes, liver, heart and kidney (Elkjaer et al., 2001; Calamita et al., 2001; Garcia et al., 2001), but its function in hematopoiesis and vasculargenesis has not been addressed so far. The vessel-specific expression of *aqp8* in zebrafish embryo indicated its veiled function in early vessel development. The last gene in this group, *yrk*, is a kinase with SH2 and SH3 domain (Sudol et al., 1993). Although the expression of this gene in zebrafish did not show any specific pattern in hematopoietic or vascular tissues, its mammalian homologues do have expression in the hematopoietic tissues (Sudol et al., 1993). In addition, consistence with our result, Gerhard J. Weber et al also found that *yrk* fell into the cluster of vascular gene in their microarray analysis (Weber et al., 2005), suggesting its function in vasculagenesis.

Taken all together, we found that 11 genes were involved in the hematopoietic or vascular development from the sequence and expression analyses. However, we still have another 7 novel genes without any known functional cues. Although a possible reason for this could be the general effects of these genes on zebrafish development,

the more likely reason is the lack of full-length sequence of these genes, and indeed, it is very true for *zvsg1* and *ncf1*. Initially, we started our expression analysis using partial cDNA sequences as probes; these two genes were omitted from our screening for the reason of the low signal intensity with very high background. Fortunately, we were able to clone the full-length of *zvsg1* and *ncf1* by using RACE, and these full-length clones allowed us to clearly view the expression of *zvsg1* in the blood vessels and *ncf1* in the myeloid cells. Hence, we believe that we can find out the potential functions of these 7 novel genes when their full-length clones are made available.

4.4 Conclusion and Future Work

We developed a new single embryo approach that facilitated the gene expression profile analysis for limited starting material. Combined with conventional approach, we have successfully identified 22 well-known hematopoietic and vascular endothelial related genes and 18 novel genes that were down-regulated in the *cloche* mutant using the Affymetrix array. Sequence and gene expression analyses revealed that 11 novel genes may be involved in the development of different hematopoietic and endothelial cells. In the future, functional analysis using full-length mRNA over-expression and morpholino knock-down could evince their roles in the hematopoiesis.

A. Protein alignment of zebrafish AQP8 with human AQP8 and mouse AQP8.

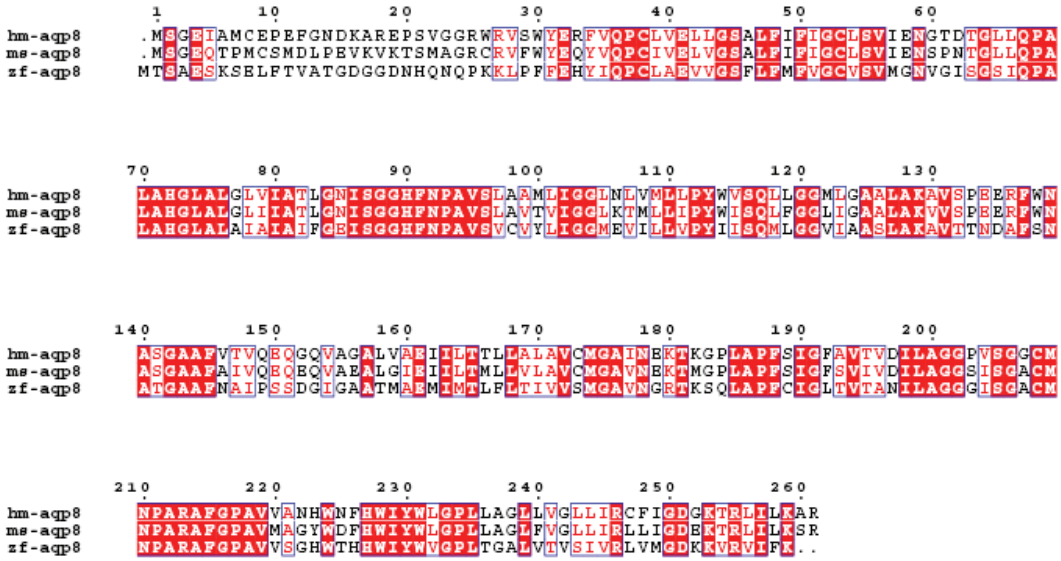

B. Protein alignment of zebrafish CAHZ with human CAHZ and mouse CAHZ.

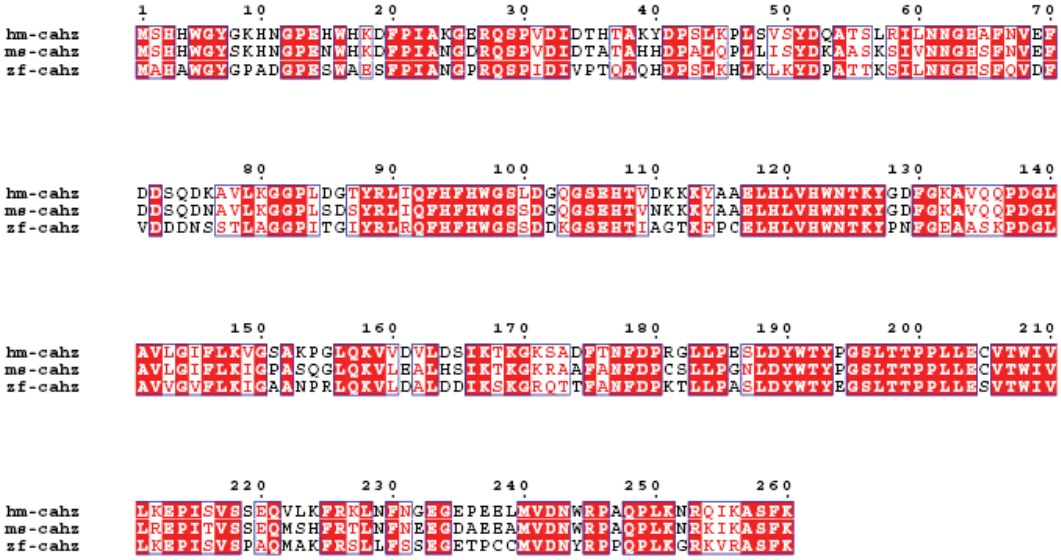

C. Protein alignment of zebrafish similar to embryonic transglutaminase with human coagulation factor XIII and mouse coagulation factor XIII.

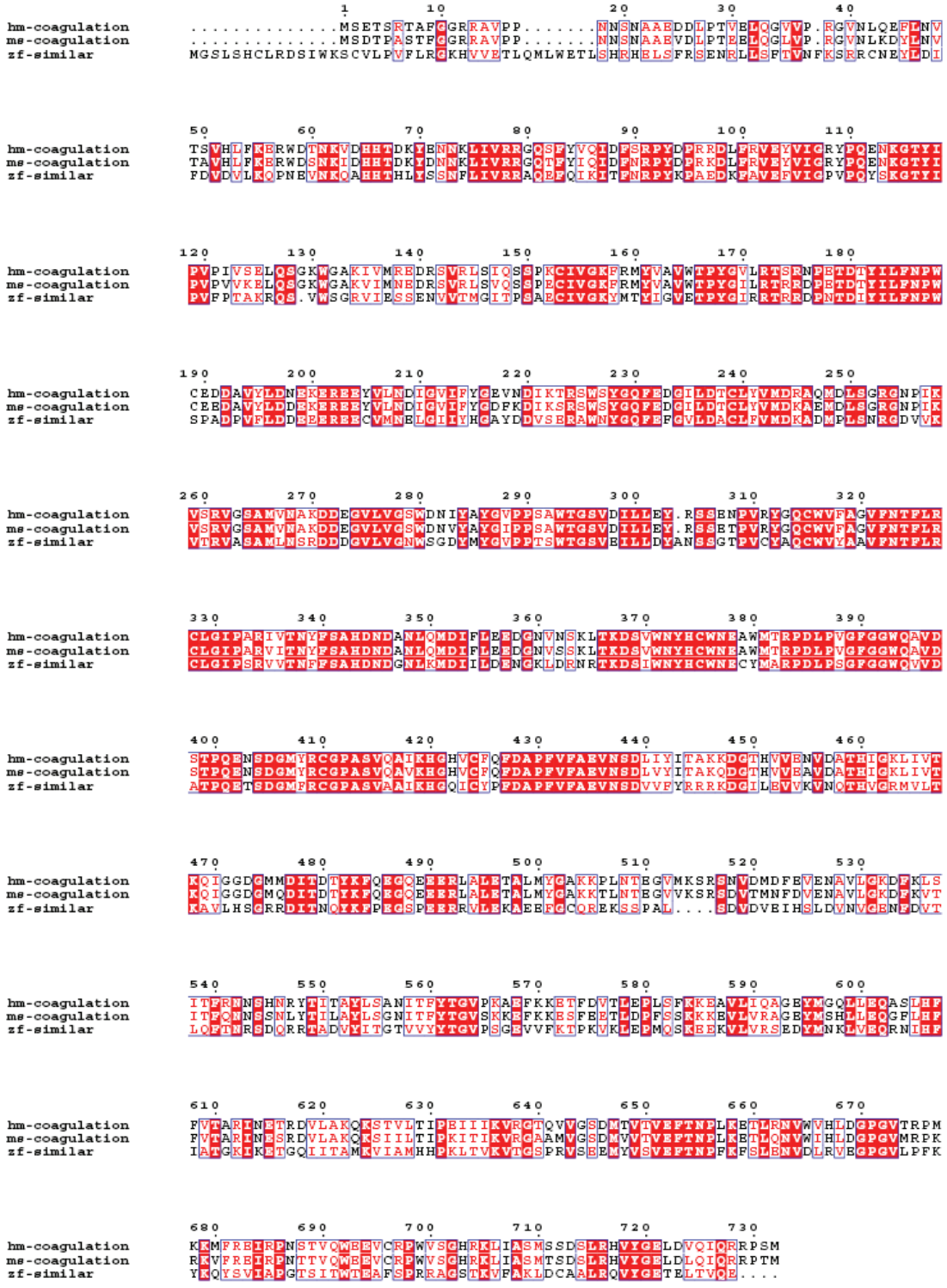

D. Protein alignment of zebrafish CLDN G with human CLAUDIN 4 and mouse CLAUDIN 4.

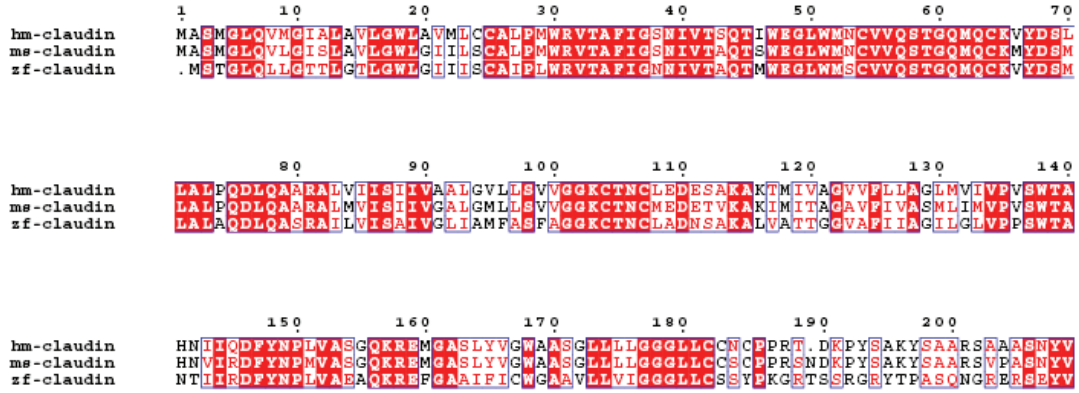

E. Protein alignment of zebrafish CPO with human CPO and mouse CPO.

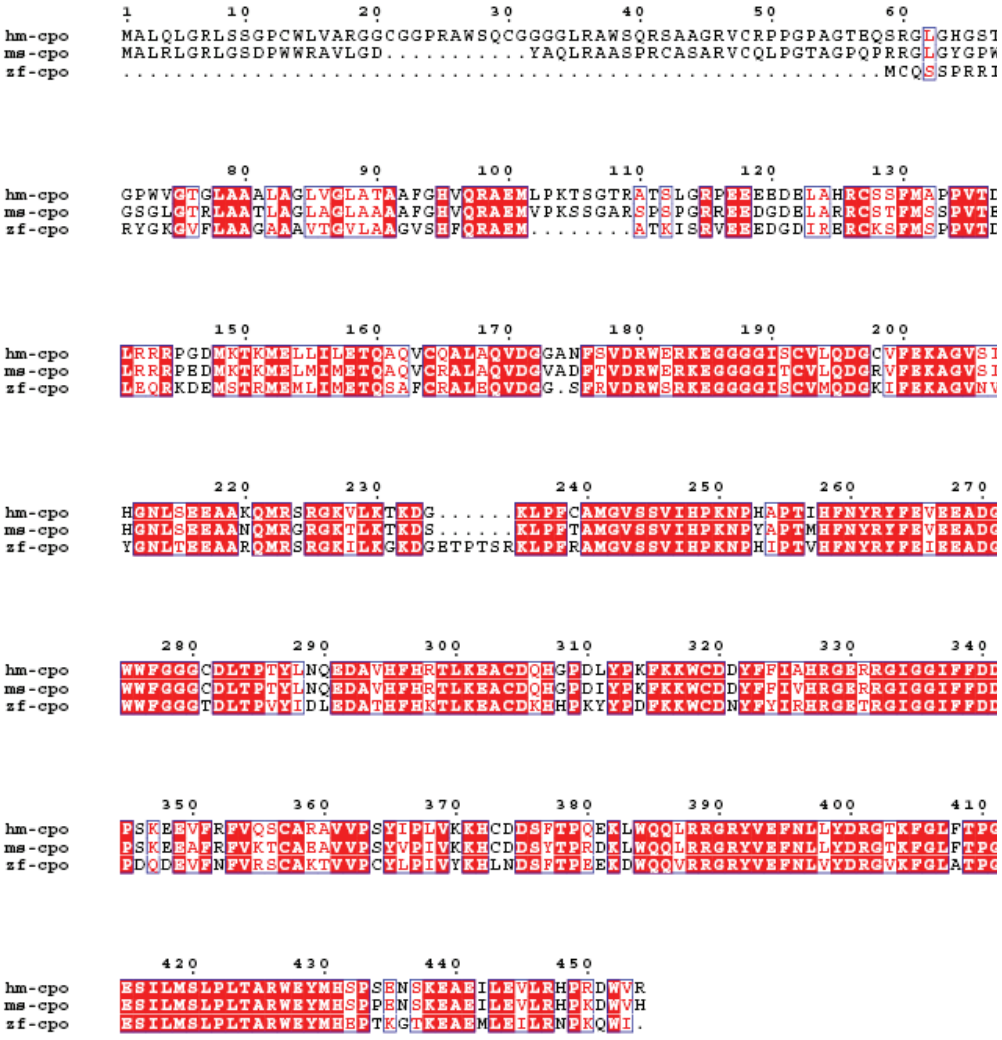

F. Protein alignment of zebrafish DUSP5 with human DUSP5 and mouse DUSP5.

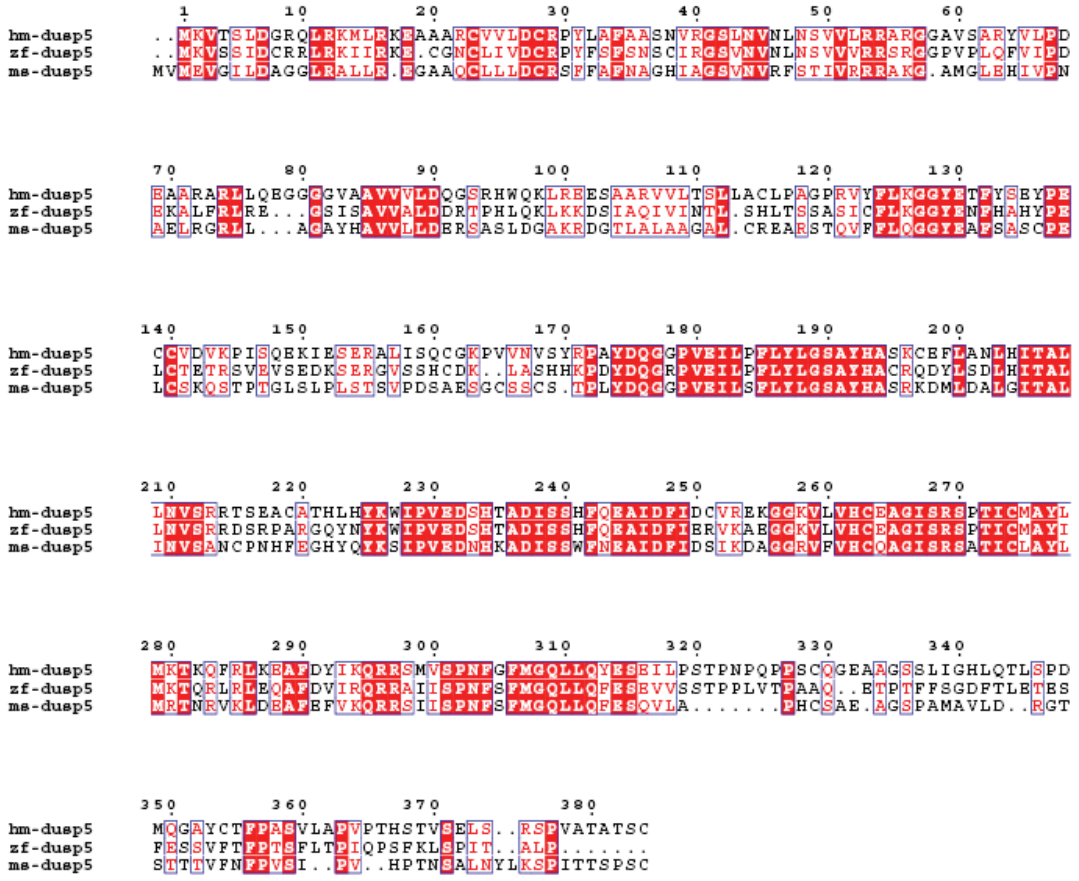

G. Protein alignment of zebrafish MMP13 with human MMP13 and mouse MMP13.

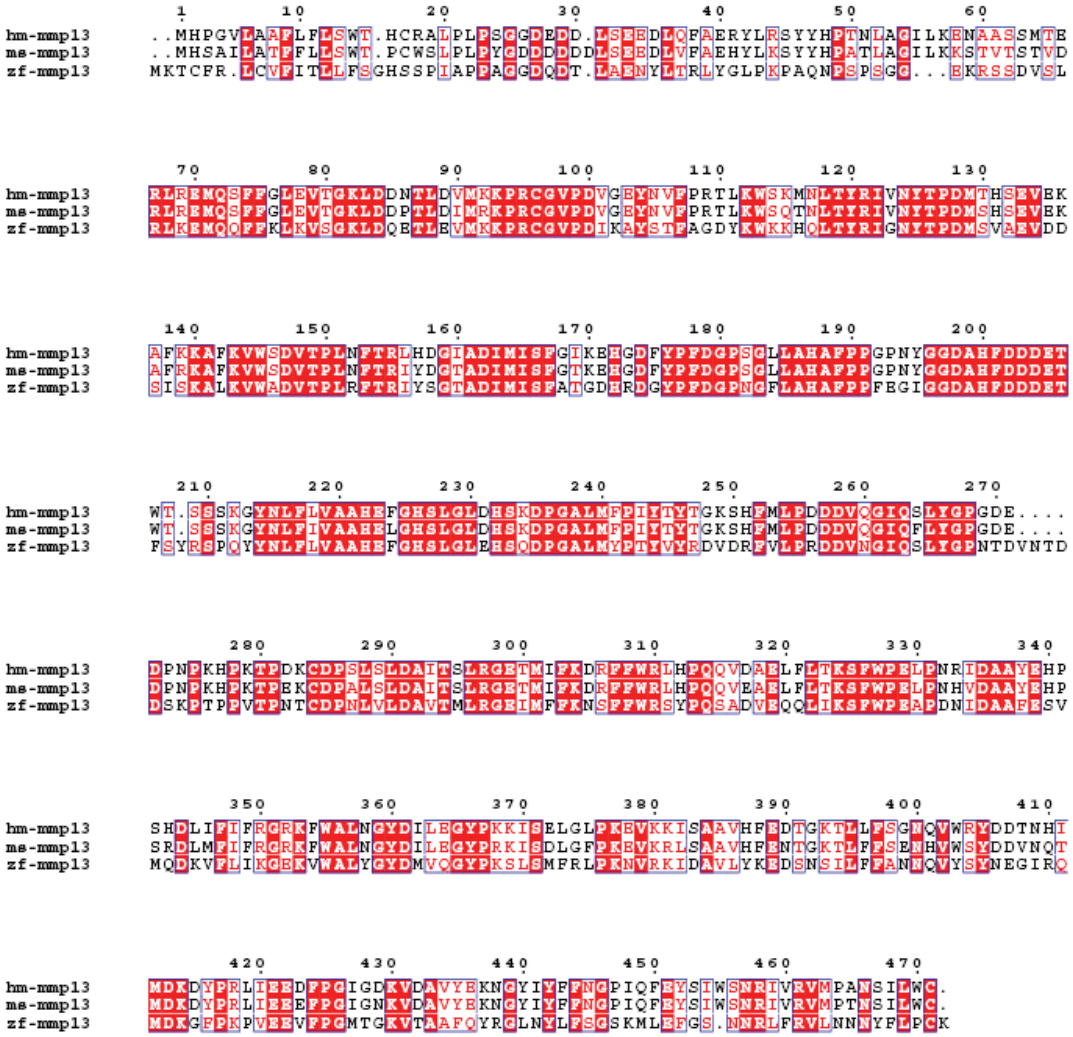

H. Protein alignment of zebrafish NCF1 with human NCF1 and mouse NCF1.

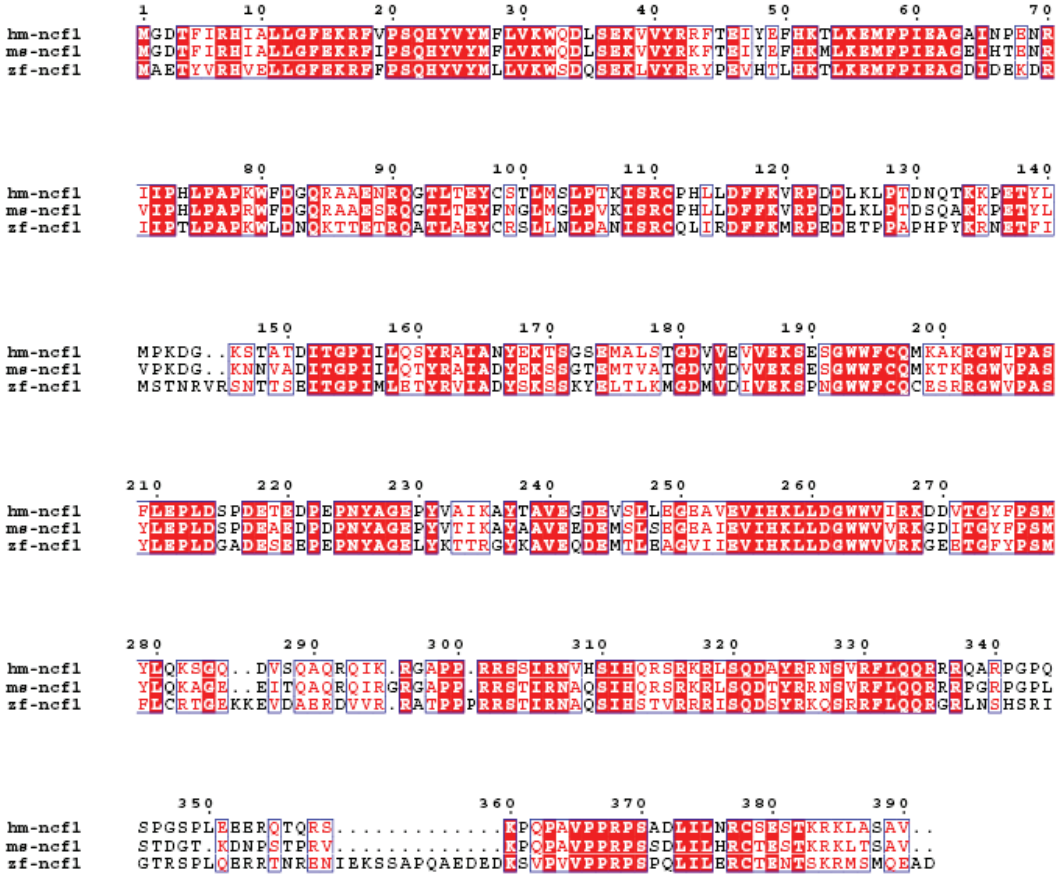

I. Protein alignment of zebrafish YRK with human YRK and mouse YRK.

J. Protein alignment of zebrafish ZNFL2 with human zinc finger protein 41 and mouse zinc finger protein 248.

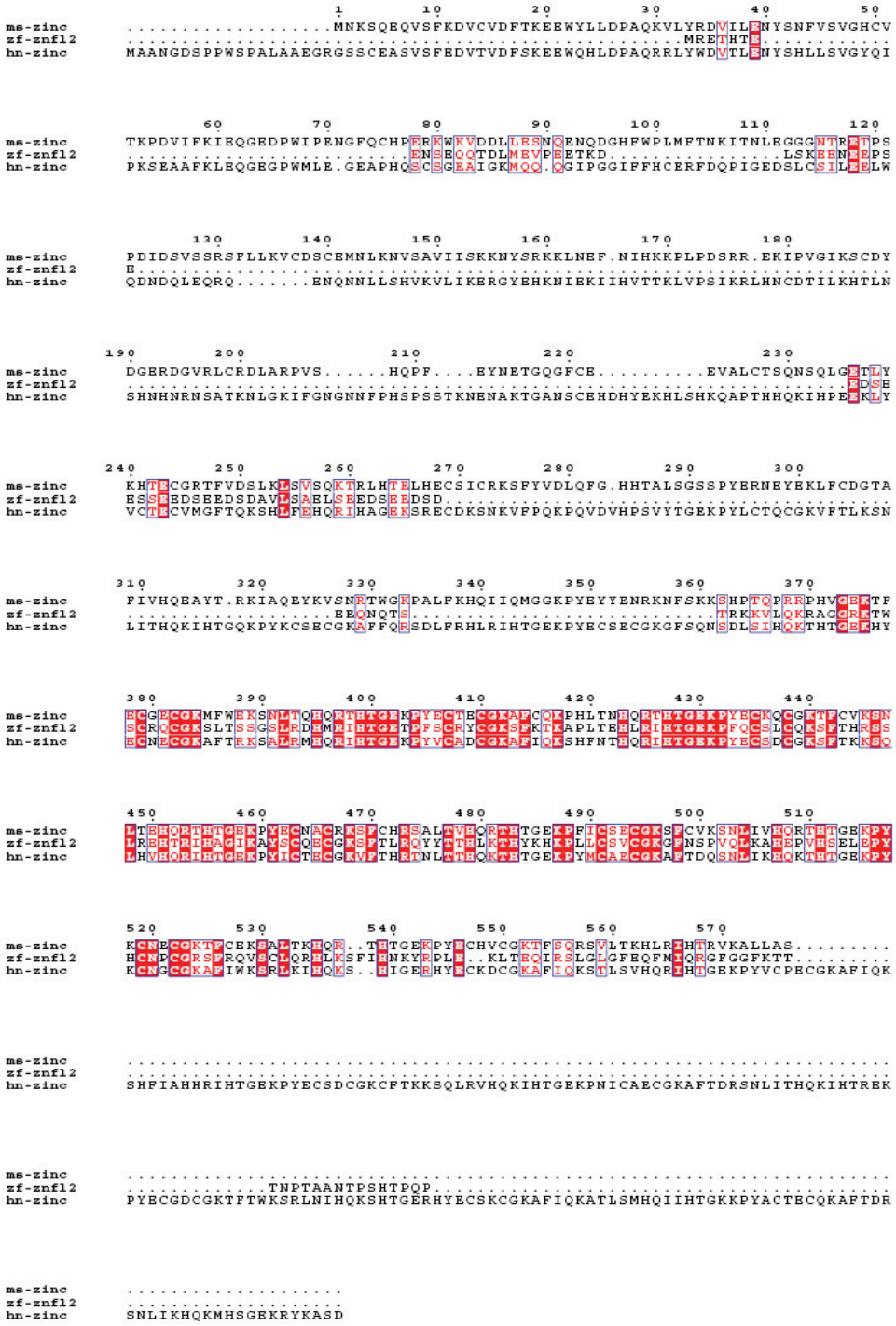

Figure 4.11 Protein Sequence Alignments of 9 Zebrafish Affymetrix Array Targets with their Mammalian Homologues.

Table 4.1 Down-Regulated Clones Identified by Amplification Method

Category I[a]			Category II[b]	
AFFX GENE ID (Unigene ID)	Gene		AFFX GENE ID (Unigene ID)	Gene
Dr.25422.1.S1_s_at	*αe1-globin*		Dr.8153.1.S1_at	*cldn g*
Dr.1450.1.S1_at	*αe3-globin*		Dr.10314.1.S1_a_at	*mmp13*
DrAffx.1.85.S1_s_at	*βe1-globin*		Dr.12726.1.S1_at	*yrk*
DrAffx.2.15.S1_at	*βe2-globin*		Dr.6834.1.A1_at	*cpo*
DrAffx.2.19.S1_at	*βe3-globin*		Dr.3201.1.S1_at	*znfl2*
Dr.355.1.S1_at	*gata1*		Dr.5365.1.A1_at	*dusp5*
Dr.20971.1.S2_at	*band3*		Dr.2973.1.A1_at	*ncf1*
Dr.2166.1.S1_at	*urod*		Dr.450.1.S1_at	*cahz*
Dr.5053.1.S1_at	*klf4*		Dr.6885.1.A1_at	*Dr.6885*
Dr.8180.1.S1_at	*alas2*		Dr.9655.1.A1_at	*Dr.9655(zvsg1)*
Dr.8039.1.S2_at	*flk1*		Dr.11977.1.A1_at	*Dr.11977*
Dr.26421.1.A1_at	*fli1*		Dr.25117.1.S1_at	*Dr.25117*
Dr.8065.1.S1_at	*lmo2*		Dr.25630.1.S1_at	*Dr.25630*
Dr.1458.1.S1_at	*scl*			
DrAffx.1.39.S1_at	*hdr*			
Dr.7612.1.A1_at	*spi1*			
Dr.8064.1.S1_at	*drl*			
Dr.8106.1.S1_at	*cmyb*			

Table 4.2 Affymetrix Quality Metrics Comparisons

Metric	Amplified Method						Standard Method						Typical Value Range
Expriments	1		2		3		1		2		3		
	Sibling	Cloche	Sibling	Cloche	Sibling	Cloche	Sibling	Cloche	Sibling	Cloche	Sibling	Cloche	
Raw Q	1.87	1.91	1.94	1.98	2.4	2.25	1.87	1.98	1.92	2.27	1.85	1.84	a
Background	47.19	48.23	51.01	54.18	63.63	58.72	47.17	50.29	51.03	60.43	46.19	47.33	20-100
Scaling Factor	4.777	4.747	5.817	5.326	3.487	5.518	4.915	4.689	6.485	5.266	5.732	3.902	<3-fold[b]
%Present Call	59.80	60.40	58.90	59.60	61.00	57.00	69.20	68.50	67.00	66.80	67.00	69.40	c
GAPDH 3'/5' Ratio	1.23	1.3	1.34	1.39	1.43	1.22	1.58	1.01	1.2	1.59	2.1	2.27	<3
Actin 3'/5' Ratio	0.92	0.92	0.91	0.87	1.03	1.04	1.71	1.59	1.95	1.94	2.26	1.83	<3

a: Noise (Raw Q) is a measure of the pixel-to-pixel variation of probe cells on a GeneChip array. The array data acquired from amplified method and standard method have comparable noise values.
b: The value of scaling/normalization factors are within the threefold range, when comparing the ratio of sibling and cloche targets in each individual set of experiment.
c: Percent Present is the percentage of the number of probe sets called “Present” relative to the total number of probe sets on array.

Table 4.3 Summary of Confirmed Target Clones

AFFX GENE ID (Unigene ID)	Gene	Amplified Method	Standard Method
Dr.25422.1.S1_s_at	*αe1-globin*	+	+
Dr.1450.1.S1_at	*αe3-globin*	+	+
DrAffx.1.85.S1_s_at	*βe1-globin*	+	+
DrAffx.2.15.S1_at	*βe2-globin*	+	+
DrAffx.2.19.S1_at	*βe3-globin*	+	+
Dr.355.1.S1_at	*gata1*	+	+
Dr.20971.1.S2_at	*band3*	+	+
Dr.2166.1.S1_at	*urod*	+	+
Dr.5053.1.S1_at	*klf4*	+	+
Dr.8180.1.S1_at	*alas2*	+	+
Dr.8039.1.S2_at	*flk1*	+	+
Dr.26421.1.A1_at	*fli1*	+	+
Dr.8065.1.S1_at	*lmo2*	+	+
Dr.1458.1.S1_at	*scl*	+	+
DrAffx.1.39.S1_at	*hdr*	+	+
Dr.7612.1.A1_at	*spi1*	+	+
Dr.8064.1.S1_at	*drl*	+	+
Dr.8106.1.S1_at	*cmyb*	+	+
Dr.8122.1.S1_a_at	*ikaros*	-	+
Dr.12704.1.A1_at	*plexinD1*	-	+
Dr.3269.1.S1_at	*hhex*	-	+
Dr.3027.1.S1_at	*band4.1*	-	+
Dr.8153.1.S1_at	*cldn g*	+	+
Dr.10314.1.S1_a_at	*mmp13*	+	+
Dr.12726.1.S1_at	*yrk*	+	+
Dr.6834.1.A1_at	*cpo*	+	+
Dr.3201.1.S1_at	*znfl2*	+	+
Dr.5365.1.A1_at	*dusp5*	+	+
Dr.2973.1.A1_at	*ncf1*	+	+
Dr.11977.1.A1_at	*Dr.11977*	+	+
Dr.450.1.S1_at	*cahz*	+	-
Dr.6885.1.A1_at	*Dr.6885*	+	-
Dr.9655.1.A1_at	*Dr.9655(zvsg1)*	+	-
Dr.25117.1.S1_at	*Dr.25117*	+	-
Dr.25630.1.S1_at	*Dr.25630*	+	-
Dr.916.1.S1_at	*aquaporin8*	-	+
Dr.1870.1.A1_at	*Dr.1870*	-	+
Dr.14448.1.A1_at	*Dr.14448*	-	+
Dr.14553.1.A1_at	*Dr.14553*	-	+
Dr.16206.1.A1_S_at	*Dr.16206*	-	+

Table 4.4 Genome Blasts of 18 Newly Identified Target Clones

AFFX GENE ID	GENE	Linkage[a] ncbi/ensembl	Domain	GeneBank ID	Funcition	Protein Similarity to Mouse
Dr.8153.1.S1_at	cldn g	24/1	PMP-22/EMP/MP20 and claudin family	NM_180965	tight junction	66.30% to CLD4_MOUSE CLAUDIN-4
Dr.10314.1.S1_a_at	mmp13	21/un	matrixin and adamalysin, Hemopexin repeat	AF506756	metalloendopeptidase activity,metallopeptidase activity,zinc ion binding	50.42% to mouse MM13_MOUSE Collagenase 3 precursor
Dr.12726.1.S1_at	yrk	21/19	SH2 motif, SH3,Protein kinase	AY169369	protein kinase activity	74.21% to mouse A44991 protein-tyrosine kinase
Dr.6834.1.A1_at	cpoIII	8/8	Coproporphyrinogen III oxidase	XM_703480.1	Coproporphyrinogen III oxidase	75.66% to human Coproporphyrinogen III oxidase
Dr.3201.1.S1_at	znfl2	un/2	zinc-finger	BC092919	N.A.	40% to human zinc finger protein 41
Dr.5365.1.A1_at	dusp5	22/22	Dual specificity protein phosphatase	BC059592	protein tyrosine/serine/threonine phosphatase activity	45.14% to mouse dual specificity phosphoprotein phosphatase
Dr.11977.1.A1_at	Dr.11977	16/24	Leucine-rich repeat	BC079491	N.A.	27.62% to mouse JG0193 G protein-coupled receptor FEX
Dr.2973.1.A1_at	Dr.2973(ncf1)	14 or 5/5	SH3 and Phox-like	NM_001030071	N.A.	45% to human Neutrophil cytosolic factor 1 (ncf1)
Dr.916.1.S1_at	aqp8	12/12	Major intrinsic protein (MIP) superfamily	NM_001004661	water channel	53% to human aquaporin 8
Dr.14448.1.A1_at	Dr.14448	un/2	N.A.	UniGene Dr.14448	N.A.	N.A.
Dr.14553.1.A1_at	Dr.14553	11/11 or 25	N.A.	UniGene Dr.14553	N.A.	N.A.

Dr.16206.1.A1_S_at	Dr.16206	20/7	Transglutaminase-like domain	XM_684690	N.A.	53% to mouse coagulation factor XIII
Dr.1870.1.A1_at	Dr.1870	1/24	N.A.	UniGene Dr.1870	N.A.	N.A.
Dr.450.1.S1_at	cahz	un/2	Carbonic anhydrase	BC065611	carbonate dehydratase activity	63.08 % to mouse homologue
Dr.9655.1.A1_at	Dr.9655(zvsg1)	24/11	N.A.	NM_001014364	N.A.	N.A.
Dr.6885.1.A1_at	Dr.6885	un/9	N.A.	Unigen Dr.6885	N.A.	N.A.
Dr.25630.1.S1_at	Dr.25630	1/1	N.A.	UniGene Dr.25630	N.A.	N.A.
Dr.25117.1.S1_at	Dr.25117	un/un	N.A.	BC053219	N.A.	N.A.

a: Genome blast from two servers, NCBI and ensembl, sometimes are different, hence, both results are presented in the table.
'un' denotes the linkage have not been defined.
N.A. denotes "not available".

Reference List

1. Akashi,K., Traver,D., Miyamoto,T., and Weissman,I.L. (2000). A clonogenic common myeloid progenitor that gives rise to all myeloid lineages. Nature *404*, 193-197.

2. Alvarez-Silva,M., Belo-Diabangouaya,P., Salaun,J., and Dieterlen-Lievre,F. (2003). Mouse placenta is a major hematopoietic organ. Development *130*, 5437-5444.

3. Amores,A., Force,A., Yan,Y.L., Joly,L., Amemiya,C., Fritz,A., Ho,R.K., Langeland,J., Prince,V., Wang,Y.L., Westerfield,M., Ekker,M., and Postlethwait,J.H. (1998). Zebrafish hox clusters and vertebrate genome evolution. Science *282*, 1711-1714.

4. Amsterdam,A., Burgess,S., Golling,G., Chen,W., Sun,Z., Townsend,K., Farrington,S., Haldi,M., and Hopkins,N. (1999). A large-scale insertional mutagenesis screen in zebrafish. Genes Dev *13*, 2713-2724.

5. Ashurst,J.L., Chen,C.K., Gilbert,J.G., Jekosch,K., Keenan,S., Meidl,P., Searle,S.M., Stalker,J., Storey,R., Trevanion,S., Wilming,L., and Hubbard,T. (2005). The Vertebrate Genome Annotation (Vega) database. Nucleic Acids Res *33*, D459-D465.

6. Babior,B.M., Lambeth,J.D., and Nauseef,W. (2002). The neutrophil NADPH oxidase. Arch. Biochem Biophys *397*, 342-344.

7. Baier,H. (2000). Zebrafish on the move: towards a behavior-genetic analysis of vertebrate vision. Curr Opin Neurobiol. *10*, 451-455.

8. Bennett,C.M., Kanki,J.P., Rhodes,J., Liu,T.X., Paw,B.H., Kieran,M.W., Langenau,D.M., Delahaye-Brown,A., Zon,L.I., Fleming,M.D., and Look,A.T. (2001). Myelopoiesis in the zebrafish, Danio rerio. Blood *98*, 643-651.

9. Berghmans,S., Murphey,R.D., Wienholds,E., Neuberg,D., Kutok,J.L., Fletcher,C.D., Morris,J.P., Liu,T.X., Schulte-Merker,S., Kanki,J.P., Plasterk,R., Zon,L.I., and Look,A.T. (2005). tp53 mutant zebrafish develop malignant peripheral nerve sheath tumors. Proc Natl Acad Sci U S A *102*, 407-412.

10. Bradbury,J. (2004). Small fish, big science. PLoS. Biol *2*, E148.

11. Brown,L.A., Rodaway,A.R., Schilling,T.F., Jowett,T., Ingham,P.W., Patient,R.K., and Sharrocks,A.D. (2000). Insights into early vasculogenesis revealed by expression of the ETS-domain transcription factor Fli-1 in wild-type and mutant zebrafish embryos. Mech Dev *90*, 237-252.

12. Brownlie,A., Donovan,A., Pratt,S.J., Paw,B.H., Oates,A.C., Brugnara,C., Witkowska,H.E., Sassa,S., and Zon,L.I. (1998). Positional cloning of the

zebrafish sauternes gene: a model for congenital sideroblastic anaemia. Nat Genet *20*, 244-250.

13. Brownlie,A., Hersey,C., Oates,A.C., Paw,B.H., Falick,A.M., Witkowska,H.E., Flint,J., Higgs,D., Jessen,J., Bahary,N., Zhu,H., Lin,S., and Zon,L. (2003). Characterization of embryonic globin genes of the zebrafish. Dev Biol *255*, 48-61.

14. Bruno,L., Hoffmann,R., McBlane,F., Brown,J., Gupta,R., Joshi,C., Pearson,S., Seidl,T., Heyworth,C., and Enver,T. (2004). Molecular signatures of self-renewal, differentiation, and lineage choice in multipotential hemopoietic progenitor cells in vitro. Mol Cell Biol *24*, 741-756.

15. Burns,C.E., DeBlasio,T., Zhou,Y., Zhang,J., Zon,L., and Nimer,S.D. (2002). Isolation and characterization of runxa and runxb, zebrafish members of the runt family of transcriptional regulators. Exp Hematol. *30*, 1381-1389.

16. Calamita,G., Mazzone,A., Cho,Y.S., Valenti,G., and Svelto,M. (2001). Expression and localization of the aquaporin-8 water channel in rat testis. Biol Reprod. *64*, 1660-1666.

17. Castilla,L.H., Wijmenga,C., Wang,Q., Stacy,T., Speck,N.A., Eckhaus,M., Marin-Padilla,M., Collins,F.S., Wynshaw-Boris,A., and Liu,P.P. (1996). Failure of embryonic hematopoiesis and lethal hemorrhages in mouse embryos heterozygous for a knocked-in leukemia gene CBFB-MYH11. Cell *87*, 687-696.

18. Chan,F.Y., Robinson,J., Brownlie,A., Shivdasani,R.A., Donovan,A., Brugnara,C., Kim,J., Lau,B.C., Witkowska,H.E., and Zon,L.I. (1997). Characterization of adult alpha- and beta-globin genes in the zebrafish. Blood *89*, 688-700.

19. Childs,S., Weinstein,B.M., Mohideen,M.A., Donohue,S., Bonkovsky,H., and Fishman,M.C. (2000). Zebrafish dracula encodes ferrochelatase and its mutation provides a model for erythropoietic protoporphyria. Curr Biol *10*, 1001-1004.

20. Choi,K., Kennedy,M., Kazarov,A., Papadimitriou,J.C., and Keller,G. (1998). A common precursor for hematopoietic and endothelial cells. Development *125*, 725-732.

21. Cormier,F. and Dieterlen-Lievre,F. (1988). The wall of the chick embryo aorta harbours M-CFC, G-CFC, GM-CFC and BFU-E. Development *102*, 279-285.

22. Cumano,A. and Godin,I. (2001). Pluripotent hematopoietic stem cell development during embryogenesis. Curr Opin Immunol *13*, 166-171.

23. Dailey,H.A. (2002). Terminal steps of haem biosynthesis. Biochem Soc. Trans. *30*, 590-595.

24. Danilova,N. and Steiner,L.A. (2002). B cells develop in the zebrafish pancreas. Proc Natl Acad Sci U S A *99*, 13711-13716.

25. Davidson,A.J., Ernst,P., Wang,Y., Dekens,M.P., Kingsley,P.D., Palis,J., Korsmeyer,S.J., Daley,G.Q., and Zon,L.I. (2003). cdx4 mutants fail to specify

blood progenitors and can be rescued by multiple hox genes. Nature *425*, 300-306.

26. Davidson,A.J. and Zon,L.I. (2004). The 'definitive' (and 'primitive') guide to zebrafish hematopoiesis. Oncogene *23*, 7233-7246.

27. de Jong,J.L. and Zon,L.I. (2005). Use of the zebrafish system to study primitive and definitive hematopoiesis. Annu Rev Genet *39*, 481-501.

28. Delassus,S. and Cumano,A. (1996). Circulation of hematopoietic progenitors in the mouse embryo. Immunity *4*, 97-106.

29. Detrich,H.W., III, Kieran,M.W., Chan,F.Y., Barone,L.M., Yee,K., Rundstadler,J.A., Pratt,S., Ransom,D., and Zon,L.I. (1995). Intraembryonic hematopoietic cell migration during vertebrate development. Proc Natl Acad Sci U S A *92*, 10713-10717.

30. Deutsch,J., Cavalieri,L.F., and Rosenberg,B.H. (1981). Effects of ethylating agents on DNA synthesis in vitro: implications for the mechanism of carcinogenesis. Carcinogenesis *2*, 363-371.

31. Dickson,M.C., Martin,J.S., Cousins,F.M., Kulkarni,A.B., Karlsson,S., and Akhurst,R.J. (1995). Defective haematopoiesis and vasculogenesis in transforming growth factor-beta 1 knock out mice. Development *121*, 1845-1854.

32. Dieterlen-Lievre,F. (1975). On the origin of haemopoietic stem cells in the avian embryo: an experimental approach. J Embryol. Exp Morphol. *33*, 607-619.

33. Dieterlen-Lievre,F. and Martin,C. (1981). Diffuse intraembryonic hemopoiesis in normal and chimeric avian development. Dev Biol *88*, 180-191.

34. Donovan,A., Brownlie,A., Dorschner,M.O., Zhou,Y., Pratt,S.J., Paw,B.H., Phillips,R.B., Thisse,C., Thisse,B., and Zon,L.I. (2002). The zebrafish mutant gene chardonnay (cdy) encodes divalent metal transporter 1 (DMT1). Blood *100*, 4655-4659.

35. Donovan,A., Brownlie,A., Zhou,Y., Shepard,J., Pratt,S.J., Moynihan,J., Paw,B.H., Drejer,A., Barut,B., Zapata,A., Law,T.C., Brugnara,C., Lux,S.E., Pinkus,G.S., Pinkus,J.L., Kingsley,P.D., Palis,J., Fleming,M.D., Andrews,N.C., and Zon,L.I. (2000). Positional cloning of zebrafish ferroportin1 identifies a conserved vertebrate iron exporter. Nature *403*, 776-781.

36. Dooley,K. and Zon,L.I. (2000). Zebrafish: a model system for the study of human disease. Curr Opin Genet Dev *10*, 252-256.

37. Dooley,K.A., Davidson,A.J., and Zon,L.I. (2005). Zebrafish scl functions independently in hematopoietic and endothelial development. Dev Biol *277*, 522-536.

38. Douagi,I., Vieira,P., and Cumano,A. (2002). Lymphocyte commitment during embryonic development, in the mouse. Semin. Immunol *14*, 361-369.

39. Driever,W., Solnica-Krezel,L., Schier,A.F., Neuhauss,S.C., Malicki,J., Stemple,D.L., Stainier,D.Y., Zwartkruis,F., Abdelilah,S., Rangini,Z., Belak,J., and Boggs,C. (1996). A genetic screen for mutations affecting embryogenesis in zebrafish. Development *123*, 37-46.

40. Dzierzak,E., Medvinsky,A., and de Bruijn,M. (1998). Qualitative and quantitative aspects of haematopoietic cell development in the mammalian embryo. Immunol Today *19*, 228-236.

41. Eckfeldt,C.E., Mendenhall,E.M., Flynn,C.M., Wang,T.F., Pickart,M.A., Grindle,S.M., Ekker,S.C., and Verfaillie,C.M. (2005). Functional analysis of human hematopoietic stem cell gene expression using zebrafish. PLoS. Biol *3*, e254.

42. Elkjaer,M.L., Nejsum,L.N., Gresz,V., Kwon,T.H., Jensen,U.B., Frokiaer,J., and Nielsen,S. (2001). Immunolocalization of aquaporin-8 in rat kidney, gastrointestinal tract, testis, and airways. Am J Physiol Renal Physiol *281*, F1047-F1057.

43. Evans,C.A., Tonge,R., Blinco,D., Pierce,A., Shaw,J., Lu,Y., Hamzah,H.G., Gray,A., Downes,C.P., Gaskell,S.J., Spooncer,E., and Whetton,A.D. (2004). Comparative proteomics of primitive hematopoietic cell populations reveals differences in expression of proteins regulating motility. Blood *103*, 3751-3759.

44. Farber,S.A., Pack,M., Ho,S.Y., Johnson,I.D., Wagner,D.S., Dosch,R., Mullins,M.C., Hendrickson,H.S., Hendrickson,E.K., and Halpern,M.E. (2001). Genetic analysis of digestive physiology using fluorescent phospholipid reporters. Science *292*, 1385-1388.

45. Farooq,A. and Zhou,M.M. (2004). Structure and regulation of MAPK phosphatases. Cell Signal. *16*, 769-779.

46. Francke,U., Hsieh,C.L., Foellmer,B.E., Lomax,K.J., Malech,H.L., and Leto,T.L. (1990). Genes for two autosomal recessive forms of chronic granulomatous disease assigned to 1q25 (NCF2) and 7q11.23 (NCF1). Am J Hum Genet *47*, 483-492.

47. Galloway,J.L. and Zon,L.I. (2003). Ontogeny of hematopoiesis: examining the emergence of hematopoietic cells in the vertebrate embryo. Curr Top. Dev Biol *53*, 139-158.

48. Garcia,F., Kierbel,A., Larocca,M.C., Gradilone,S.A., Splinter,P., LaRusso,N.F., and Marinelli,R.A. (2001). The water channel aquaporin-8 is mainly intracellular in rat hepatocytes, and its plasma membrane insertion is stimulated by cyclic AMP. J Biol Chem *276*, 12147-12152.

49. Gekas,C., Dieterlen-Lievre,F., Orkin,S.H., and Mikkola,H.K. (2005). The placenta is a niche for hematopoietic stem cells. Dev Cell *8*, 365-375.

50. Georgopoulos,K., Bigby,M., Wang,J.H., Molnar,A., Wu,P., Winandy,S., and Sharpe,A. (1994). The Ikaros gene is required for the development of all lymphoid lineages. Cell *79*, 143-156.

51. Godin,I.E., Garcia-Porrero,J.A., Coutinho,A., Dieterlen-Lievre,F., and Marcos,M.A. (1993). Para-aortic splanchnopleura from early mouse embryos contains B1a cell progenitors. Nature *364*, 67-70.

52. Gregory,M. and Jagadeeswaran,P. (2002). Selective labeling of zebrafish thrombocytes: quantitation of thrombocyte function and detection during development. Blood Cells Mol Dis. *28*, 418-427.

53. Griffin,K.J., Amacher,S.L., Kimmel,C.B., and Kimelman,D. (1998). Molecular identification of spadetail: regulation of zebrafish trunk and tail mesoderm formation by T-box genes. Development *125*, 3379-3388.

54. Haar,J.L. and Ackerman,G.A. (1971). A phase and electron microscopic study of vasculogenesis and erythropoiesis in the yolk sac of the mouse. Anat Rec. *170*, 199-223.

55. Habeck,H., Odenthal,J., Walderich,B., Maischein,H., and Schulte-Merker,S. (2002). Analysis of a zebrafish VEGF receptor mutant reveals specific disruption of angiogenesis. Curr Biol *12*, 1405-1412.

56. Haffter,P., Granato,M., Brand,M., Mullins,M.C., Hammerschmidt,M., Kane,D.A., Odenthal,J., van Eeden,F.J., Jiang,Y.J., Heisenberg,C.P., Kelsh,R.N., Furutani-Seiki,M., Vogelsang,E., Beuchle,D., Schach,U., Fabian,C., and Nusslein-Volhard,C. (1996). The identification of genes with unique and essential functions in the development of the zebrafish, Danio rerio. Development *123*, 1-36.

57. Hammerschmidt,M., Pelegri,F., Mullins,M.C., Kane,D.A., Brand,M., van Eeden,F.J., Furutani-Seiki,M., Granato,M., Haffter,P., Heisenberg,C.P., Jiang,Y.J., Kelsh,R.N., Odenthal,J., Warga,R.M., and Nusslein-Volhard,C. (1996). Mutations affecting morphogenesis during gastrulation and tail formation in the zebrafish, Danio rerio. Development *123*, 143-151.

58. Heasman,J. (2002). Morpholino oligos: making sense of antisense? Dev Biol *243*, 209-214.

59. Henry,R.P. and Swenson,E.R. (2000). The distribution and physiological significance of carbonic anhydrase in vertebrate gas exchange organs. Respir. Physiol *121*, 1-12.

60. Herbomel,P., Thisse,B., and Thisse,C. (1999). Ontogeny and behaviour of early macrophages in the zebrafish embryo. Development *126*, 3735-3745.

61. Herbomel,P., Thisse,B., and Thisse,C. (2001). Zebrafish early macrophages colonize cephalic mesenchyme and developing brain, retina, and epidermis through a M-CSF receptor-dependent invasive process. Dev Biol *238*, 274-288.

62. Heyworth,P.G., Cross,A.R., and Curnutte,J.T. (2003). Chronic granulomatous disease. Curr Opin Immunol *15*, 578-584.

63. Hill,D.J. and Rowley,A.F. (1996). The thromboxane mimetic, U-46619, induces the aggregation of fish thrombocytes. Br. J Haematol. *92*, 200-211.

64. Hsia,N. and Zon,L.I. (2005). Transcriptional regulation of hematopoietic stem cell development in zebrafish. Exp Hematol. *33*, 1007-1014.

65. Huber,T.L., Kouskoff,V., Fehling,H.J., Palis,J., and Keller,G. (2004). Haemangioblast commitment is initiated in the primitive streak of the mouse embryo. Nature *432*, 625-630.

66. Ibraham,N.G., Friedland,M.L., and Levere,R.D. (1983). Heme metabolism in erythroid and hepatic cells. Prog Hematol. *13*, 75-130.

67. Inada,M., Wang,Y., Byrne,M.H., Rahman,M.U., Miyaura,C., Lopez-Otin,C., and Krane,S.M. (2004). Critical roles for collagenase-3 (Mmp13) in development of growth plate cartilage and in endochondral ossification. Proc Natl Acad Sci U S A *101*, 17192-17197.

68. Iscove,N.N., Barbara,M., Gu,M., Gibson,M., Modi,C., and Winegarden,N. (2002). Representation is faithfully preserved in global cDNA amplified exponentially from sub-picogram quantities of mRNA. Nat Biotechnol. *20*, 940-943.

69. Isogai,S., Horiguchi,M., and Weinstein,B.M. (2001). The vascular anatomy of the developing zebrafish: an atlas of embryonic and early larval development. Dev Biol *230*, 278-301.

70. Ivanova,N.B., Dimos,J.T., Schaniel,C., Hackney,J.A., Moore,K.A., and Lemischka,I.R. (2002). A stem cell molecular signature. Science *298*, 601-604.

71. Jagadeeswaran,P., Sheehan,J.P., Craig,F.E., and Troyer,D. (1999). Identification and characterization of zebrafish thrombocytes. Br. J Haematol. *107*, 731-738.

72. Jin,H., Xu,J., Qian,F., Du,L., Tan,C.Y., Lin,Z., Peng,J., and Wen,Z. (2005a). The 5' zebrafish scl promoter targets transcription to the brain, spinal cord, and hematopoietic and endothelial progenitors. Dev Dyn.

73. Jin,S.W., Beis,D., Mitchell,T., Chen,J.N., and Stainier,D.Y. (2005b). Cellular and molecular analyses of vascular tube and lumen formation in zebrafish. Development *132*, 5199-5209.

74. Johnson,G.R. and Moore,M.A. (1975). Role of stem cell migration in initiation of mouse foetal liver haemopoiesis. Nature *258*, 726-728.

75. Joseph Sambrook,D.W.R. (2001). Molecular Cloning: A Laboratory Manual. Cold Spring Harbor Laboratory Press; 3rd Labmn edition).

76. Kaczynski,J., Cook,T., and Urrutia,R. (2003). Sp1- and Kruppel-like transcription factors. Genome Biol *4*, 206.

77. Kalev-Zylinska,M.L., Horsfield,J.A., Flores,M.V., Postlethwait,J.H., Vitas,M.R., Baas,A.M., Crosier,P.S., and Crosier,K.E. (2002). Runx1 is required for zebrafish blood and vessel development and expression of a human RUNX1-CBF2T1 transgene advances a model for studies of leukemogenesis. Development *129*, 2015-2030.

78. Kataoka,H., Ochi,M., Enomoto,K., and Yamaguchi,A. (2000). Cloning and embryonic expression patterns of the zebrafish Runt domain genes, runxa and runxb. Mech Dev *98*, 139-143.

79. Kau,C.L. and Turpen,J.B. (1983). Dual contribution of embryonic ventral blood island and dorsal lateral plate mesoderm during ontogeny of hemopoietic cells in Xenopus laevis. J Immunol *131*, 2262-2266.

80. Kawahara,A. and Dawid,I.B. (2000). Expression of the Kruppel-like zinc finger gene biklf during zebrafish development. Mech Dev *97*, 173-176.

81. Kawahara,A. and Dawid,I.B. (2001). Critical role of biklf in erythroid cell differentiation in zebrafish. Curr Biol *11*, 1353-1357.

82. Keller,G., Lacaud,G., and Robertson,S. (1999). Development of the hematopoietic system in the mouse. Exp Hematol. *27*, 777-787.

83. Kennedy,M., Firpo,M., Choi,K., Wall,C., Robertson,S., Kabrun,N., and Keller,G. (1997). A common precursor for primitive erythropoiesis and definitive haematopoiesis. Nature *386*, 488-493.

84. Kimmel,C.B., Ballard,W.W., Kimmel,S.R., Ullmann,B., and Schilling,T.F. (1995). Stages of embryonic development of the zebrafish. Dev Dyn. *203*, 253-310.

85. Kishimoto,Y., Lee,K.H., Zon,L., Hammerschmidt,M., and Schulte-Merker,S. (1997). The molecular nature of zebrafish swirl: BMP2 function is essential during early dorsoventral patterning. Development *124*, 4457-4466.

86. Kollmar,R., Nakamura,S.K., Kappler,J.A., and Hudspeth,A.J. (2001). Expression and phylogeny of claudins in vertebrate primordia. Proc Natl Acad Sci U S A *98*, 10196-10201.

87. Kondo,M., Wagers,A.J., Manz,M.G., Prohaska,S.S., Scherer,D.C., Beilhack,G.F., Shizuru,J.A., and Weissman,I.L. (2003). Biology of hematopoietic stem cells and progenitors: implications for clinical application. Annu Rev Immunol *21*, 759-806.

88. Kondo,M., Weissman,I.L., and Akashi,K. (1997). Identification of clonogenic common lymphoid progenitors in mouse bone marrow. Cell *91*, 661-672.

89. Kosswig,C. (1973). Genetics and Mutagenesis of Fish.

90. Koyama,N., Ishibashi,K., Kuwahara,M., Inase,N., Ichioka,M., Sasaki,S., and Marumo,F. (1998). Cloning and functional expression of human aquaporin8 cDNA and analysis of its gene. Genomics *54*, 169-172.

91. Kwak,S.P. and Dixon,J.E. (1995). Multiple dual specificity protein tyrosine phosphatases are expressed and regulated differentially in liver cell lines. J Biol Chem *270*, 1156-1160.

92. Lambert,J.F., Liu,M., Colvin,G.A., Dooner,M., McAuliffe,C.I., Becker,P.S., Forget,B.G., Weissman,S.M., and Quesenberry,P.J. (2003). Marrow stem cells shift gene expression and engraftment phenotype with cell cycle transit. J Exp Med *197*, 1563-1572.

93. Langenau,D.M., Feng,H., Berghmans,S., Kanki,J.P., Kutok,J.L., and Look,A.T. (2005). Cre/lox-regulated transgenic zebrafish model with conditional myc-induced T cell acute lymphoblastic leukemia. Proc Natl Acad Sci U S A *102*, 6068-6073.

94. Langenau,D.M., Ferrando,A.A., Traver,D., Kutok,J.L., Hezel,J.P., Kanki,J.P., Zon,L.I., Look,A.T., and Trede,N.S. (2004). In vivo tracking of T cell development, ablation, and engraftment in transgenic zebrafish. Proc Natl Acad Sci U S A *101*, 7369-7374.

95. Langenau,D.M., Traver,D., Ferrando,A.A., Kutok,J.L., Aster,J.C., Kanki,J.P., Lin,S., Prochownik,E., Trede,N.S., Zon,L.I., and Look,A.T. (2003). Myc-induced T cell leukemia in transgenic zebrafish. Science *299*, 887-890.

96. Lassila,O., Eskola,J., Toivanen,P., Martin,C., and Dieterlen-Lievre,F. (1978). The origin of lymphoid stem cells studied in chick yold sac-embryo chimaeras. Nature *272*, 353-354.

97. Lassila,O., Martin,C., Toivanen,P., and Dieterlen-Lievre,F. (1982). Erythropoiesis and lymphopoiesis in the chick yolk-sac-embryo chimeras: contribution of yolk sac and intraembryonic stem cells. Blood *59*, 377-381.

98. Leeman,M.F., Curran,S., and Murray,G.I. (2002). The structure, regulation, and function of human matrix metalloproteinase-13. Crit Rev Biochem Mol Biol *37*, 149-166.

99. Liao,E.C., Paw,B.H., Oates,A.C., Pratt,S.J., Postlethwait,J.H., and Zon,L.I. (1998). SCL/Tal-1 transcription factor acts downstream of cloche to specify hematopoietic and vascular progenitors in zebrafish. Genes Dev *12*, 621-626.

100. Liao,E.C., Paw,B.H., Peters,L.L., Zapata,A., Pratt,S.J., Do,C.P., Lieschke,G., and Zon,L.I. (2000). Hereditary spherocytosis in zebrafish riesling illustrates evolution of erythroid beta-spectrin structure, and function in red cell morphogenesis and membrane stability. Development *127*, 5123-5132.

101. Liao,E.C., Trede,N.S., Ransom,D., Zapata,A., Kieran,M., and Zon,L.I. (2002). Non-cell autonomous requirement for the bloodless gene in primitive hematopoiesis of zebrafish. Development *129*, 649-659.

102. Liao,W., Bisgrove,B.W., Sawyer,H., Hug,B., Bell,B., Peters,K., Grunwald,D.J., and Stainier,D.Y. (1997). The zebrafish gene cloche acts upstream of a flk-1 homologue to regulate endothelial cell differentiation. Development *124*, 381-389.

103. Lieschke,G.J., Oates,A.C., Crowhurst,M.O., Ward,A.C., and Layton,J.E. (2001). Morphologic and functional characterization of granulocytes and macrophages in embryonic and adult zebrafish. Blood *98*, 3087-3096.

104. Lieschke,G.J., Oates,A.C., Paw,B.H., Thompson,M.A., Hall,N.E., Ward,A.C., Ho,R.K., Zon,L.I., and Layton,J.E. (2002). Zebrafish SPI-1 (PU.1) marks a site of myeloid development independent of primitive erythropoiesis: implications for axial patterning. Dev Biol *246*, 274-295.

105. Liu,F. and Wen,Z. (2002). Cloning and expression pattern of the lysozyme C gene in zebrafish. Mech Dev *113*, 69-72.

106. Lo,J., Lee,S., Xu,M., Liu,F., Ruan,H., Eun,A., He,Y., Ma,W., Wang,W., Wen,Z., and Peng,J. (2003). 15000 unique zebrafish EST clusters and their future use in microarray for profiling gene expression patterns during embryogenesis. Genome Res *13*, 455-466.

107. Lohnes,D. (2003). The Cdx1 homeodomain protein: an integrator of posterior signaling in the mouse. Bioessays *25*, 971-980.

108. Long,Q., Meng,A., Wang,H., Jessen,J.R., Farrell,M.J., and Lin,S. (1997). GATA-1 expression pattern can be recapitulated in living transgenic zebrafish using GFP reporter gene. Development *124*, 4105-4111.

109. Lynch,M. and Conery,J.S. (2000). The evolutionary fate and consequences of duplicate genes. Science *290*, 1151-1155.

110. Lyons,S.E., Lawson,N.D., Lei,L., Bennett,P.E., Weinstein,B.M., and Liu,P.P. (2002). A nonsense mutation in zebrafish gata1 causes the bloodless phenotype in vlad tepes. Proc Natl Acad Sci U S A *99*, 5454-5459.

111. Lyons,S.E., Shue,B.C., Lei,L., Oates,A.C., Zon,L.I., and Liu,P.P. (2001). Molecular cloning, genetic mapping, and expression analysis of four zebrafish c/ebp genes. Gene *281*, 43-51.

112. Ma,C., Fan,L., Ganassin,R., Bols,N., and Collodi,P. (2001). Production of zebrafish germ-line chimeras from embryo cell cultures. Proc Natl Acad Sci U S A *98*, 2461-2466.

113. Manley,N.R. (2000). Thymus organogenesis and molecular mechanisms of thymic epithelial cell differentiation. Semin. Immunol *12*, 421-428.

114. Martin,C., Beaupain,D., and Dieterlen-Lievre,F. (1978). Developmental relationships between vitelline and intra-embryonic haemopoiesis studied in avian 'yolk sac chimaeras'. Cell Differ *7*, 115-130.

115. Maximow AA. (1909). Untersuchungen uber blut und bindegewebe 1. Die fruhesten entwicklungsstadien der blut- und binde- gewebszellan bein saugetierembryo, bis zum anfang der blutbilding unden leber. Arch Mikroskop Anat *73*, 444-561.

116. Medvinsky,A. and Dzierzak,E. (1996). Definitive hematopoiesis is autonomously initiated by the AGM region. Cell *86*, 897-906.

117. Medvinsky,A.L., Samoylina,N.L., Muller,A.M., and Dzierzak,E.A. (1993). An early pre-liver intraembryonic source of CFU-S in the developing mouse. Nature *364*, 64-67.

118. Mombaerts,P., Iacomini,J., Johnson,R.S., Herrup,K., Tonegawa,S., and Papaioannou,V.E. (1992). RAG-1-deficient mice have no mature B and T lymphocytes. Cell *68*, 869-877.

119. Moore,M.A. and Metcalf,D. (1970). Ontogeny of the haemopoietic system: yolk sac origin of in vivo and in vitro colony forming cells in the developing mouse embryo. Br. J Haematol. *18*, 279-296.

120. Moore,M.A. and Owen,J.J. (1967). Chromosome marker studies in the irradiated chick embryo. Nature *215*, 1081-1082.

121. Mucenski,M.L., McLain,K., Kier,A.B., Swerdlow,S.H., Schreiner,C.M., Miller,T.A., Pietryga,D.W., Scott,W.J., Jr., and Potter,S.S. (1991). A functional c-myb gene is required for normal murine fetal hepatic hematopoiesis. Cell *65*, 677-689.

122. Mullins,M.C., Hammerschmidt,M., Haffter,P., and Nusslein-Volhard,C. (1994). Large-scale mutagenesis in the zebrafish: in search of genes controlling development in a vertebrate. Curr Biol *4*, 189-202.

123. Nasevicius,A. and Ekker,S.C. (2000). Effective targeted gene 'knockdown' in zebrafish. Nat Genet *26*, 216-220.

124. Nehls,M., Pfeifer,D., Schorpp,M., Hedrich,H., and Boehm,T. (1994). New member of the winged-helix protein family disrupted in mouse and rat nude mutations. Nature *372*, 103-107.

125. Neuhauss,S.C., Biehlmaier,O., Seeliger,M.W., Das,T., Kohler,K., Harris,W.A., and Baier,H. (1999). Genetic disorders of vision revealed by a behavioral screen of 400 essential loci in zebrafish. J Neurosci. *19*, 8603-8615.

126. Nichogiannopoulou,A., Trevisan,M., Neben,S., Friedrich,C., and Georgopoulos,K. (1999). Defects in hemopoietic stem cell activity in Ikaros mutant mice. J Exp Med *190*, 1201-1214.

127. Oates,A.C., Brownlie,A., Pratt,S.J., Irvine,D.V., Liao,E.C., Paw,B.H., Dorian,K.J., Johnson,S.L., Postlethwait,J.H., Zon,L.I., and Wilks,A.F. (1999). Gene duplication of zebrafish JAK2 homologs is accompanied by divergent embryonic expression patterns: only jak2a is expressed during erythropoiesis. Blood *94*, 2622-2636.

128. Oates,A.C., Pratt,S.J., Vail,B., Yan,Y., Ho,R.K., Johnson,S.L., Postlethwait,J.H., and Zon,L.I. (2001). The zebrafish klf gene family. Blood *98*, 1792-1801.

129. Ottersbach,K. and Dzierzak,E. (2005). The murine placenta contains hematopoietic stem cells within the vascular labyrinth region. Dev Cell *8*, 377-387.

130. Palis,J., Robertson,S., Kennedy,M., Wall,C., and Keller,G. (1999). Development of erythroid and myeloid progenitors in the yolk sac and embryo proper of the mouse. Development *126*, 5073-5084.

131. Palis,J. and Yoder,M.C. (2001). Yolk-sac hematopoiesis: the first blood cells of mouse and man. Exp Hematol. *29*, 927-936.

132. Patterson,L.J., Gering,M., and Patient,R. (2005). Scl is required for dorsal aorta as well as blood formation in zebrafish embryos. Blood *105*, 3502-3511.

133. Paw,B.H., Davidson,A.J., Zhou,Y., Li,R., Pratt,S.J., Lee,C., Trede,N.S., Brownlie,A., Donovan,A., Liao,E.C., Ziai,J.M., Drejer,A.H., Guo,W., Kim,C.H., Gwynn,B., Peters,L.L., Chernova,M.N., Alper,S.L., Zapata,A., Wickramasinghe,S.N., Lee,M.J., Lux,S.E., Fritz,A., Postlethwait,J.H., and Zon,L.I. (2003). Cell-specific mitotic defect and dyserythropoiesis associated with erythroid band 3 deficiency. Nat Genet *34*, 59-64.

134. Peterson,R.E., Tu,C., and Linser,P.J. (1997). Isolation and characterization of a carbonic anhydrase homologue from the zebrafish (Danio rerio). J Mol Evol. *44*, 432-439.

135. Pevny,L., Simon,M.C., Robertson,E., Klein,W.H., Tsai,S.F., D'Agati,V., Orkin,S.H., and Costantini,F. (1991). Erythroid differentiation in chimaeric mice blocked by a targeted mutation in the gene for transcription factor GATA-1. Nature *349*, 257-260.

136. Poirot,O., Suhre,K., Abergel,C., O'Toole,E., and Notredame,C. (2004). 3DCoffee@igs: a web server for combining sequences and structures into a multiple sequence alignment. Nucleic Acids Res *32*, W37-W40.

137. Porcher,C., Swat,W., Rockwell,K., Fujiwara,Y., Alt,F.W., and Orkin,S.H. (1996). The T cell leukemia oncoprotein SCL/tal-1 is essential for development of all hematopoietic lineages. Cell *86*, 47-57.

138. Qian,F., Zhen,F., Ong,C., Jin,S.W., Meng,S.H., Stainier,D.Y., Lin,S., Peng,J., and Wen,Z. (2005). Microarray analysis of zebrafish cloche mutant using amplified cDNA and identification of potential downstream target genes. Dev Dyn. *233*, 1163-1172.

139. Ransom,D.G., Bahary,N., Niss,K., Traver,D., Burns,C., Trede,N.S., Paffett-Lugassy,N., Saganic,W.J., Lim,C.A., Hersey,C., Zhou,Y., Barut,B.A., Lin,S., Kingsley,P.D., Palis,J., Orkin,S.H., and Zon,L.I. (2004). The zebrafish moonshine gene encodes transcriptional intermediary factor 1gamma, an essential regulator of hematopoiesis. PLoS. Biol *2*, E237.

140. Ransom,D.G., Haffter,P., Odenthal,J., Brownlie,A., Vogelsang,E., Kelsh,R.N., Brand,M., van Eeden,F.J., Furutani-Seiki,M., Granato,M., Hammerschmidt,M., Heisenberg,C.P., Jiang,Y.J., Kane,D.A., Mullins,M.C., and Nusslein-Volhard,C.

(1996). Characterization of zebrafish mutants with defects in embryonic hematopoiesis. Development *123*, 311-319.

141. Robb,L., Elwood,N.J., Elefanty,A.G., Kontgen,F., Li,R., Barnett,L.D., and Begley,C.G. (1996). The scl gene product is required for the generation of all hematopoietic lineages in the adult mouse. EMBO J *15*, 4123-4129.

142. Robb,L., Lyons,I., Li,R., Hartley,L., Kontgen,F., Harvey,R.P., Metcalf,D., and Begley,C.G. (1995). Absence of yolk sac hematopoiesis from mice with a targeted disruption of the scl gene. Proc Natl Acad Sci U S A *92*, 7075-7079.

143. Schorpp,M., Leicht,M., Nold,E., Hammerschmidt,M., Haas-Assenbaum,A., Wiest,W., and Boehm,T. (2002). A zebrafish orthologue (whnb) of the mouse nude gene is expressed in the epithelial compartment of the embryonic thymic rudiment. Mech Dev *118*, 179-185.

144. Shafizadeh,E., Paw,B.H., Foott,H., Liao,E.C., Barut,B.A., Cope,J.J., Zon,L.I., and Lin,S. (2002). Characterization of zebrafish merlot/chablis as non-mammalian vertebrate models for severe congenital anemia due to protein 4.1 deficiency. Development *129*, 4359-4370.

145. Shalaby,F., Rossant,J., Yamaguchi,T.P., Gertsenstein,M., Wu,X.F., Breitman,M.L., and Schuh,A.C. (1995). Failure of blood-island formation and vasculogenesis in Flk-1-deficient mice. Nature *376*, 62-66.

146. Shivdasani,R.A., Mayer,E.L., and Orkin,S.H. (1995). Absence of blood formation in mice lacking the T-cell leukaemia oncoprotein tal-1/SCL. Nature *373*, 432-434.

147. Solnica-Krezel,L., Schier,A.F., and Driever,W. (1994). Efficient recovery of ENU-induced mutations from the zebrafish germline. Genetics *136*, 1401-1420.

148. Sprague,J., Doerry,E., Douglas,S., and Westerfield,M. (2001). The Zebrafish Information Network (ZFIN): a resource for genetic, genomic and developmental research. Nucleic Acids Res *29*, 87-90.

149. Stainier,D.Y., Weinstein,B.M., Detrich,H.W., III, Zon,L.I., and Fishman,M.C. (1995). Cloche, an early acting zebrafish gene, is required by both the endothelial and hematopoietic lineages. Development *121*, 3141-3150.

150. Stickens,D., Behonick,D.J., Ortega,N., Heyer,B., Hartenstein,B., Yu,Y., Fosang,A.J., Schorpp-Kistner,M., Angel,P., and Werb,Z. (2004). Altered endochondral bone development in matrix metalloproteinase 13-deficient mice. Development *131*, 5883-5895.

151. Sudol,M., Greulich,H., Newman,L., Sarkar,A., Sukegawa,J., and Yamamoto,T. (1993). A novel Yes-related kinase, Yrk, is expressed at elevated levels in neural and hematopoietic tissues. Oncogene *8*, 823-831.

152. Sumanas,S., Jorniak,T., and Lin,S. (2005). Identification of novel vascular endothelial-specific genes by the microarray analysis of the zebrafish cloche mutants. Blood *106*, 534-541.

153. Summerton,J. and Weller,D. (1997). Morpholino antisense oligomers: design, preparation, and properties. Antisense Nucleic Acid Drug Dev *7*, 187-195.

154. Terskikh,A.V., Miyamoto,T., Chang,C., Diatchenko,L., and Weissman,I.L. (2003). Gene expression analysis of purified hematopoietic stem cells and committed progenitors. Blood *102*, 94-101.

155. Thompson,M.A., Ransom,D.G., Pratt,S.J., MacLennan,H., Kieran,M.W., Detrich,H.W., III, Vail,B., Huber,T.L., Paw,B., Brownlie,A.J., Oates,A.C., Fritz,A., Gates,M.A., Amores,A., Bahary,N., Talbot,W.S., Her,H., Beier,D.R., Postlethwait,J.H., and Zon,L.I. (1998). The cloche and spadetail genes differentially affect hematopoiesis and vasculogenesis. Dev Biol *197*, 248-269.

156. Thummel,R., Burket,C.T., Brewer,J.L., Sarras,M.P., Jr., Li,L., Perry,M., McDermott,J.P., Sauer,B., Hyde,D.R., and Godwin,A.R. (2005). Cre-mediated site-specific recombination in zebrafish embryos. Dev Dyn. *233*, 1366-1377.

157. Tiwari-Woodruff,S.K., Buznikov,A.G., Vu,T.Q., Micevych,P.E., Chen,K., Kornblum,H.I., and Bronstein,J.M. (2001). OSP/claudin-11 forms a complex with a novel member of the tetraspanin super family and beta1 integrin and regulates proliferation and migration of oligodendrocytes. J Cell Biol *153*, 295-305.

158. Traver,D., Herbomel,P., Patton,E.E., Murphey,R.D., Yoder,J.A., Litman,G.W., Catic,A., Amemiya,C.T., Zon,L.I., and Trede,N.S. (2003a). The zebrafish as a model organism to study development of the immune system. Adv. Immunol *81*, 253-330.

159. Traver,D., Paw,B.H., Poss,K.D., Penberthy,W.T., Lin,S., and Zon,L.I. (2003b). Transplantation and in vivo imaging of multilineage engraftment in zebrafish bloodless mutants. Nat Immunol *4*, 1238-1246.

160. Trede,N.S., Zapata,A., and Zon,L.I. (2001). Fishing for lymphoid genes. Trends Immunol *22*, 302-307.

161. Turksen,K. and Troy,T.C. (2004). Barriers built on claudins. J Cell Sci *117*, 2435-2447.

162. Turpen,J.B. and Knudson,C.M. (1982). Ontogeny of hematopoietic cells in Rana pipiens: precursor cell migration during embryogenesis. Dev Biol *89*, 138-151.

163. Turpen,J.B., Knudson,C.M., and Hoefen,P.S. (1981). The early ontogeny of hematopoietic cells studied by grafting cytogenetically labeled tissue anlagen: localization of a prospective stem cell compartment. Dev Biol *85*, 99-112.

164. Ueda,K., Arakawa,H., and Nakamura,Y. (2003). Dual-specificity phosphatase 5 (DUSP5) as a direct transcriptional target of tumor suppressor p53. Oncogene *22*, 5586-5591.

165. Valge-Archer,V.E., Osada,H., Warren,A.J., Forster,A., Li,J., Baer,R., and Rabbitts,T.H. (1994). The LIM protein RBTN2 and the basic helix-loop-helix

protein TAL1 are present in a complex in erythroid cells. Proc Natl Acad Sci U S A *91*, 8617-8621.

166. van Eeden,F.J., Granato,M., Odenthal,J., and Haffter,P. (1999). Developmental mutant screens in the zebrafish. Methods Cell Biol *60*, 21-41.

167. Volpp,B.D., Nauseef,W.M., Donelson,J.E., Moser,D.R., and Clark,R.A. (1989). Cloning of the cDNA and functional expression of the 47-kilodalton cytosolic component of human neutrophil respiratory burst oxidase. Proc Natl Acad Sci U S A *86*, 7195-7199.

168. Wadman,I.A., Osada,H., Grutz,G.G., Agulnick,A.D., Westphal,H., Forster,A., and Rabbitts,T.H. (1997). The LIM-only protein Lmo2 is a bridging molecule assembling an erythroid, DNA-binding complex which includes the TAL1, E47, GATA-1 and Ldb1/NLI proteins. EMBO J *16*, 3145-3157.

169. Wang,E., Miller,L.D., Ohnmacht,G.A., Liu,E.T., and Marincola,F.M. (2000). High-fidelity mRNA amplification for gene profiling. Nat Biotechnol. *18*, 457-459.

170. Wang,H., Long,Q., Marty,S.D., Sassa,S., and Lin,S. (1998). A zebrafish model for hepatoerythropoietic porphyria. Nat Genet *20*, 239-243.

171. Wang,Q., Stacy,T., Binder,M., Marin-Padilla,M., Sharpe,A.H., and Speck,N.A. (1996). Disruption of the Cbfa2 gene causes necrosis and hemorrhaging in the central nervous system and blocks definitive hematopoiesis. Proc Natl Acad Sci U S A *93*, 3444-3449.

172. Warren,A.J., Colledge,W.H., Carlton,M.B., Evans,M.J., Smith,A.J., and Rabbitts,T.H. (1994). The oncogenic cysteine-rich LIM domain protein rbtn2 is essential for erythroid development. Cell *78*, 45-57.

173. Weber,G.J., Choe,S.E., Dooley,K.A., Paffett-Lugassy,N.N., Zhou,Y., and Zon,L.I. (2005). Mutant-specific gene programs in the zebrafish. Blood *106*, 521-530.

174. Weinstein,B.M., Schier,A.F., Abdelilah,S., Malicki,J., Solnica-Krezel,L., Stemple,D.L., Stainier,D.Y., Zwartkruis,F., Driever,W., and Fishman,M.C. (1996). Hematopoietic mutations in the zebrafish. Development *123*, 303-309.

175. Wienholds,E., Kloosterman,W.P., Miska,E., Alvarez-Saavedra,E., Berezikov,E., de Bruijn,E., Horvitz,H.R., Kauppinen,S., and Plasterk,R.H. (2005). MicroRNA expression in zebrafish embryonic development. Science *309*, 310-311.

176. Wienholds,E. and Plasterk,R.H. (2005). MicroRNA function in animal development. FEBS Lett *579*, 5911-5922.

177. Wienholds,E., Schulte-Merker,S., Walderich,B., and Plasterk,R.H. (2002). Target-selected inactivation of the zebrafish rag1 gene. Science *297*, 99-102.

178. Wienholds,E., van Eeden,F., Kosters,M., Mudde,J., Plasterk,R.H., and Cuppen,E. (2003). Efficient target-selected mutagenesis in zebrafish. Genome Res *13*, 2700-2707.

179. Willett,C.E., Cherry,J.J., and Steiner,L.A. (1997a). Characterization and expression of the recombination activating genes (rag1 and rag2) of zebrafish. Immunogenetics *45*, 394-404.

180. Willett,C.E., Cortes,A., Zuasti,A., and Zapata,A.G. (1999). Early hematopoiesis and developing lymphoid organs in the zebrafish. Dev Dyn. *214*, 323-336.

181. Willett,C.E., Kawasaki,H., Amemiya,C.T., Lin,S., and Steiner,L.A. (2001). Ikaros expression as a marker for lymphoid progenitors during zebrafish development. Dev Dyn. *222*, 694-698.

182. Willett,C.E., Zapata,A.G., Hopkins,N., and Steiner,L.A. (1997b). Expression of zebrafish rag genes during early development identifies the thymus. Dev Biol *182*, 331-341.

183. Wingert,R.A., Brownlie,A., Galloway,J.L., Dooley,K., Fraenkel,P., Axe,J.L., Davidson,A.J., Barut,B., Noriega,L., Sheng,X., Zhou,Y., and Zon,L.I. (2004). The chianti zebrafish mutant provides a model for erythroid-specific disruption of transferrin receptor 1. Development *131*, 6225-6235.

184. Winnier,G., Blessing,M., Labosky,P.A., and Hogan,B.L. (1995). Bone morphogenetic protein-4 is required for mesoderm formation and patterning in the mouse. Genes Dev *9*, 2105-2116.

185. Wortis,H.H., Nehlsen,S., and Owen,J.J. (1971). Abnormal development of the thymus in "nude" mice. J Exp Med *134*, 681-692.

186. Xu,M.J., Matsuoka,S., Yang,F.C., Ebihara,Y., Manabe,A., Tanaka,R., Eguchi,M., Asano,S., Nakahata,T., and Tsuji,K. (2001). Evidence for the presence of murine primitive megakaryocytopoiesis in the early yolk sac. Blood *97*, 2016-2022.

187. Yamada,Y., Warren,A.J., Dobson,C., Forster,A., Pannell,R., and Rabbitts,T.H. (1998). The T cell leukemia LIM protein Lmo2 is necessary for adult mouse hematopoiesis. Proc Natl Acad Sci U S A *95*, 3890-3895.

188. Yang,B., Song,Y., Zhao,D., and Verkman,A.S. (2005). Phenotype analysis of aquaporin-8 null mice. Am J Physiol Cell Physiol *288*, C1161-C1170.

189. Yoda,H., Momoi,A., Esguerra,C.V., Meyer,D., Driever,W., Kondoh,H., and Furutani-Seiki,M. (2003). An expression pattern screen for genes involved in the induction of the posterior nervous system of zebrafish. Differentiation *71*, 152-162.

190. Yoder,M.C. (2001). Introduction: spatial origin of murine hematopoietic stem cells. Blood *98*, 3-5.

191. Yoder,M.C., Hiatt,K., Dutt,P., Mukherjee,P., Bodine,D.M., and Orlic,D. (1997). Characterization of definitive lymphohematopoietic stem cells in the day 9 murine yolk sac. Immunity *7*, 335-344.

192. Zhu,Y.Y., Machleder,E.M., Chenchik,A., Li,R., and Siebert,P.D. (2001). Reverse transcriptase template switching: a SMART approach for full-length cDNA library construction. Biotechniques *30*, 892-897.

193. Zon,L.I. (1995). Developmental biology of hematopoiesis. Blood *86*, 2876-2891.